Project Number GXP - 1401

FIBRIN-BASED MICROVASCULAR NETWORK FOR THE MODULAR DESIGN OF A CARDIAC PATCH

A Major Qualifying Project Report

Submitted to the Faculty

Of

Worcester Polytechnic Institute

In partial fulfillment of the requirements for the

Degree of Bachelor of Science

By:

_____ _____

Alyssa Bornstein Keith Gagnon

_____ _____

Thomas Moutinho Kevin Reyer

Approved By:

_____

Professor George Pins, Advisor

AUTHORSHIP

All members contributed equally to writing, editing, and formatting of this paper.

ACKNOWLEDGEMENTS

The design team would like to give a special thanks to our advisor, Professor George Pins, as well as his graduate students, Megan O'Brien and Alexander Hallet. The design team would also like to thank Professor Glenn Gaudette for the original design idea and Professor Dirk Albrecht, Ross Lagoy, and Laura Aurilio for their help with microfabrication techniques. We would like to thank Professor Sakthikumar Ambady for his help with fluorescent imaging and Professor Stephen Kmiotek for his help with diffusion analysis. The team would further like to thank Lisa Wall and Professor Zoe Reidinger for their support within the lab.

Table of Contents

ABSTRACT

Heart failure is the leading cause of death in the United States, creating a clinical need for a tissue scaffold to repair the heart post-myocardial infarction. A major limitation hindering the development of a cardiac tissue scaffold with a clinically relevant thickness is the lack of adequate vascularization. In this project, a thin fibrin hydrogel was engineered with a microvascular network to create a perfusable system that delivers nutrients to a layer-by-layer constructed cardiac tissue scaffold. These scaffolds were shown to have a high fidelity when patterned against PDMS and these engineered channels were shown to contain perfusate. The team utilized computational modeling to optimize the microvascular network for uniform flow velocity and shear stresses. Finally, mass diffusion from a single channel cast in fibrin was quantified and cells were seeded atop a medium perfused gel. Results suggest that perfusion of medium through the central channel enhanced cellular survival when cultured on the surface. Therefore, a fibrin microvascular network may be a viable solution as a perfusable construct.

TABLE OF FIGURES

TABLE OF TABLES

TABLE OF EQUATIONS

CHAPTER 1: INTRODUCTION

The American Heart Association (AHA) estimates that 85.6 million U.S. citizens suffer from heart disease (Mozaffarian et al., 2015). Additionally, the AHA reports that a U.S. citizen dies every 40 seconds as a result of heart disease, making it one of the top three killers of both men and women in the United States (Mozaffarian et al., 2015).

Recent studies have shown that 40% of patients who are diagnosed with heart failure will succumb to the illness within two and half years (Pocock et al., 2013). Heart failure is often the result of an acute myocardial infarction (AMI), most commonly referred to as a 'heart attack', an episode in which a blockage in a coronary artery leads to myocardial cell death. Lacking endogenous repair abilities, the body lays down a collagenous scar tissue in the region of cell death (W.-H. Zimmermann et al., 2006). Ultimately, the development of scar tissue in the heart hinders cardiac function and can lead to a progressive decrease in the pumping efficiency of the heart due to ventricular remodeling. If this pumping efficiency is no longer sufficient to meet the perfusion demands of the body, the patient is considered to have a condition known as total heart failure (Ertl & Frantz, 2005). To remedy this, an alternative mechanism of pumping blood is needed.

Currently, treatment options for patients with heart failure are limited. The gold standard in complete heart failure treatment is a heart transplant. While there have been significant improvements in successful transplants over the last few decades, matching a patient with a viable donor heart remains a challenge and many patients on the waitlist for a heart transplant often die before a viable match is found (Cowie et al., 1997; Hunt & Haddad,

2008; Zimmermann & Eschenhagen, 2003). For those patients who require immediate intervention, a ventricular assist device (VAD) is implanted as a short term solution in order to extend the patient's life long enough to receive a viable heart for transplantation. While an effective short term solution, VADs are only temporarily effective, with a two year survival rate of only 58% (Slaughter et al., 2009). Thus, there is a need for a more effective, long-term solution to treat heart disease.

Due to limited endogenous cardiac regeneration and the lack of treatment options available, cardiac tissue engineering has been a focus of recent research efforts in attempts to repair damaged myocardium (W. H. Zimmermann et al., 2006). One promising strategy being attempted by a number of groups is the development of an *in vitro* cultured layer of functional myocardial tissue for implantation at the site of scar tissue formation. It has been hypothesized that such a "cardiac patch" would help to restore the pumping capacity of the heart, as well as provide a conduit for the electrical signal to restore electrical synchronicity in the heart (Godier et al., 2010; Radisic & Christman, 2013). While several groups have made slight progress developing a functional cardiac patch, the vast majority have shown poor clinical relevancy and functional outcomes. Many of these groups have found that one of the major limitations of engineering a functional cardiac tissue patch is the difficulty of delivering nutrients and oxygen into a construct that is thick enough to support relevant heart function (Novosel, Kleinhans, & Kluger, 2011). The addition of a vascular network to such a construct has the ability to enhance nutrient and oxygen delivery throughout, thus allowing for a thicker patch of more clinically relevant size.

In this project, the design team was assigned the task of designing and fabricating a microvascular network in a thin-film fibrin hydrogel to be used as a vascular layer in a layer-by-layer constructed cardiac patch. After being tasked with the project, the design team conducted a thorough literature review of vascularization strategies for tissue engineered constructs. Interviews with the client, Dr. George Pins, and users, Megan O'Brien and Alex Hallet, were also conducted in order to assess the expectations and desires of each stakeholder in this project. Once these interviews were completed, the team formalized a revised client statement, from which a series of milestones were drafted in order to guide the logical progression of the project from start until completion.

The overview of project milestones can be seen in Figure 1. Note that the first milestone was the successful engineering of a fibrin microvascular network, which was important to demonstrate that fibrin could be patterned and could retain an imprinted geometry. Using a natural capillary bed as design inspiration, a microvascular system was created which had a single inlet, a branching region, and a functional vascular area, which was designed to be the region of diffusion into and out of the vascular network. Once designed, the networks were fabricated onto a silicon wafer using a standard photolithography protocol. A polydimethylsiloxane (PDMS) replicate of the wafer was

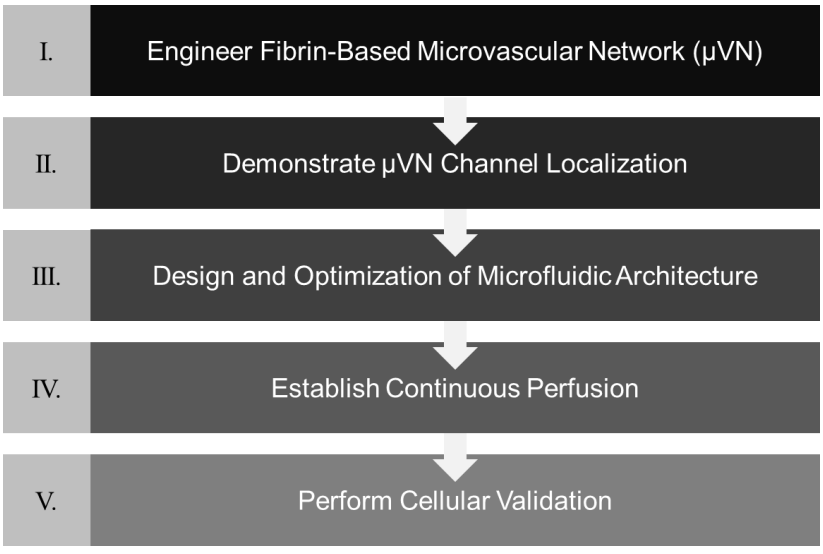

Figure 1: Schematic of Project Strategy

created, from which fibrin was patterned into a thin film. After 20 minutes, the fibrin was removed from the mold, leaving a very high-fidelity replicate to the PDMS mold in the fibrin sheet. Using this technology, the 20 mg/mL fibrin gels used were shown to have very high pattern fidelity, showing a maximal deviation in width of 8% from the PDMS mold from which they were cast.

Once the microvascular network had been engineered into a thin film of fibrin, the next step was to demonstrate that the channels could localize flow in their lumens. This step was critical if the channels were to enhance the rate of perfusion through the construct to levels greater than bulk diffusion alone. In order to demonstrate this channel localization, 1 μm latex microparticles were introduced into a patterned fibrin gel using capillary action. Examination of these particles during loading revealed that they remained in the lumen of the channels while flowing and remained in the channels once the flow had ceased. Microscopic examination showed minimal leaching of the particles into the surrounding gels, suggesting that flow through the channels was easier than bulk gel transport. This suggested that these micropatterned fibrin films were capable of serving as a conduit for flow.

The third step of the design process was the optimization of the microfluidic vessel architecture. Three width profiles (constant width, a linearly decreasing channel width and a width profile that obeyed Murray's Law) were tested in Comsol (Comsol, Burlington) to assess for the uniformity of flow throughout the system. Murray's law was determined to have the most uniform flow, however, its rapid growth from one branch to the next had potential to generate fabrication difficulties. Different junction geometries (square branching, circular branching and triangular branching) were also tested in Comsol and the velocity flow profiles

were assessed based on how well each design reduced flow stagnations. Qualitative analysis did not suggest that any one design outperformed the others, so elements of all three designs were combined into the final, optimized geometry. Simulations suggested that this optimized geometry had a lower fluidic resistance than any of the other channel designs and qualitatively, this architecture produced a highly homogenous flow pattern with minimal regions of flow stagnation.

The fourth phase of the project was the generation of continuous perfusion within the thin-film layers and quantification of diffusion from a continuously perfused channel. Most of the perfusion attempts for continuous perfusion of a thin-film network resulted in significant backflow around the needle, though anecdotally, some thin films were able to be perfused. In order to quantify diffusion, the team moved to a single channel system through which continuous perfusion was reliably achieved. As a model molecule, fluorescein isothiocyanate (FITC, Sigma Aldrich) was continuously perfused through the channels and diffusion of the fluorescent particle from the channel into the surrounding gel was monitored. Ultimately, the diffusivity of FITC in fibrin was measured to be 1.5×10^{-7} cm^2/sec.

The final phase of this project was a validation of cellular viability in order to show that this system could adequately supply nutrients to cells in adjacent layers. Again, the single channel system was used, due to its ability to be continuously perfused and the large (600 µm) separation between the channel and the cells; if cells were able to be nourished from a channel 600 µm away, their survival in layers thinner than that would be likely. To test this, cells were seeded on a single channel perfusion system and bathed in DPBS, while DMEM was perfused through the channel for 24 hours. Calcein AM/ EthD staining suggested that some cells in the

DMEM perfused channels were still alive, while none of the cells in the gels perfused with DPBS were still alive. This demonstrated that nutrient perfusion through the channels could enhance cellular survival atop a perfused gel.

Taken together, the results of these five steps demonstrated that a thin film, continuously perfused fibrin microvasculature could support cellular survival on adjacent layers of a tissue construct. Thus, this MQP served to validate the feasibility of the thin film microvasculature concept. In the future, these two systems will need to be integrated prior to the fabrication of a continuously perfusable thin film hydrogel for use in a layer-by-layer constructed cardiac tissue element.

CHAPTER 2: LITERATURE REVIEW

This chapter provides a comprehensive overview of the pathophysiology of heart failure as well as the current treatments available. It provides the necessary information to understand the need for a vascularized scaffold, as well as an overview of previous attempts to engineer vascularized scaffolds. This chapter concludes with an anatomy overview of native microvascular and design principles for engineering microfluidic based vasculature.

2.1 HEART FAILURE

Heart failure, clinically defined as "an abnormality of cardiac structure or function leading to failure of the heart to deliver oxygen at a rate commensurate with the requirements of the metabolizing tissues, despite normal filling pressures (McMurray et al., 2012)." affects approximately 5.7 million United States citizens and is projected to increase in prevalence by 46% by 2030, at which point it will affect over 8 million people in the U.S. alone (Mozaffarian et al., 2015). While current treatments for this disease have shown improvements in survival rates, 5% of hospital admissions and one in nine overall deaths is attributed to heart failure, which costs approximately $35 billion per year to treat. (Mozaffarian et al., 2015; Mulloy et al., 2013). Additionally, the average five year survival of patients with heart failure is approximately 50%, which is largely attributed to the limited endogenous regeneration in the tissue after damage has occurred (Mulloy et al., 2013). Due to its prevalence, new and improved medical treatments for heart failure are in constant demand (Shin, Ishii, Sueda, & Vacanti, 2004).

2.1.1 Pathophysiology of Heart Failure

Heart failure is often the result of a traumatic cardiac event, such as an acute myocardial infarction (AMI), which is more commonly known as a heart attack. During an AMI, blood supply to the myocardial tissue is reduced, often due to a clot in a coronary artery, resulting in hypoxia of the tissue downstream of the blockage. Due to their high metabolic activity, cardiomyocytes are extremely sensitive to a reduced supply of oxygen, which results in gradual, irreparable tissue death beginning within four hours of the onset of hypoxia (Boersma et al., 2003; Elsasser, Suzuki, Lorenz-Meyer, Bode, & Schaper, 2001; Vunjak-Novakovic et al., 2009). The longer the blockage persists, the greater the amount of cellular death and the greater the size of the necrotic region of the myocardium.

Current treatment techniques for clearing a blockage involve chemical vasodilation or percutaneous coronary intervention, the manual clearing of a blockage via angioplasty (Boersma et al., 2003). Once the blockage has been cleared and perfusion is reestablished, the region of cellular death begins to remodel, a process where the necrotic area is digested and a collagenous scar tissue layer develops. The remodeling of contractile healthy myocardium to rigid scar tissue, which is non-contractile and non-conductive, limits the flexibility and expansion of the adjacent regions of myocardial tissue. This lack of contractility and flexibility inferred by the scar tissue reduces the overall pumping efficiency (measured by ventricular ejection fraction) of the heart, though the degree to which the efficiency is reduced is ultimately dependent upon the size of the necrotic region (Bolooki, 2010; Vunjak-Novakovic et al., 2009).

Once the infarction has been cleared, scar tissue ultimately remains at the site of the infarct. Over time, the ventricular walls of an infarcted heart are remodeled due to the differential stress state created by the presence of the scar tissue, resulting in a degradation in pumping efficiency until it has reached a point where the heart is no longer able to provide adequate perfusion to the remainder of the body, a situation known as end stage heart failure (Godier et al., 2010).

2.1.2 Current Treatments

Currently, there are three clinically available therapies for end stage heart failure including pharmacological therapy, Left Ventricular Assist Devices (LVADs) or total heart transplants (Rose et al., 2001). These three options are typically successful in extending the lives of patients who suffer from end stage heart failure, though none are permanent solutions.

Pharmacological Therapy

Typically the first treatment regimen in heart failure patients, pharmacological therapy aims to reduce the overall degradation of the heart by relieving symptoms and preventing future myocardial damage (Dickstein et al., 2008). One of the major drugs used in the treatment of heart failure is an angiotensin-converting enzyme (ACE) inhibitor, which serves to dilate arteries throughout the body and reduce blood pressure, both of which can lead to an increased nutrient delivery throughout the myocardium and a decreased risk of subsequent occlusions (Bakris, Weir, DeQuattro, & McMahon, 1998; Dickstein et al., 2008; McMurray et al., 2012; Swedberg et al., 2005).

In addition to the administration of ACE inhibitors, beta-blockers or digoxin, if well tolerated by patients, are commonly used to depress myocardial function, reducing the

myocardial workload for heart failure patients ("A Trial of the Beta-Blocker Bucindolol in Patients with Advanced Chronic Heart Failure," 2001; Dickstein et al., 2008). Other chemical therapies include aldosterone antagonists and hydralazine, both diuretics which reduce blood pressure, as well as angiotensin receptor blockers (ARBs), which work to lower blood pressure by acting directly on angiotensin receptors in the kidneys (Dickstein et al., 2008). This decreased blood pressure reduces the necessary force of contraction of the heart, allowing the weakened heart to pump blood more effectively.

Overall, while cardiovascular drugs are one of the most common treatment methods, there is potential for a number of adverse side-effects to these drugs. Additionally, the long-term effects (and side-effects) of these drugs, while mostly positive, are just now being understood (Flather et al., 2000). Furthermore, certain patients may not be able to receive specific drugs, due to contraindications with their other medications. Most significantly, none of these drugs induce myocardial repair- they all treat the symptoms and once a patient is started on these drugs, they will continue to use them, or similar drugs, for the remainder of their lives (McMurray et al., 2012).

Left Ventricular Assist Devices

Left Ventricular Assist Devices (LVADs) are large, electromechanical pumps designed to replace the pumping capacity of a failing left ventricle. They consist of a tube attached to the left ventricle that collects pooling blood and pumps it to the aorta, inducing flow though the circulatory system (Holley, Harvey, & John, 2014; Mulloy et al., 2013; Slaughter et al., 2009). An example of an implanted LVAD can be seen in Figure 2.

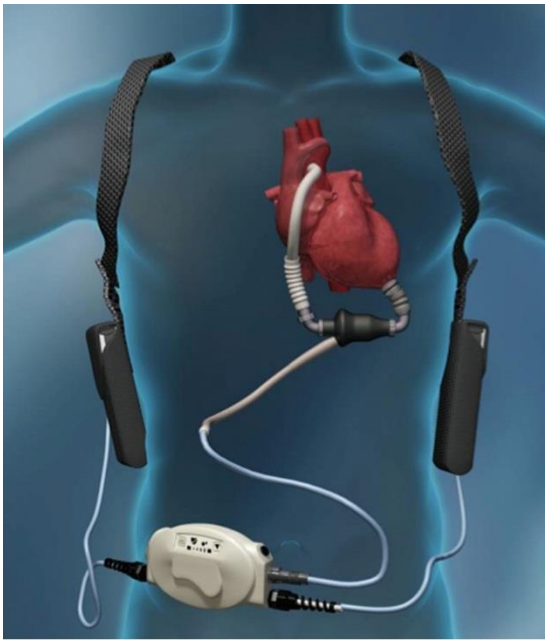

Figure 2: Schematic of an LVAD. Note the large size of the pump and connection between the apex of the heart and the aorta (Holley et al., 2014).

In 2009, the two-year survival rate for a patient with an LVAD was 58%, and though survival rates have increased over time, LVADs still are not considered long-term solutions to heart failure due to the lifespan of their components and the physiological response (Holley et al., 2014; Slaughter et al., 2009). For example, patients using LVADs have been shown to develop aortic insufficiencies and flattened ventricles, changes in the endothelium histology, and to have increased chances of developing a serious gastrointestinal bleed (Cowger et al., 2010; Holley et al., 2014; Stern et al., 2010). The risk of infection is another concern associated with LVADs. For example, in 2004, 65% of implanted LVADs needed revision surgery after one year of use, and the main reason for this surgery is infection due to the implantation of the device (Holley et al., 2014; Topkara et al., 2010). Thus, LVADs are a functional, clinically available temporary solution for end stage heart failure, but do not provide a long-term treatment for heart failure.

Heart Transplant

The current clinical gold standard for the treatment of end stage heart failure is a total heart transplant. While LVADs are typically used to provide an immediate, short-term treatment for acute heart failure when a viable, transplantable heart is unavailable, a total orthotropic heart transplant is designed for longer-term use. In an orthotropic heart transplant (OHT), a patient's heart is removed and replaced with a donor heart that is an immunologically acceptable match via a dangerous procedure that results in operative death rates of 5-10% (Beltrami et al., 1994; Jung et al., 2011). In 2011, only 4,096 heart transplants were attempted worldwide, with approximately 2000 conducted in the United States, which suggests the difficulty of the procedure is and the lack of available hearts (Lund et al., 2013; Mulloy et al., 2013). In 2011, the one-year survival rate for orthotropic heart transplants was 85% and the five year survival rate, calculated by examining the 103,299 OHTs conducted between 1981 and June 2011, was measured to be 69%, with a median survival rate of 11 years (Jung et al., 2011; Lund et al., 2013; Stehlik et al., 2011). Although OHTs extend the lifetime of patients, the 11 years granted via an OHT is not considered a "permanent" solution to heart failure, as the mean age of recipients of transplanted hearts in a study of 154 men was 43 years old (Jung et al., 2011).

In addition to a difficult surgery, patients with orthotropic heart transplants are at an increased risk of rejection. Of all transplants between 2001 and 2009, 26% of patients were hospitalized for immune rejection within the first year, while 44% were hospitalized for rejection within 5 years (Stehlik et al., 2011). In order to address the risk of rejection, immunosuppressive drugs are used, which increase the risk of infection and sepsis as well as a

whole host of other undesirable side-effects, including opportunistic diseases and cancer (Jung et al., 2011; Lindenfeld et al., 2004). While rejection and infection are concerns, the leading source of graft failure, occurring in more than 50% of OHTs, is cardiac allograph vasculopathy (CAV), a complication that is a combination of intimal hyperplasia, traditional atherosclerosis, and autoimmune rejection that results in the narrowing of coronary arteries that ultimately kills the transplant (Jentzer, Hickey, & Khandhar, 2014; Weis & von Scheidt, 1997).

Clearly, both the LVAD and the OHT offer limited to moderate success for patients suffering from advanced heart failure. Both treatments seek to augment the heart mechanically, either in the form of a pump or a new heart, yet neither treatment seeks to repair the existing heart tissue, which would greatly reduce the risk of infection and foreign body response. Theoretically, the repair of the damaged heart tissue would allow for restoration of heart function and negate the concerns of CAV associated with OHT, as well as the issues associated with LVAD use. For these reasons, the development of an engineered myocardial tissue layer has been a goal in regenerative medicine over the last few years (Radisic & Christman, 2013; Vunjak-Novakovic et al., 2009).

2.2 Cardiac Tissue Engineering

Cardiac tissue engineering has been an area of research in the broader tissue engineering field for quite some time, and though there have been significant advances in this field, there are no clinically available treatments at this time.

2.2.1 Clinical Need

Tissue engineering is defined as "an interdisciplinary field that applies the principles of engineering and the life sciences towards the development of biological substitutes that restore, maintain or improve function" (Langer & Vacanti, 1993). As the definition suggests, this field of engineering seeks to design and develop functional tissue substitutes for implantation. As has been previously explained, there is no real, long term solution to heart failure. LVADs are temporary fixes and patients receiving OHTs often suffer from complications of rejection, infection and CAV. *Thus, there is a need for a clinically relevant solution to heart failure which has potential to restore functionality to the scarred heart without risk of rejection and other complications associated with OHT and LVAD use.*

A number of different labs have attempted to generate myocardial tissue constructs to enhance the contractility and electrical synchronicity of the collagenous scar tissue formed post-AMI (Radisic & Christman, 2013; Vunjak-Novakovic et al., 2009). Many researchers believe that tissue engineered myocardial constructs could provide the functional recovery necessary while negating the concerns of immune rejection seen in OHT (Vunjak-Novakovic et al., 2009). Despite its promise, the field of cardiac tissue engineering is a particularly challenging field of tissue engineering, due to the high density and non-proliferative nature of myocytes in native myocardium, the large volumes of oxygen required to fuel these metabolically active cells, and the coupling between adjacent cells which allows for electromechanical synchronicity (Mulloy et al., 2013; Vunjak-Novakovic et al., 2009).

2.2.2 Current Strategies

The two main fields of cardiac tissue engineering include myocardial tissue element (MTE) culture and injectable hydrogels. In contrast to injectable hydrogels, which seek to deliver a cell-laden hydrogel to the region of myocardial damage, myocardial tissue element research aims for the formation of a functional layer of *in vitro* cultured myocardial tissue which can be used as replacement tissue for damaged or diseased heart tissue (Radisic & Christman, 2013). The advantages of this strategy, as compared to an injectable hydrogel, are numerous including a high level of control over the mechanical properties of the patch, the ability to utilize anisotropy to control cellular orientation and the ability to pre-vascularize the patch. Additional concerns with injectable hydrogels include their ability to localize the cells and their ultimate effectiveness in supporting cellular proliferation and growth (Radisic & Christman, 2013). Due to these concerns, many recent cardiac regeneration attempts have focused on MTE fabrication.

2.2.3 Fundamental Limitations

While a diverse number of strategies have been used to develop these tissue elements, all suffer from a number of fundamental limitations. One major concern is the invasive nature of the implantation procedure; in order to effectively deliver the construct to the heart, the thoracic cavity must be opened and the patch must be sown into the myocardial wall. Additionally, the size of the patch is a major concern, as a number of studies have indicated that the regenerative effect is limited by the size of the patch (Singelyn & Christman, 2010). The largest concern with these tissue elements is the lack of vascularization, which limits the size of the patches. Therefore, there is a clinical relevancy for vascularized tissue constructs to provide

a constant supply of nutrient delivery and removal of waste to support the growth and proliferation of cells. (Radisic & Christman, 2013; Taylor, Sampaio, & Gobin, 2014; W.-H. Zimmermann et al., 2006).

Numerous groups have been begun developing vascularized tissue elements which are able to be thicker to create more clinically relevant cardiac tissue elements (J. T. Borenstein & Vunjak-Novakovic, 2011). For example, one group, which has used cardiomyocyte cell sheets was only able to support sheets stacked 3 to 4 layers high, to a thickness of approximately 80μm, before necrotic regions began appearing within the tissue (Shimizu, 2011). Once vascularized, however, these cells sheets were able to be stacked to thicknesses approaching 1 mm before seeing the formation of necrotic regions (Masuda, Shimizu, Yamato, & Okano, 2008). Thus, it is evident that vascularization of MTEs, which are naturally a metabolically active tissue, is paramount to the successful development of a tissue engineered construct that can be used in a clinical setting.

2.3 Cardiac Tissue Engineering in Dr. Pins' Lab

As alluded to previously, one of the major drawbacks of most *in vitro* cultivated cardiac patches is their lack of vascularization, which ultimately leads to failure of the graft and death of any cells contained within the patch (Montgomery, Zhang, & Radisic, 2014). In order to address this concern, Professor Pins' lab is pioneering a novel strategy for the creation of a vascularized myocardial tissue element which is fabricated using a layer-by-layer approach in which thin layers (~200 μm) of myocardial tissue are alternated with thin layers of perfused vascular tissue. This design, theoretically, would allow for the creation of a cardiac tissue patch of a clinically relevant thickness, as the vascular layer should be no more than 200 μm from any

cell in the muscular layer, thus falling within the diffusion limit of oxygen (Carmeliet & Jain, 2000).

Functionally, this layer-by-layer construction allows for the introduction of multi-functionality into the design of the cardiac patch. Each layer will have a distinct function (contraction, electrical synchronicity, perfusion, etc.), and by stacking one layer atop the next, multiple functionalities could be incorporated into the design of the cardiac patch. At its most basic level, Pins lab has identified two layers that are critical to the success of this patch: the muscular layer and the vascular layer. The myocardial layer of the patch will be a functional, contractile tissue composed of aligned cardiomyocytes that will provide contractility and mechanical integrity to the patch. In contrast, the vascular layer will consist of an engineered, perfusable vascular network designed to provide nutrients to not only the other cells of the vascular layer, but also to the cells of the muscular layer.

This MQP focuses on the development of the vascular layer of this layer-by-layer composite system. This layer is crucial to the success of the patch, as it will deliver the nutrients necessary for cellular survival throughout the patch, allowing for the creation of a patch far thicker than 400μm, or twice the diffusion limit of oxygen (since oxygen can diffuse in both directions). Research suggests that as long as all cells are located within 200μm of a vascular layer, they will receive sufficient diffusion from a perfusion system to support cellular survival. Thus, this vascular layer plays a pivotal role in the cardiac patch, as it allows for the development of a cardiac patch of clinically relevant size. It is the role of this MQP team to design, fabricate and validate these vascular layers.

Ultimately, the two layers, the myocardial and vascular layers, will be stacked atop one another, as displayed in Figure 3.

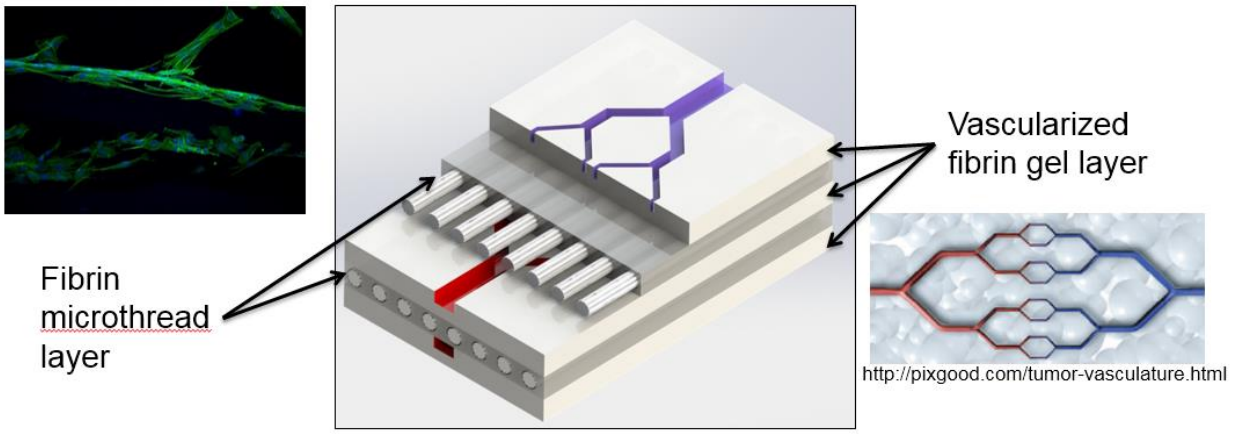

Figure 3: Diagram of layer-by-layer Fabricated Cardiac Patch. Note that the red layers are the vascular layers and the more translucent layers are the muscular layers.

Alternating layers of aligned myocardial tissue and vasculature ensures that the active myocardial layer receives adequate nutrients for survival and function.

2.4 Tissue Engineered Vasculature

A number of different groups have attempted to vascularize tissue constructs. In general, vascularization strategies fall into one of two categories: *de novo* vasculogenesis and engineered vasculature (Phelps & García, 2010). While fundamentally different processes, both of these strategies arrive at the same outcome: tissue construct vascularization. The groups who have succeeded using *de novo* vasculogenesis have managed to induce the formation of new blood vessels *de novo* by endothelial cells. In contrast, the groups who have pursued engineered vasculature use fabrication techniques to form channels in the scaffold, which can then be perfused with medium. These scaffolds also often support angiogenesis, which is the sprouting and formation of small vessels and capillaries from intact blood vessels (Risau, 1997;

Risau & Flamme, 1995). Due to the nature of this project, a cursory overview of the *de novo* vasculogenesis will be provided, followed by a more in-depth description of engineered vasculature, which was deemed more pertinent to the project.

2.4.1 De Novo Vasculogenesis

A number of groups have synthesized vasculature using *de novo* vasculogenesis. These techniques rely on cellular vascularization of the channels, in which cells are placed on or in the construct and induced into an angiogenic state through the use of growth factors, topographical cues and co-culture conditions ((Patan), 2000). In general, these techniques fall into two categories, *in vivo* based approaches and *in vitro* approaches, seminal works of which are summarized in Table 1.

Table 1: Summary of Studies Achieving the Vascularization of Engineered Tissue

Concept	Outcome	Reference
In Vivo Vascularization		
Omental Implantation	Vascularization of implanted scaffold and integration into host vasculature	(Dvir et al., 2009)
Subcutaneous Implantation	Perfusable vasculature with a natural morphology and vascular sprouting.	(Hegen et al., 2011)
VEGF- Overexpression	Over-expression of VEGF induced increased angiogenesis of tissue element implanted atop the myocardium.	(Marsano et al., 2013)
HUVEC Sandwiching	Subcutaneous implantation of multilayer cardiomyocyte sheets with HUVECs between each layer showed micro-vessel formation after one week.	(Sasagawa et al., 2010)
In Vitro Vascularization		
Co-Culture	Co-culture of cardiomyocytes, endothelial cells and fibroblasts showed the creation of a large, perfusable vascular plexus with native myocardial-like properties	(Auger, Gibot, & Lacroix, 2013; Chen et al., 2010; Stevens et al., 2009)
Artificial Vascular Bed Sprouting	Culture of cell sheets atop a collagen gel with microchannels showed anastomoses between lumens in cellular layers and microchannels.	(Sakaguchi et al., 2013; Hidekazu Sekine et al., 2008; H. Sekine et al., 2013)
Decellularized Vascular Network	Decellularized veins and organs have been shown to be perfusable and capable of supplying nutrients to the developing tissue.	(Badylak, Taylor, & Uygun, 2011; Ott et al., 2008; Schaner et al., 2004)

2.4.2 Engineered Vasculature

A different vascularization strategy which has been used to vascularize tissue constructs is engineered vasculature. This strategy revolves around the addition of perfusable vascular channels to the scaffold during scaffold fabrication. Cells are then seeded on the scaffold and the scaffold is perfused, supplying nutrients to the cells.

Engineered vasculature offers a number of advantages over *de novo* vasculogenesis. One major advantage of this strategy is the control which it offers the designer. In the *de novo* process, cells move in a pseudorandom fashion, forming vascular networks as they go. In contrast, in an engineered approach, the channels are exactly where they are designed to be. This control gives the designer the ability to ensure that all portions of the scaffold are equally perfused.

Another major advantage of the engineered approach is its timeliness. In general, perfusion of engineered vascular constructs occurs at the same time as, or shortly after, scaffold synthesis. In most cases, these channels can be immediately perfused, allowing cells to be added to the scaffold weeks sooner than if *de novo* vascularization, which relies on cells to migrate and develop their own networks, had been used. For this reason, it has been posited that microfluidic-based microvasculature can lead to a more developed microvasculature in a fixed amount of time, as compared to the other two methods (Golden & Tien, 2007).

One drawback of these engineered channels is that their diffusion capacity decreases over time, as the channel becomes endothelialized, which due to their barrier function, limits diffusion in and out of the channel, thus limiting diffusion out of the channels. In *de novo* vascularization, this change in diffusion is not an issue, since the endothelialized vessel is fabricated as the vessel extends (Alberts et al., 2013) .

A brief summary of some of the engineered vascular strategies which have been used for engineered vascular synthesis is shown in Table 2.

Table 2: Engineered Vasculature Studies

Scaffold Mediated Fabrication		
Silicon Imprinting	PGS scaffolds were cast on a silicon master-mold. Once sealed, the scaffold was perfusable and able to be successfully endothelialized	(Fidkowski et al., 2005)
Sacrificial Layer	Sacrificial gelatin patterns were made in a PDMS mold and a collagen gel was cast around the gelatin patterns. Once melted, the gelatin was capable of being perfused and endothelialized	(Golden & Tien, 2007)
Soft Lithography	Silk was patterned on a PDMS mold and attached to a porous scaffold. Perfusion of medium through the silk channels was able to keep cells in the porous scaffold alive	(Wray, Tsioris, Gi, Omenetto, & Kaplan, 2013)
Silicon Micromachining	Machined features down to 1 µm were in silicon were then imprinted in a biocompatible polymer and endothelialized on a capillary size scale.	(Jeffrey T. Borenstein et al., 2002)
Silicon Imprinting	Calcium-alginate hydrogels are molded from a silicon pattern. Fluorescent markers were then perfused to study diffusion through the hydrogel	(Choi et al., 2007)
3D Printing	A sugar-glass vasculature was printed used as a sacrificial layer for gel casting. Once the gel was cast, the sugar-glass was sacrificed, revealing 800 µm diameter, perfusable channels	(Miller et al., 2012)

Silicon Imprinting

As microfabrication and Biomicroelectromechanical systems (BioMEMS) have become more accessible in recent years, direct incorporation of perfusable vessels into scaffolds has been attempted. One of the first groups to engineer a vascular network for tissue engineering applications utilized a poly(glycerol sebacate) (PGS) scaffold which was imprinted with channels by patterning it against a microfabricated silicon wafer. This PGS scaffold was then bonded to a flat layer of PGS, forming sealed channels. These channels were then perfused and endothelialized. After endothelialization, the patency of the channels was found to be quite high, as perfused dyes remained localized to the lumens of the channels (Fidkowski et al., 2005).

Sacrificial Layer

A similar approach towards the direct fabrication of a vascular network was attempted two years later. This approach utilized soft lithography to form channels in a collagen gel. Golden et al. at Boston University have used soft lithography to template a sacrificial layer of gelatin. A collagen gel was then cast around this sacrificial layer, which was sacrificed by increasing the temperature and allowing the gelatin to be flushed out of the channels. This ultimately left channels in the shape of the initial sacrificial layer, that the authors were able to perfuse with media and endothelialize, forming engineered vessels (Golden & Tien, 2007). An example of these channels is shown in Figure 4.

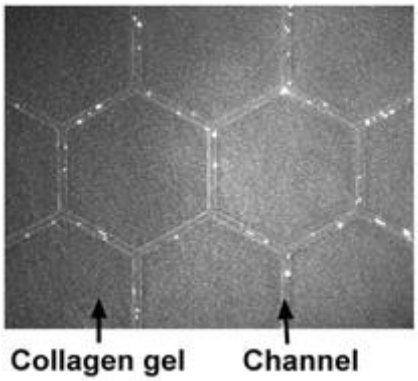

Figure 4: Micropatterned Collagen Gel. Note that the channels have been seeded with endothelial cells, which are the brighter specks seen in the figure (Golden & Tien, 2007)

Notice the complex hexagonal architecture of these channels and their relative uniformity. This work established sacrificial layers as a viable means of generating channels in a hydrogel construct.

Soft Lithography

A group at Tufts University recently published similar results featuring a micropatterned silk scaffold for use in engineered vasculature. Wray et al. demonstrated the fabrication of a silk-

based microfluidic microvascular network atop of a porous scaffold. After endothelializing the channels, researchers were able to show successful survival and endothelialization of hMSCs that were being cultured in the porous scaffold (Wray et al., 2013). This research suggests that a microfluidic layer can support cells in the bulk of the scaffold, relatively distant from the microfluidic region.

In a similar study, Bick et al. demonstrated that methacrylated hyaluronic acid hydrogels (MeHA) could be cross-linked against a PDMS mold, developing channels within the hydrogel. These channels were then crosslinked to flat layers of MeHA, creating enclosed channels, which were then coated with collagen and endothelialized. After 3 days, these channels were seen to have confluent layers of endothelial cells (Bick et al.). Similar results have been seen by a number of groups (Fidkowski et al., 2005; Janakiraman, Kienitz, & Baskaran, 2007; Kaihara et al., 2000; Ling et al., 2007; Shin et al., 2004)

3D Printing

In contrast to the conventional soft lithography fabrication methods, which generate thin, 2D-esque constructs, other groups have attempted to synthesize three-dimensional vasculature networks using 3D printing technologies. A group at the University of Pennsylvania has shown that a 3D printed carbohydrate glass scaffold can be printed in the shape of the desired vasculature and used as a sacrificial layer to form vasculature in a wide variety of scaffold materials, including agarose, alginate, fibrin and Matrigel (Miller et al., 2012). Using such a method, researchers were able to generate channels that could be perfused at a physiologically relevant flow rate of approximately 10μL/s (Miller et al., 2012). Example cross-sections of these cell-seeded channels can be seen in Figure 5.

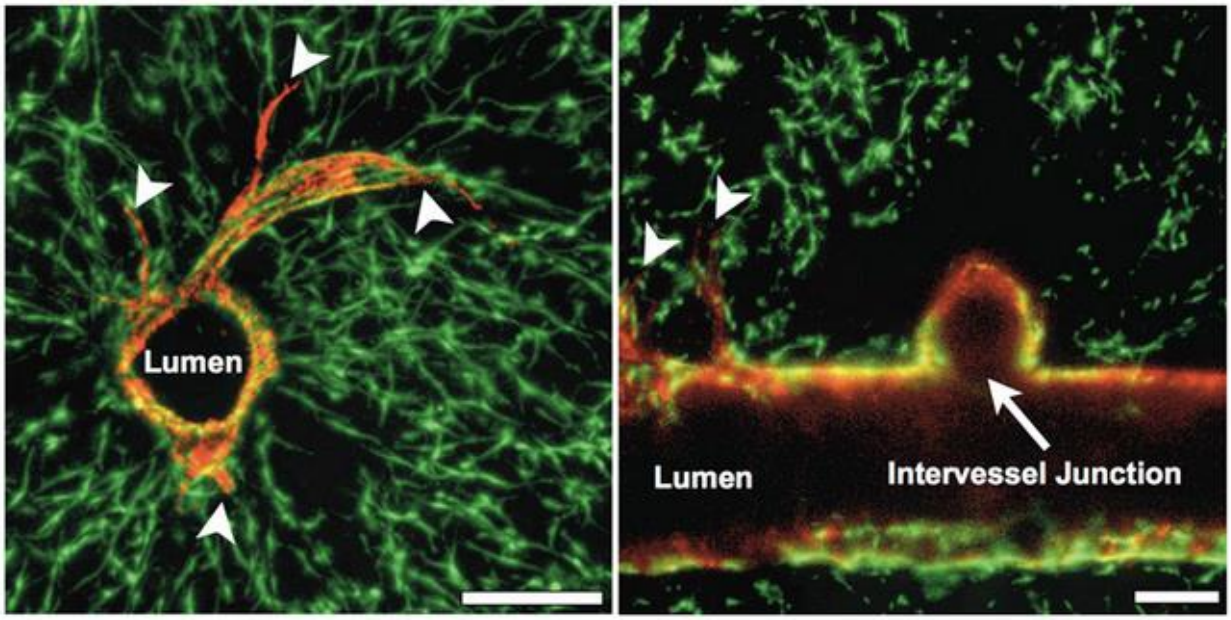

Figure 5: Endothelialized 3D Printed Vasculature. Note that red cells are mCherry expressing HUVEC. These results show not only the existence of intact vasculature, but also the also the junction of two discrete vessels. The scale bars are both 200 µm (Miller et al., 2012).

Note that this figure suggests that the authors were able to grow a confluent layer of endothelial cells within their 3D fabricated microvasculature.

Another group is working on the 3D fabrication of vasculature by 3D printing a modified Pluronics, which exhibit LCST behavior. This layer acts as a sacrificial layer around which a gel could be cast. Once polymerized, the fibrin is cooled and flushed, generating intact, 3D vasculature (Kolesky et al., 2014) Still an emerging technology, 3D sacrificial layers appear to have potential to play a large role in the development of a vascularized scaffold.

Similarly, a group at The Scripps Research Institute developed and studied a 3D printed fibrin based scaffold loaded with human microvascular endothelial cells (HMVEC) (Cui, 2009). The cells were combined with the gel to form a "bio-ink" which was then printed layer by layer

to form sealed vascular layers within a gel. Cui et. al. used a drop-to-gelation method using 60 mg/ml fibrinogen and 50 unit/ml thrombin. These concentrations formed a very dense fibrin gel which polymerized quickly and maintained properly printed geometries. Using a modified HP Deskjet printer, thrombin loaded with the HMVECs was printed concurrently with fibrin to create the polymerization of the polymer. The HMVECs were observed as migrating and aligning toward the channels, forming confluent linings inside the gel (Cui, 2009). An example of this 3D printed vasculature can be seen in Figure 6.

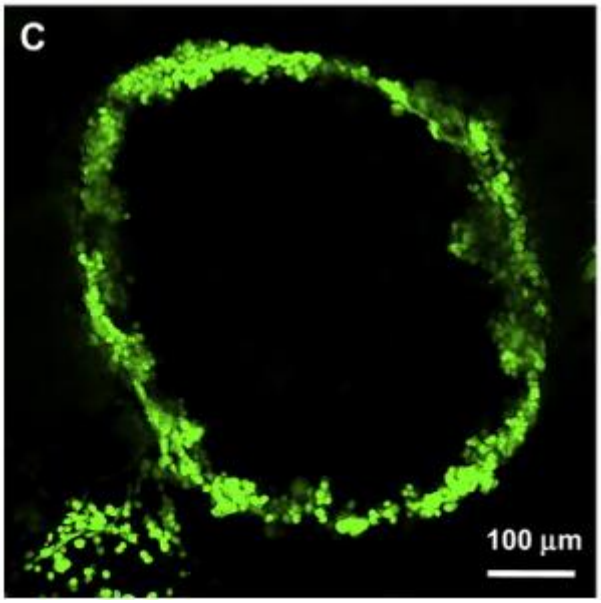

Figure 6: Endothelial Layer of 3D Printed Microvessel. Note that these endothelial cells were printed directly within the gel; they were not seeded onto the surface after fabrication (Cui & Boland, 2009)

Note that the endothelialized lining seen in this figure was not seeded after channel fabrication; instead the HUVECs were printed with the scaffold by the 3D printing apparatus. Although still a very novel technology, this example does show promise for 3D printing of vascularized tissue layers.

While promising, engineered fabrication methods suffer from a variety of drawbacks that have limited their current clinical applicability. Firstly, the flat walls and sharp corners that result from lithography and other BioMEMS techniques lead to challenges in seeding cells into the channels, as well as their ultimate adhesion, both of which can be detrimental to the formation of an intact endothelial layer (Green et al., 2009). Additionally, these sharp edges and flat walls lead to non-homogenous shear stresses, which can also affect the ultimate survival of any endothelial layer. Another challenge with direct fabrication, particularly with 2D fabrication strategies (lithography) is that the sealing between layers often proves to be challenging and the entire process is fairly slow and time consuming (Miller et al., 2012).

2.4.3 Challenges in Vascular Design

When designing a vascular network, there are a number of important parameters to keep in mind. One of the first parameters that should be considered is the size of the channels. It is important that vessels in the engineered construct have a physiologic size, such that physiological flow rates do not generate pressures that are too large or too small. A study by Skalak et al. suggests that the average capillary in skeletal muscle has a diameter of 6µm with a total length of approximately 75µm (Skalak & Schmid-Schönbein, 1986). The total arteriolar to venule length was reported to be between 0.5 mm and 1.5mm (Less, Skalak, Sevick, & Jain, 1991). Additionally, it is important to note that arterioles at a given branching level were, on average, smaller than venules at the same level, and arterioles at the lower branching levels were reported to have diameters between 200 and 250µm. Prior to fusing with capillaries, arterioles have been reported to have diameters of approximately 20µm (Marieb & Hoehn, 2013). The first order venules, closest to the capillaries, have diameters of approximately 30µm

, while the larger venules closer to the veins were measured to have diameters on the order of 650μm (Less et al., 1991).

Another important aspect of vascular design that must be considered in the design of a vascular tissue is the branching pattern, including the size and shape of the branches. One of the most frequently used vascular models is Murray's Law. Created based on the relation between the diameters of parent and daughter vessels *in vivo*, Murray's Law relates the diameters of daughter vessels with the diameters of parent vessels based on the assumption that the system operates under a least work paradigm (Emerson, Cieslicki, Gu, & Barber, 2006; Murray, 1926; Painter, Eden, & Bengtsson, 2006).

This law is often presented as:

$$\sum r_p^3 = \sum r_d^3$$

Equation 1: Murray's Law where r_p = parent radius which is the radius of the larger vessel and r_d = daughter radius, which is the radius of each subsequent branch after bifurcation.

In this form, it is clear that this law indicates that volumetric flow rates into a branch are equal to volumetric flow rates out of the branching, making an assumption of a steady-state flow (no accumulation). When vasculature is designed according to this law, it can be shown that the shear stresses on the walls of each branch are the same, which suggests a physiological reason as to the evolution of such a relation in organisms (Emerson et al., 2006; Sherman, 1981). Although Equation 1 applies only to circular channels, this design principle, with its accompanying implications, can be applied to channels of any shape; using rectangular channels, for instance, requires that the radius term in Equation 1 be replaced with the

hydraulic diameter of the square channels. These channels, in of themselves, have distinct challenges in regards to cellular seeding and flow stagnation (Miller et al., 2012).

In terms of branching geometry, significantly less quantification has been made, however, arteriolar branching patterns similar to those shown in Figure 7.

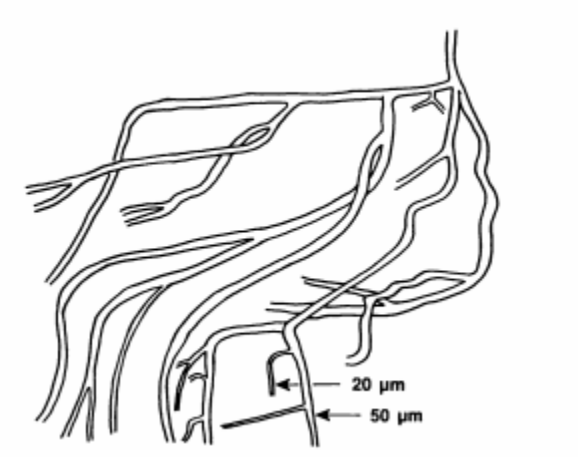

Figure 7: Arteriolar Branching Pattern. Note the long, non-interconnected channels in this pattern. From (Less et al., 1991)

Notice how the typical arterioles are long and largely not interconnected from one arteriole to another.

Yet another important parameter to consider is the flow velocity in the channel. Natural flow rate through a physiologic capillary bed was reported to be on the order of 300 µm/sec, and many groups have shown the importance of physiologic flow rates on vascular function, particularly in regards to channel endothelialization (Isenberg, Williams, & Tranquillo, 2006; Lichtenberg et al.; Marieb & Hoehn, 2013). Thus, inadequate flow velocities could have severely detrimental effects on the development of intact vasculatures, and should not be an engineering parameter which is overlooked.

2.5 SUMMARY AND NEED

Given the increasing incidence rate of heart disease worldwide, there exists a dire need for engineered vasculature as a means for regenerating ischemic cardiac tissue. Currently, an implantable, vascularized tissue scaffold does not exist and therefore, heart disease patients must eventually resort to invasive and dangerous procedures such as LVAD implantation and orthotropic heart transplants. Clinically, the access to a reliable, *in vitro* fabricated cardiac patch would prevent the need for such procedures, as well as generate a patient-specific regenerative scaffold for myocardial repair. Although a significant amount of research has already been conducted in attempt to engineer a regenerative cardiac scaffold, the creation of a vascularized construct that encourages diffusion and cell proliferation while mimicking the mechanical properties of cardiac tissue has yet to be achieved, largely due to a lack of vascularization of the engineered myocardial tissue element. The field of cardiac tissue engineering can be greatly accelerated with the development of a clinically relevant vascular construct, which can be integrated into multilayered tissue construct.

CHAPTER 3: PROJECT STRATEGY

In this section, an overview of the project strategy used towards the design of a microvascular network for implementation in a cardiac patch will be presented. The strategy of this project was based off of the engineering design process outlined in Dym & Little (2009). As such, this section will begin with an overview of the users, clients and designers, and shows the logical progression of this project transitioning from an initial client statement to the revised client statement, which incorporates objectives and constraints identified by the design team. This section closes with a summary of the overall approach of the project.

3.1 STAKEHOLDERS

According to Dym & Little, there are three parties involved in the design of any product (2009): The client, who contracts the design; the users, or the people for whom the design is intended; and the design team, who design the product for the users based on the requirements specified by the client. It is the responsibility of the design team to develop a product that satisfies the needs of both the clients and the users. In the scope of this project, the design team is the MQP team: Alyssa Bornstein, Keith Gagnon, Thomas Moutinho and Kevin Reyer. The client has been identified as the project advisor- George Pins, who came to the MQP team seeking the development of a microvascular element for his cardiac patch. Megan O'Brien and Alexander Hallet, two graduate students in Pins' lab working towards the development of a modular cardiac patch, have been identified as the users of this microvascular element. As the users, these two graduate students require a functional product from the design team that will aid them in the development of their clinically relevant cardiac patch. The relationship between the client, the users and the design team can be seen in Figure 8.

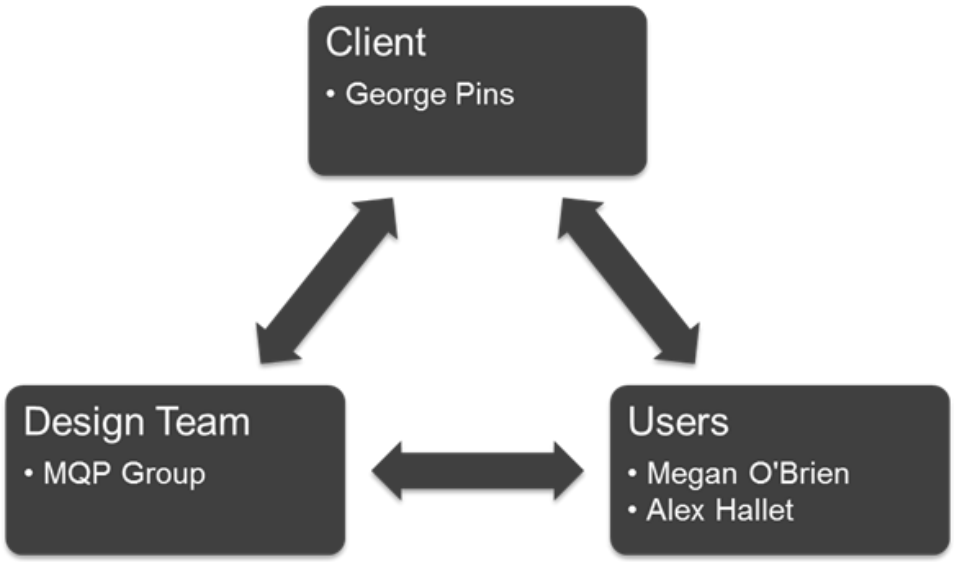

Figure 8: Summary of Clients, Designers and Users

3.2 Initial Client Statement and Clarification

The initial client statement was presented to the design team by the client, as follows:

> *Design, develop and characterize a fibrin-based scaffold with microfluidics-based vascular network that will facilitate the perfusion of a multilayered tissue construct.*

Upon inspection of this initial client statement, a number of project aspects were readily apparent to the design team. One of the first traits noted was the overall goal of creating a "microfluidics-based vascular network." The capabilities of the said vascular network were noted; it must facilitate the "perfusion of a multilayered tissue construct." This was interpreted to indicate that the vascular network must be capable of maintaining cellular viability within multiple layers of the biomaterial when perfused with medium. Other important aspects that were ascertained from this simple initial client statement included that the scaffold must be "fibrin-based" and that certain properties of the scaffold must be characterized; the two most

readily apparent and relevant properties that the team discussed were diffusion of nutrients out of the channels and the perfusion characteristics of the channels.

In order to develop a better understanding of the client statement, the design team researched the current role of vascularization and microfluidics in the field of vascular tissue engineering. Additionally, the team conducted a number of user and client interviews, as well as organized a brainstorming session with the users, in order to better determine which attributes the clients and users desired in the final product. The following list of attributes, sorted by their topic, was generated:

1. Mimics physiological vasculature
    a. Simulates native tissue stiffness
        i. Fibrin-based
        ii. Maintains high pattern fidelity
    b. Mimics physiological shear stresses
        i. Contains perfusate
        ii. Flow must be characterizable
            1. Steady state flow
            2. Pulsatile flow
    c. Incorporates natural geometries
        i. Physiological interchannel spacing
2. Capable of perfusion
    a. Allows for sufficient oxygen diffusion
    b. Allows for diffusion of small molecules
    c. Allows for diffusion of small proteins
3. Maintains cellular viability
    a. Biocompatible
        i. Sustains fibroblasts
        ii. Sustains endothelial cells
    b. Not cytotoxic
    c. Sterilizable
4. Easy to handle
    a. Maneuverable
    b. Stackable
        i. Can be bonded to other gels
    c. Capable of alignment
5. Easy to produce
    a. Reproducible
    b. Precise
    c. Low unit cost
    d. Minimal waste
6. Size
    a. 1 cm x 1 cm
    b. 200 microns thick

Once the list was created, the design team sorted the attribute list into objectives, constraints and functions. Objectives are what the product should do, constraints are limits to the design space, and functions are how an objective is achieved. These three categories are displayed below:

OBJECTIVES:

- Mimics physiological vasculature
- Simulates native tissue stiffness
- Mimics physiological shear stresses
- Steady state flow
- Incorporates natural geometries
- Capable of perfusion
- Allows for sufficient oxygen diffusion
- Allows for diffusion of small molecules
- Allows for diffusion of small proteins
- Maintains cellular viability
- Sustains fibroblasts
- Sustains endothelial cells
- Easy to handle
- Maneuverable
- Stackable
- Capable of alignment
- Easy to produce
- Reproducible
- Precise
- Low unit cost
- Minimal waste

CONSTRAINTS:

- Biocompatible
- Sterilizable
- Fibrin-based
- 3 week degradation time
- Flow must be characterizable
- Spending within MQP budget
- Completed within MQP timeframe
- 1x1 cm
- 200 µm thick

FUNCTION:

- Material harnessed high pattern fidelity
- Permits oxygen diffusion
- Encourages cell adhesion
- Contains perfusate
- Consists of physiological interchannel spacing
- Manage pulsatile flow
- Sustains

Having this list of objectives, constraints and functions, the design team was then able to further classify the objectives into sub-objective categories.

3.3 OBJECTIVES AND SUB-OBJECTIVES

In order to make all of the objectives easier to visualize and understand, they were sorted into thematic groups, in which the theme of the group was designated to be a high level objective. This hierarchical sorting can be seen in Figure 9.

One of the first high-level objectives created was to create a vascular network that mimics the physiologic architecture of a capillary bed. It was determined that this is important as physiologic perfusion rates and geometries generate biomechanical cues for endothelial cell growth and development.

A second high level objective developed was that the engineered microvascular network must be perfusable, meaning that fluid can continuously flowed through the network with discrete localization of the fluid in the channels. The perfusion of nurteint rich medium is critical for the continuous delivery of nutrients throughout the construct, allowing for the survival of cells in or on the hydrogel..

A third high level objective developed was that the construct must maintain cellular viability. The need for this objective should speak for itself, as this is the overall premise of the vascular layer. Sub-objectives identified for this high tier objective include sufficient diffusion of oxygen, small molecules (glucose, small signaling molecules, etc.) and proteins. Sufficient concentrations of all three of these must be established in order to ensure cellular survival.

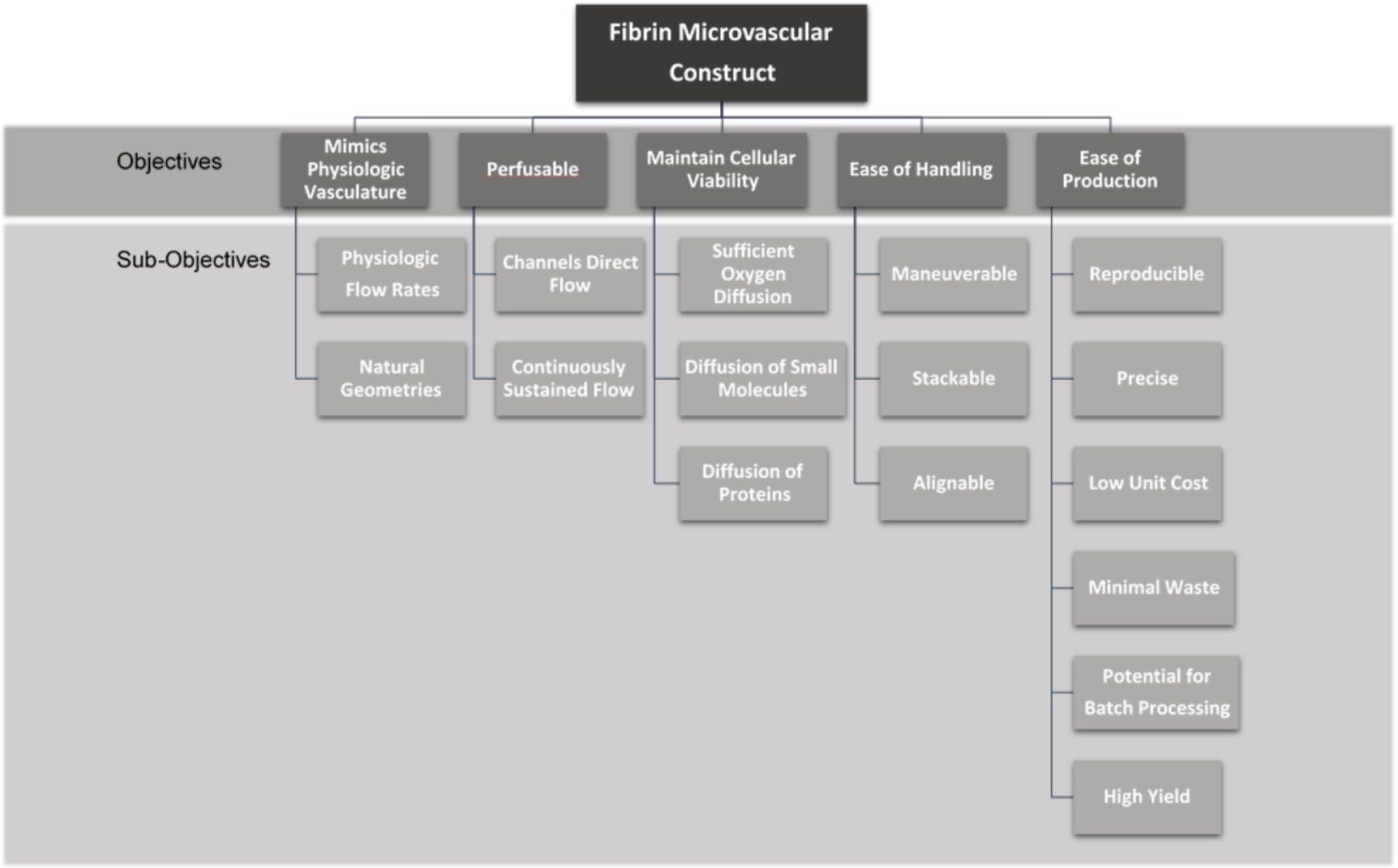

Figure 9: Objectives tree with high-level objective and sub-objectives

A fourth high-level objective created from the list of objectives was that the ultimate microvascular construct must be easy to handle, such that it can be easily added to a layer-by-layer constructed modular cardiac tissue patch with a clinically relevant thickness. Important sub-objectives in this category include maneuverable, suggesting that the construct is easy to move around; stackable, suggesting that the layers can be stacked, a necessity for layer-by-layer fabrication; and alignable, which suggests that the vascular layers can be rotated and stacked in any orientation the user would see necessary.

A fifth high-level objective created was ease of production the construct should be relatively easy to fabricate. This suggests that the fabrication method must be reproducible and precise. Additionally, the users desire a low unit cost, with minimal waste and potential for batch processing.

The success of this project depends on the completion of the five major objectives summarized about. In reference to the high-level objectives and the sub-objectives, the design team will be able to determine the progression of the project and the overall success.

3.4 Quantitative Analysis of Objectives

In order to quantitatively assess the importance of the various objectives stated above, the team created a pairwise comparison chart (PCC), an engineering tool which allows for the systematic comparison of one objective against a different objective and ultimately ranks objectives in terms of their importance. In order to complete a PCC, a PCC matrix is used, which has the objectives listed as both row and column headers. Moving across a row, if the row element is more important than the column element, a 1 is recorded in the cell corresponding

to their intersection. If the column element is more important than the row element, a 0 is recorded. If the two are equally important, a 0.5 is recorded. Ultimately, the elements across each row are tallied and reported in the right-most "Total" column. This gives the ultimate importance of each objective, with the higher scoring objectives being deemed more important.

Table 3 shows the PCC, for the high-level objectives, completed by both the design team and the user. Each of the five objective columns is further divided into two sub-columns: the left column contains the PCC results of the designer, MQP team, and the right column contains the results of the user, Megan O'Brien.

Table 3: Pairwise Comparison Chart of High-Level Project Objectives

Project Objectives	I		II		III		IV		V		Score
I.Mimics Physiologic Vasculature			0.0	0.0	0.0	0.0	0.0	0.0	0.0	0.0	0.0
II. Perfusable	1.0	1.0			0.0	0.5	1.0	1.0	1.0	1.0	6.5
III.Maintain Cellular Viability	1.0	1.0	1.0	0.5			1.0	1.0	1.0	1.0	7.5
IV.Ease of Handling	1.0	1.0	0.0	0.0	0.0	0.0			0.5	1.0	4.5
V. Ease of Production	1.0	1.0	0.0	0.0	0.0	0.0	0.5	0.0			2.5

Ranking the objectives by score, the following order was produced:

Table 4: Ranking of High Level Objectives, summing results of design team and user

Ranking	Objective
1	Maintain Cellular Viability
2	Perfusable
3	Ease of Handling
4	Ease of Production
5	Mimics Physiologic Vasculature

The most important objective of this project was determined to be that the engineered microvascular construct supports and maintains cellular viability. This is crucial, as it is the purpose of this project. The second most important objective was that the construct is perfusable, which is required for the successful maintenance of cellular viability. Ease of handling was identified to be the next most important objective; handling these devices is important in order to successfully create the modular cardiac patch construct. Ease of production was ranked fourth; as long as the product was fabricated and satisfied the first four high-level objectives, the user was not concerned with the ease of the overall fabrication process. Finally, physiologic mimicry was ranked last; neither the user nor the design team ranked the physiological relevancy of the vascular network's geometry as highly important; as long as the network was able to maintain cellular viability, the construct would be deemed successful.

3.5 Quantitative Analysis of Sub-Objectives

After quantifying each of the high level objectives, the sub-objectives were ranked. This analysis allowed the design team to quantitatively understand which sub-objectives were most important in terms of achieving the high-level objectives.

3.5.1 Physiologic Mimicry Sub-Objective

Two sub-objectives for physiologic mimicry were identified: Physiologic Flow Rates and Natural Geometries. For only two sub-objectives, no PCC was needed, as it is a fairly binary decision. It was ultimately decided that achieving physiologic flow rates was more important than fabricating a network with natural geometries, as natural flow rates would induce physiologically relevant shear stresses, an important characteristic for vessel endothelialization.

3.5.2 Perfusable Sub-Objectives

Two sub-objectives were identified for the "perfusable" high level sub objective: (i) the channels should direct flow and (ii) the channels should be continuously perfusable. The first sub-objective describes the ability of the channels to contain flow. Without this ability, any perfusate would disperse itself throughout the gel. This removes the need for channels and would slow the ultimate perfusion of the patch, ultimately relying on diffusion of nutrients through the gel. The second sub-objective can be described as the ability for continuous replenishment of new medium and exit of nutrient depleted medium. After much discussion, it was determined that these two objectives were equally important, as a deficiency in either would defeat the purpose of the patch.

3.5.3 Maintain Cellular Viability Sub-Objectives

Three sub-objectives were identified under the ”maintain cellular viability” objective. The first sub-objective is that the network provides sufficient oxygen diffusion for cellular growth, proliferation and viability. The second sub-objective is that the network is capable of providing sufficient diffusion of small molecules (<1000 Da, i.e. small molecule growth factors, chemokines, cytokines, etc.) from the channels to the cells. The final sub-objective is that the microvascular layer is capable of supplying cells with a high enough supply of vital proteins for cellular function. As multiple sub-objectives were identified for this high-level objective, the completion of a PCC was necessary. The rating of each of these sub-objectives is seen below, in Table 5.

Table 5: Pairwise Comparison Chart of Sub-Objective "Maintains Cellular Viability".

III. Maintain Cellular Viability	A	B	C	Score
A. Sufficient Oxygen Diffusion (m.w. = 32 Da)		0.5	0.5	1.0
B. Diffusion of Small Molecules(m.w. <1000 Da)	0.5		0.5	1.0
C. Diffusion of Proteins	0.5	0.5		1.0

Based on the results of this PCC, it is clear that all three nutrients are important to maintaining viability. Without all three categories of molecules being delivered to the cells, viability will be greatly hindered. Oxygen will need to be present as quickly as possible to cells in order to maintain viability, however it cannot be over-valued compared to larger nutrients and proteins.

3.5.4 Ease of Handling Sub-Objective

Three sub-objectives were identified under the “ease of handling” objective. These were maneuverable, stackable and alignable. In order to satisfy the maneuverable sub-objective, it

is necessary that the microvascular construct is capable of being moved around readily, whether in solution or out of solution. The stackable objective indicates that these layers needed to be able to stack one atop the next, generating a series of sealed layers. The third sub-objective, which states that the constructs should be alignable, indicates that the directionality of the constructs' vasculature should be evident and that they should be easily rotated and manipulated, allowing manual alignment of the individual layers and corresponding vasculature in any direction needed. The quantitative analysis of these three objectives can be seen in Table 6.

Table 6: Pairwise Comparison Chart of Sub-Objective "Ease of Handling".

IV. Ease of Handling	A	B	C	Score
A. Maneuverable		1.0	1.0	2.0
B. Stackable	0.0		1.0	1.0
C. Alignable	0.0	0.0		0.0

Based on the results of this PCC, it is clear that maneuverable was deemed most important, followed by stackable. Alignable was designated to be the least important of the three objectives.

3.5.5 Ease of Production Sub-Objective

The last high-level objective, ease of production, had five sub-objectives. The first sub-objective, reproducible, indicated that the production method of the final design must generate the same series of channels each time it is used. The next sub-objective, precise, indicates that the production method needed to be capable of generating channels with dimensions of similar size to those of the mold pattern used to template the channels. The third

sub-objective, low unit cost, indicates that the constructs must ultimately be inexpensive to produce. Another sub-objective, minimal waste, denotes to limiting the overall waste of resources (fibrin, thrombin, etc.) used during the fabrication process. The final sub-objective under this high level objective was the potential for batch processing, indicating that the production method was capable of being readily expanded such that multiple constructs could be created within a short time span.

In order to quantify the overall importance of these sub-objectives, a pairwise comparison chart was used. This chart can be seen in Table 7.

Table 7: Pairwise Comparison Chart of Sub-Objective "Ease of Production".

V. Ease of Production	A	B	C	D	E	Score
A. Reproducible		1.0	1.0	1.0	1.0	4.0
B. Precise	0.0		1.0	1.0	1.0	3.0
C. Low Unit Cost	0.0	0.0		0.0	0.0	0.0
D. Minimal Waste	0.0	0.0	1.0		0.0	1.0
E. Potential for Batch Processing	0.0	0.0	1.0	1.0		2.0

Note that reproducibility and precision were rated to be the most important sub-objectives, while minimal cost and low waste were deemed to be fairly unimportant.

3.6 CONSTRAINTS

Information from the initial client statement, as well as the list of attributes brainstormed with the users (presented in section 3.2), was used to formulate a list of constraints of the project. One important constraint of this project is that the scaffold must ultimately be biocompatible; nothing that will (directly or indirectly) hinder cellular survival can

be used in the construction of the microvascular layer. Another constraint of the product is that it must be sterilizable, such that these constructs can be made in a sterile fashion.

Additionally, according to the client and user, the construct must be fabricated from a fibrin-based material and must have a degradation time of three weeks or greater. Additional constraints arose from the official guidelines of the MQP- the project had to be completed within the four-term limit and the total cost of the project had to be less than $624.

3.7 REVISED CLIENT STATEMENT

After extensive communications with the user and designer, as well as a quantitative analysis of the objectives and sub-objectives, the design team was able to revise the client statement to the following:

> *Design and develop a 1x1 cm, 200μm thick, fibrin-based scaffold which contains a physiologically relevant, microfluidics-based, branched vascular network to support cellular growth and proliferation in a multilayered cardiac tissue construct. The scaffold will contain and promote the survival of endothelial cells and myocytes in a luminal or bulk gel fashion, or if cultured on the surface of the network. Additionally, the network will permit the diffusion of nutrients, small molecules and oxygen from the perfusate to the surrounding tissue. The construct must be perfusable, manufacturable and maneuverable and last up to three weeks in an in vivo environment.*

This revised client statement clearly states the end goal of the project: a branched microvascular network capable of supporting cells. Additionally, it incorporates a number of

the important high level objectives and project constraints. This statement guided the team's design process over the course of the year.

3.8 Project Approach

In order to appropriately structure the project, the team organized the design strategy into a series of manageable milestones. The first milestone to be completed was validation that micropatterning of fibrin was possible. Once this was completed, the team had to show that the channels localized flow; if this was not the case, the channels would serve no purpose, as all perfusate would simply pass into the gel immediately. After showing the localization ability of the channels, the team developed an optimal microfluidic architecture, seeking to maximize flow uniformity and minimize fluid dead-spaces. Once the optimization of microfluidic architecture was completed, the team sought to generate successful continuous perfusion of the channels. The final stage of the design process was cellular validation of the microvascular system. This schematic is summarized in Figure 10.

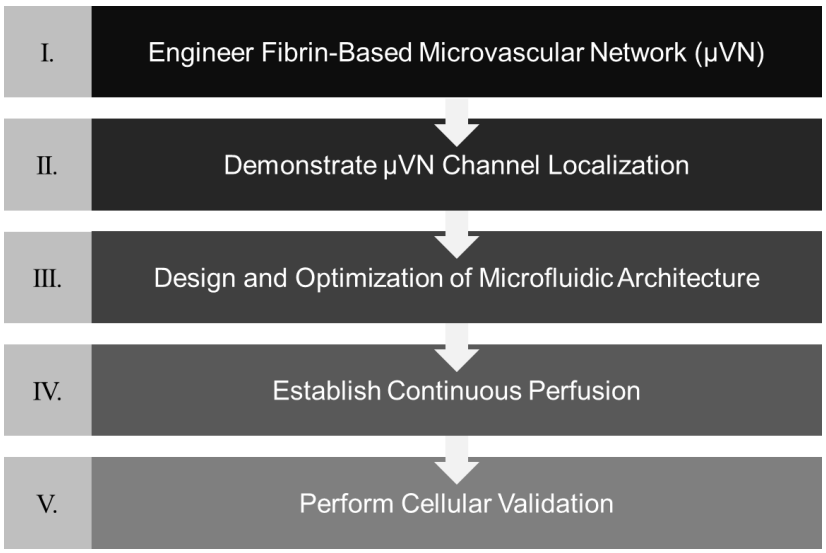

Figure 10: Schematic of Project Strategy

In order to quantify the success of each of these steps, milestones were created along with specifications shown in Table 8. These milestones served to further segment each of the important steps listed above; once all of the milestones for a given phase were completed, the phase could be considered to be complete. A table presenting the milestones for each step of the project, along with their desired value and method of evaluation can be found in Table 8.

Table 8: Milestones of Project. Note that LM is light microscopy, FM is fluorescence microscopy, CLSM is confocal laser scanning microscopy, CFD is computation fluid dynamics, PIV is particle image velocimetry, CFDA/PI is carboxygluorrescein diacetate succinimidyl ester/propidium iodide,, MTT is 3-(4,5-dimethylthiazol-2-ly)-2,5-diphenyltetrazolium and vWBF is von Willebrand Factor

Step	*Criterion*	*Desired Value*	*Evaluation*
Pattern Fibrin	Successful Patterning	Width = 100μm	LM
	High Pattern Fidelity	± 10% Mold	LM
	Reproducible Results	± 10% between gels	LM
	Thin Gels	≤300μm	
Demonstrate Channel Localization	Microparticle Loading	Observed	LM
	Microparticle Localization	Observed	LM
	Multilayer Loading	Observed	LM
	Multilayer Localization	Observed	LM
Design and Optimization of Microfluidic Architecture	Minimization of "Dead Spaces"	Qualitative	CFD
	Minimal Pressure Drop in Branching	Qualitative	CFD
Successful Continuous Perfusion	Perfusable at physiologic flow rates	300μm/sec *	LM, PIV
	Laminar, deterministic flow		LM, PIV
Cellular Validation	Cardiomyocytes survive on top surface	>80%	CFDA/PI, MTT
	Cardiomyocytes survive in bulk of gel	>80%	CFDA/PI, MTT
	Cardiomyocytes survive on fibrin microthread alignment layer	>80%	CFDA/PI, MTT
	Endothelializtion of Lumen	Confluent layer	vWBF

*Note that this value was obtained from (Marieb & Hoehn, 2013)

The completion of these milestones, specifically the criteria listed above, was vital in order to accomplish each step of the project, and ultimately to engineer a vascular tissue construct. By segmenting the project into sections, each with important, quantitative milestones, a logical outline to the project was created.

CHAPTER 4: ALTERNATIVE DESIGNS

After the design analysis, the team had a fundamental conceptual idea of the project. Based on the initial client statement, which mentioned "microfluidics", the design team focused on a photolithographic approach for the fabrication of the channels, as this is fairly common in microfluidics research, however, other options were still considered. Additionally, based off of preliminary concept art, the team visualized a final network design that appeared similar that seen in the schematic of the proposed patch, shown in Figure 11.

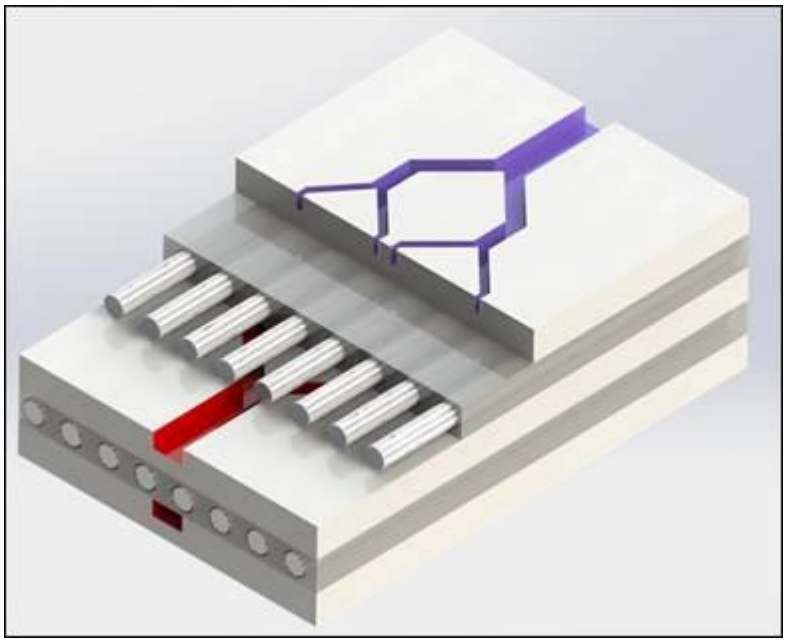

Figure 11: Proposed Patch Architecture. Note that the vascular tree is a simple branching network.

This conceptual design was then conferred onto the five step project strategy, previously described, in order to logically progress towards the creation of a continuously perfused thin-film hydrogel vasculature.

Once the general project strategy had been formulated, the design process was begun. Four of the five steps in general project schematic, seen in Figure 10, require engineering. For Step 1: Pattern

Fibrin Scaffold, the team determined that a mechanism of successfully generating channels needs to be created. Step 2: Demonstrate Channel Localization, required the design of a process for creating multi-layered constructs by confirming that the channels could serve as boundary for the containment of perfusate. Step 3: Design and Optimization of Microfluidic Architecture, required the design of a microfluidic microvascular network and the ultimate optimization of the design to achieve uniformity of flow with minimized low flow zones (or reduced wasted space within the network). The second to last major design project occurred in Step 4: Successful Continuous Perfusion, which required the creation of a method or device that would allow for the successful continuous perfusion of the channels. The last major design milestone is Step 5: Conduct Cellular Viability studies. This milestone will ultimately determine diffusion of nutrients through fibrin gel from a perfused channel can proved cells with enough nutrition for survival.

For each of these design components, the team held a brainstorming session, in which they analyzed the functions of each design and hypothesized ways in which that function could be achieved. The remainder of this chapter details the multiple design alternatives for the different design aspects of the project and the ultimate evaluation of each design alternative.

4.1 Channel Fabrication

One of the first design challenges that needed to be addressed was the creation of discrete channels that could be perfused. As stipulated by the objectives and constraints identified previously, the mechanism of channel creation needed to generate reproducible channels with appropriate biomimetic geometries while also facilitating easy maneuvering and stacking of the gels.

Another important aspect of the channel fabrication step was identifying a means of holding and securing these gels. The client requested a convenient means of manipulating and moving the constructs around, such that they could be aligned and stacked, ultimately enabling construction of the cardiac patch.

In order to create a list of as many different means of fabricating channels as possible, the team held a brainstorming session, in which different ideas for fabricating channels were proposed. The results of this session are summarized in the function-means diagram show in Table 9.

Table 9: Channel Fabrication Function-Means

Function	Means					
Channel Creation	PDMS Mold	Sacrificial Layer	Pressure Stamping	Decellularized Scaffold	Injection Molded	3D Printing
Hold gel	PDMS Ring	Vellum Film Ring	Coverslip	3D Printed Frame		

While many of these means are self-explanatory, they are all explained below. The first six ideas pertain to methods of fabricating micro-patterned gels, while the subsequent four pertain to methods to move the fabricated gel.

4.1.1 PDMS Contact Casting

One idea that the team brainstormed to create channels in the fibrin hydrogel was PDMS contact casting, a strategy in which fibrin would be cast over a PDMS negative mold, thus generating channels in the fibrin gel once removed from the PDMS. This patterned hydrogel would then be stacked atop a flat fibrin gel to create closed channels, as can be seen in Figure 12.

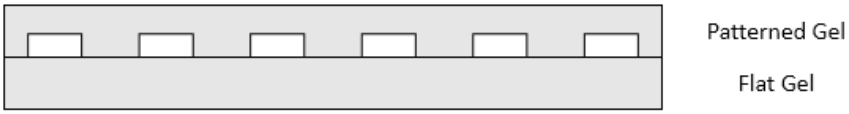

Figure 12: PDMS Contact Casting Channel Creation. Notice how the patterned gel, created via contact casting, is placed atop a flat gel, thus closing the channels to the environment

Expected pros and cons of this method can be seen in Table 10.

Table 10: Pros and Cons of PDMS Contact Printing

Pros	Cons
• Ease of creating gel • High pattern fidelity • High volume output potential	• Must pre-treat mold for easy removal • Creating patterns requires expensive step of photolithography • Sealing of fibrin gels can be difficult

4.1.2 Sacrificial Layer

Production of a fibrin gel via a sacrificial layer consists of fabricating a fibrin gel around a sacrificial material, similar to the procedure performed by Golden et al. (2007). The sacrificial layer would consist of gelatin, agar or another material which would behave as a gel at lower temperatures (where the fibrin could be molded around it), but could be dissolved away at higher temperatures, leaving a void where the sacrificial layer once was. It was expected that these voids would form perfusable channels. Pros and cons of using a sacrificial layer can be seen in Table 11.

Table 11: Pros and Cons of Sacrificial Layer

Pros	Cons
• High pattern fidelity • Eliminates need to seal gels to enclose patterned channels • Sacrificial layers can be patterned in various geometries	• Difficult to produce • Residue of sacrificial layer • Time required to sacrifice layer before perfusion can be performed • Mounting of the sacrificial layer such that it is totally embedded in the gel could be difficult.

4.1.3 Pressure Stamping

Another idea considered for channel creation was pressure stamping. Pressure stamping would involve imprinting the gel with channels via compression or removal of material in a flat, previously cast gel. The tool used for this technique would consist of an apparatus capable of stamping the mold pattern into the gel. Pros and cons of using pressure stamping can be seen in Table 12.

Table 12: Pros and Cons of Pressure Stamping

Pros	Cons
• Simple processing • Cheap • Potential for rapid production	• Unknown precision • Questionable channel retention • Error would be inconsistent from gel to gel • Force required for imprinting might destroy gel • Relatively little literature on stamping cast hydrogels with patterns.

4.1.4 Decellularized Vascular Scaffold

This channel creation strategy would involve the creation of a fibrin gel around a decellularized vascular bed from an organism. Pros and cons of using a decellularized scaffold can be seen in Table 13.

Table 13: Pros and Cons of Decellularized Vasculature

Pros	Cons
• Design is optimized due to natural development • Casting fibrin around decellularized material will be easy • Vasculature on physiologic size scale	• Must have donor source • Immunogenic concerns, if decellularization does not remove all traces of donor organism • Not consistent pattern • Decellularization can use harsh chemicals which can affect fibrin gel

One immediate concern of the team with this fabrication method was the availability of donor vasculature to be decellularized. While an idea to decellularize a leaf was transiently considered, nothing ultimately became of the idea, due to concerns over the large amount of cellulose, a structural carbohydrate not found in humans, in leaf vasculature.

4.1.5 Injection Molding

The team considered a strategy of injection molding to create channels in fibrin. For this strategy, two halves of a PDMS mold, one side being flat and the other containing a channel template, would be assembled and fibrin would be injected into the void. While similar to the PDMS contact casting, this method would allow for the creation of gels with a specific thickness. A sample set-up can be seen in Figure 13.

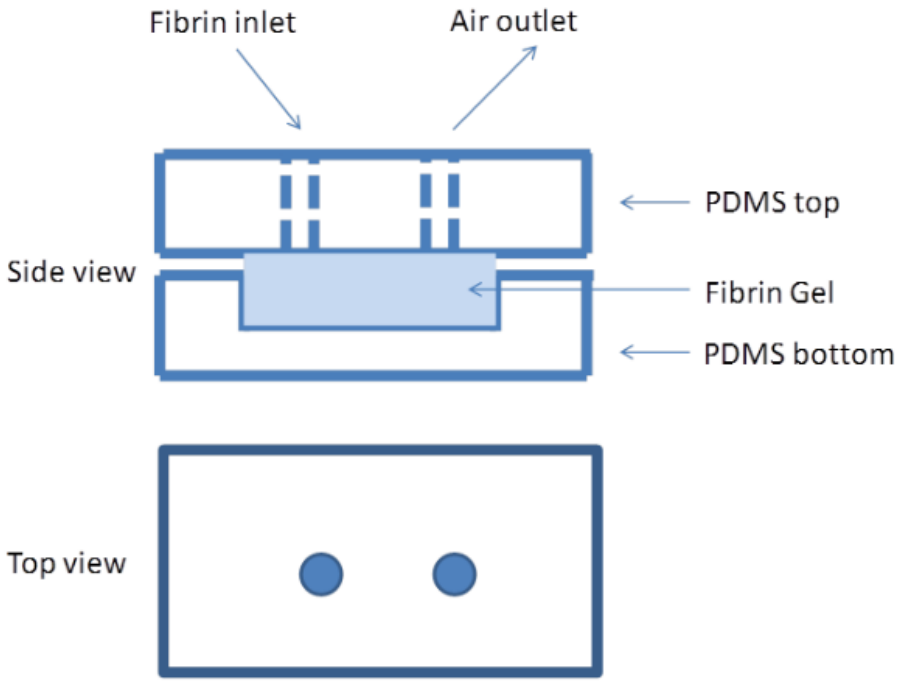

Figure 13: Injection molding sketch

The team generated a list of pros and cons for the injection molding technique, which are summarized in Table 14.

Table 14: Pros and Cons of Injection Molding

Pros	Cons
• Creates a gel of very specific thickness • Simple production due to ease of injecting fibrin solution into an inlet • High pattern fidelity	• Leakage at interface of two halves if not adequately sealed • Fibrin may stick to the PDMS, causing gel damage upon removal • Requires precise stacking of PDMS molds

4.1.6 3D Printing

Another design alternative proposed by the team was a layer-by-layer 3D printing mechanism for generating channels in fibrin. This printer would lay down thin layers of fibrin in a bath of HEPES buffer. After each layer clotted, a new layer would be printed atop the clotted layer, stacking layers to form complex internal architectures, such as channels. Pros and cons of using a 3D printer can be seen in Table 15.

Table 15: Pros and cons of 3D printing

Pros	Cons
• Ability to customize geometry • Potential to incorporate cells into gel during printing • High degree of precision	• Very expensive start-up costs; a machine would need to be designed. • Gel would need to set quickly, requiring large amounts of cross-linking, thus limiting diffusion potential • Printing error could block channels

4.1.7 PDMS Well

PDMS is a very versatile polymeric material that is biocompatible and easily formed into a variety of shapes (2012; Crapo, Gilbert, & Badylak, 2011). Due to these two important properties, the team proposed the creation of a well for holding and manipulating the gel. Once patterned, the hydrogel could be securely placed in this well and moved to wherever it was needed. Preliminary tests suggested that fibrin would adhere to PDMS securely when in air, but would readily detach once submerged. It was proposed that a PDMS well would provide a secure means of moving and manipulating cast fibrin gels. Pros and cons of using PDMS as a vessel for holding fibrin gels can be seen in

Table 16.

Table 16: Pros and Cons for using a PDMS ring

Pros	Cons
• Able to image through (if thin) • Fibrin sticks moderately well to PDMS • Easily maneuverable	• Need to submerge in water to remove fibrin

4.1.8 Vellum Film Ring

Vellum film is a specific paper advertised for use by artists as tracing paper. It is made from plasticized cotton, has a higher stiffness than normal paper and is slightly translucent. After discussions with Meg, a user of the product, the team learned that the client, Meg, fabricates gels, loaded with aligned fibrin threads, by casting fibrin in a vellum film ring on a Dacron slide (Figure 14). Other materials for the structural ring were not considered in order to maintain a consistent fabrication method with the client. The team considered this idea as method for the fabrication of microfluidic gels, as it provides a lightweight, durable structure which can hold fibrin gels independently. Pros and cons of using vellum film as a means to hold fibrin gels can be seen in Table 17.

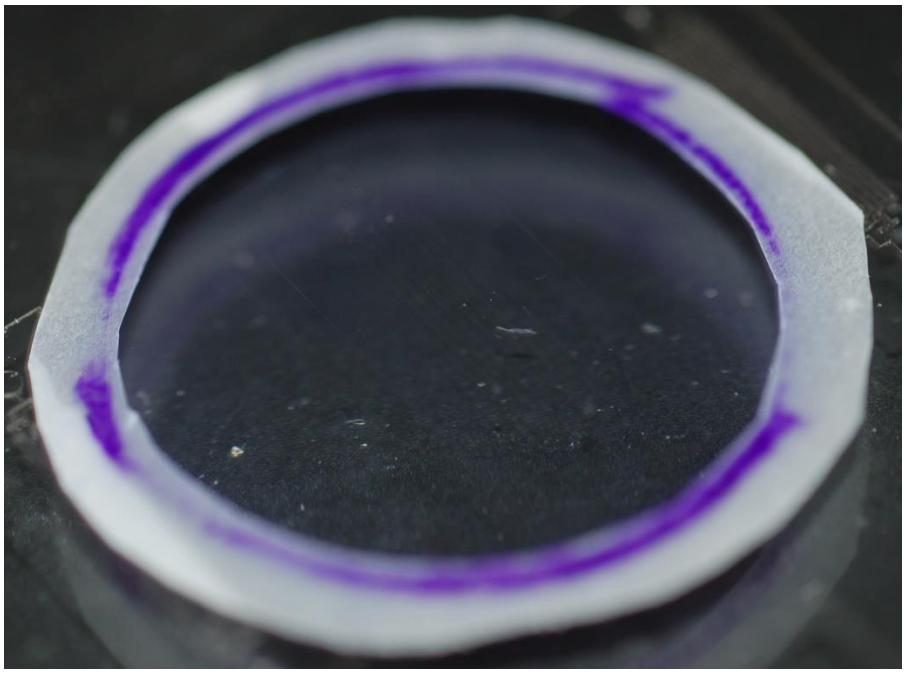

Figure 14: Example vellum ring for holding thin fibrin layer

Table 17: Pros and cons of using a vellum ring

Pros	Cons
• Easily maneuverable • Robust frame • Fibrin sticks well to vellum paper • Creates thin gels • Compatible with existing system	• Unknown cytotoxicity • Unknown sterilization technique

4.1.9 Cover Slip

Another idea contemplated by the team was the use of a coverslip as a bottom foundation layer to the fibrin gels. If the fibrin was placed on top of a mold, a cover slip could be placed over the solution, effectively trapping the fibrin between the mold and the coverslip. This method was developed by a team member and had been previously show to generate patterned gels with moderate reliability (approximately 80% success). The pros and cons of using the cover slip can be seen in Table 18.

Table 18: Pros and Cons of using a cover slip

Pros	Cons
• Clear to allow imaging • Easy maneuverability and compatibility with imaging on most microscopes	• Removal from the coverslip (if needed) is difficult • Coverslip is fragile, dropping can fracture the coverslip and destroy the gel

4.1.10 3D Printed Frame

A 3D printed frame for the hydrogel could satisfy several of the design requirements, including providing a mechanism to support an inlet/outlet port, such that the frame could also be used as a bioreactor. However, these parts often have optical properties incompatible with imaging and questionable biocompatibility. A further pro/con summary can be seen in Table 19.

Table 19: Pros and Cons of 3D Printed Frame

Pros	Cons
• Highly Customizable • Outlet and inlet anchors • Strong material allows for robust frame and enhanced maneuverability	• Cheap materials may not be biocompatible • Inadequate optical properties for imaging • 3D printing dimensions on the microfluidic level may be difficult or cost prohibitive

4.2 DESIGN OF A MULTI-LAYER CONSTRUCT

The second phase of this project involved demonstrating the boundary function of the channels. A large number of channel fabrication methods (except for the sacrificial layer and decellularized vasculature) generate channels that are open to the environment. In order to demonstrate channel localization, it is important to seal one of these patterned gels to a flat gel, such that the fluid cannot simply travel along the interface between gels. For this reason, it was important to consider mechanisms for bonding one gel layer to the next. Additionally, it was determined that the client would ultimately need a method of bonding multiple thin layers of hydrogels in order to create

a functional tissue construct with muscle and engineered vasculature components. To accomplish gel -gel adhesion, the team identified and brainstormed various methods to induce adhesion between fibrin hydrogels. These ideas are summarized in the function-means table presented in Table 20.

Table 20: Multi-Layer Sealing Function-Means Table

Function	Means								
Gel/Gel Adhesion	Surface Tension	$CaCl_2$	Thrombin Only	$CaCl_2$ & Thrombin	Fibrinogen Glue	Fibrin Glue	Differential Sealing	UV Crosslinking	EDC Crosslinking

Each of the proposed methods above is explained in more detail in the following sections.

4.2.1 Surface Tension

The first proposed method of gel sealing involved the use of the cohesive properties of water to hold the gels together. Previous work in the lab has shown surface tension capable of holding two gels together sufficiently such that fluids cannot pass between them (Gagnon, and Pins, unpublished data). While not a robust method of sealing gels, due to its known efficacy, it was considered. A list of pros and cons for this method can be found in Table 21.

Table 21: Pros and Cons of Hydrated Stacking

Pros	Cons
• Maintains channel geometry • Ease of production • No additional "glue" needed • Proven to work	• Weak bonding • Unreliable adhesion strength of layers • Unreliable distinct loading of channels

4.2.2 $CaCl_2$ Bonding

Another method considered for sealing gel layers to one another involved the use of calcium chloride. Calcium chloride is one component used in producing fibrin gels, as the divalent calcium ions activate thrombin, allowing it to cleave fibrinogen and initiating the polymerization reaction (Ahmed, Dare, & Hincke, 2008)(Ahmed, Dare, & Hincke, 2008)(Ahmed, Dare, & Hincke, 2008)(Ahmed, Dare, &

Hincke, 2008)(Ahmed, Dare, & Hincke, 2008)(Ahmed, Dare, & Hincke, 2008). This method operates under the assumption that application of calcium ions would activate any residual thrombin in the gels. This activated thrombin would then cleave any entrapped fibrinogen at the surface, potentially crosslinking the layer together. Pros and cons of this approach can be found in Table 22.

Table 22: Pros and Cons of Calcium Chloride Solution Bath

Pros	Cons
• Maintains channel geometry • Enhances attachment of gels over simple stacking • Easy application	• Unknown adhesion strength • Creates potential liquid barrier

4.2.3 Thrombin

Similar to sealing with calcium chloride, the team also considered application of thrombin to seal the gels. It was hypothesized that supplemental thrombin could be activated by residual $CaCl_2$ in the gel and again cleave residual fibrinogen, sealing the two layers together. Pros and cons of the approach can be found in Table 23.

Table 23: Pros and Cons of Thrombin Coating

Pros	Cons
• Maintains channel geometry • Enhanced gel sealing vs. surface tension • Easy application	• Unknown bond strength • Variable availability of non-polymerized fibrinogen • Potential liquid barrier could prevent flow

4.2.4 $CaCl_2$ and Thrombin

The application of a combination of calcium chloride and thrombin would remove the dependence on residual $CaCl_2$ and thrombin. The procedure would be the same as described in the two sections above, but the combination of these two materials guarantees the presence of activated

thrombin between the two layers, which should enhance layer to layer linkage. Pros and cons for this approach can be found in Table 24

Table 24: Pros and Cons of Calcium Chloride + Thrombin Coating

Pros	Cons
• Maintains channel geometry • Enhanced gel sealing compared to each material individually • Easy application	• Requires use of additional thrombin and calcium chloride • Weak bonding • Less cost effective

4.2.5 Fibrinogen

Similar to the calcium chloride and thrombin strategies posed above, the fibrinogen glue strategy would be applied to the face of one gel prior to application of a second gel. Preliminary studies by Meg demonstrated that application of small volumes of fibrinogen to the surface of the constructs could effectively seal one layer to the next. It is hypothesized that the fibrinogen would be cleaved by residual activated thrombin and polymerize into both of the layers, effectively sealing them together. While promising for flat gels, the team was concerned that the fibrinogen, which form the bulk material of the gel, might fill in the channels that were trying to be sealed. A further pro and con analysis can be seen in Table 25.

Table 25: Pros and Cons of Fibrinogen Glue

Pros	Cons
• Maintains channel geometry • Increased maneuverability • Potentially stronger seal between layers	• Not uniform bonding • Large scale use could become expensive • Potential for channel blockage

4.2.6 Fibrin Glue

Yet another iteration of the intrinsic fibrin crosslinks (exploiting fibrin polymerization reactions to seal the layers) outlined above involves the use of a fibrin glue weld to seal the layers. The fibrin

glue welding technique consists of stacking molded fibrin gels and then pipetting a combination of activated thrombin and fibrinogen around the edges of the gel. Theoretically, this should "glue" the gels together and form a sealed stack of gels. The outside "weld" as opposed to the direct surface treatment, as described in the above methods, was preferred, since the fibrin might fill in the channels of the gel were it is applied directly to the face of the microvascular layer. Pros and cons for this means of sealing stacked layers can be found in Table 26.

Table 26: Pros and Cons of Fibrin Glue Weld

Pros	Cons
• Maintains channel geometry • Increased maneuverability • Potentially stronger seal between layers	• Not uniform bonding • Large scale use could become expensive • Potential for channel blockage

4.2.7 Differential Casting

Another method of sealing distinct layers together that was contemplated was known as differential sealing. This method required the creation of one gel, followed by the casting of another. After a certain amount of time, the first gel would be applied to the second (casting) gel. It was assumed that the polymerizing gel would then permanently bind to the gel atop of it, effectively sealing the two layers. The major concern of this fabrication method was that, due to the slightly viscous nature of the polymerizing layer, the channels of the cast layer could be filled as the casting gel finishes casting. If an appropriate procedure could be created such that the casting gel has polymerized enough to not fill in the channel but still has fibrinogen that is available to bond with the second layer, then this method could create a 'single' gel that has sealed channels throughout. The anticipated pros and cons of this method can be seen in

Table 27.

Table 27: Pros and Cons of Differential Casting

Pros	Cons
• Maintains channel geometry • Increased bond strength • Allows for cell to be cast with gels	• Potential filling of channels • Cast time of fibrin is not exact • Manufacturing is more difficult and takes more time

4.2.8 UV Crosslinking

Ultraviolet light has been used to crosslink fibrin and increase material stiffness in fibrin microthreads (Cornwell & Pins, 2007). The team determined that this method might be able bond to two gels together by placing the gels in contact with each other and applying a UV light to induce crosslinking between the layers.

Table 28: Pros and Cons of UV Crosslinking

Pros	Cons
• Maintains channel geometry • Potentially sealed channels • Simple process that requires only one round of casting fibrin	• May result in sub-optimal material properties for cellular integration • May not create complete sealing of channels • Does not allow cells to be cast in gels

4.3 Design And Optimization of Microfluidic Network

In the third phase of this project, the design and optimization of a microfluidic network was attempted. Though the preliminary design of these architectures started at the beginning of the project (coinciding with Step 1), and an initial wafer was printed early on, it wasn't until after the channel boundary function (Step 2) was verified that this geometry was optimized.

The most fundamental function of this design component is the delivery of perfusate throughout the hydrogel. The most optimized model of a vascular network is a natural capillary bed. The design team used Figure 15 as motivation for the design of a microfluidic network.

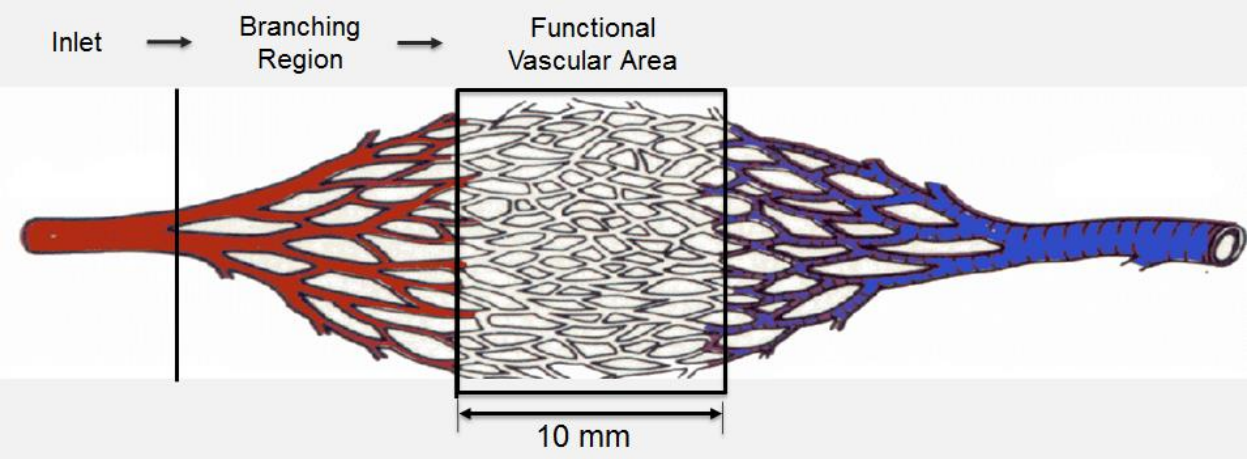

Figure 15: Capillary schematic used as design inspiration for microfluidics designed networks

In terms of the microvascular design, a number of different ideas for channel architectures were brainstormed. Ultimately, the team identified three regions of the microvascular network, each of which could be independently designed. These three regions included the loading regions, the branching region and the functional vascular area. As the names suggest, the loading region is the area in which the flow is initiated and driven, while the branching regions are the regions of microvascular that serve to divide a single flow into multiple discrete flows. The final region, the functional vascular area (FVA), is the area of the patch in which the network will serve as a surrogate capillary bed; the other two regions of the patch serve only as a source of flow and a means of flow division. A schematic of the relationship between these three regions can be seen in Figure 16.

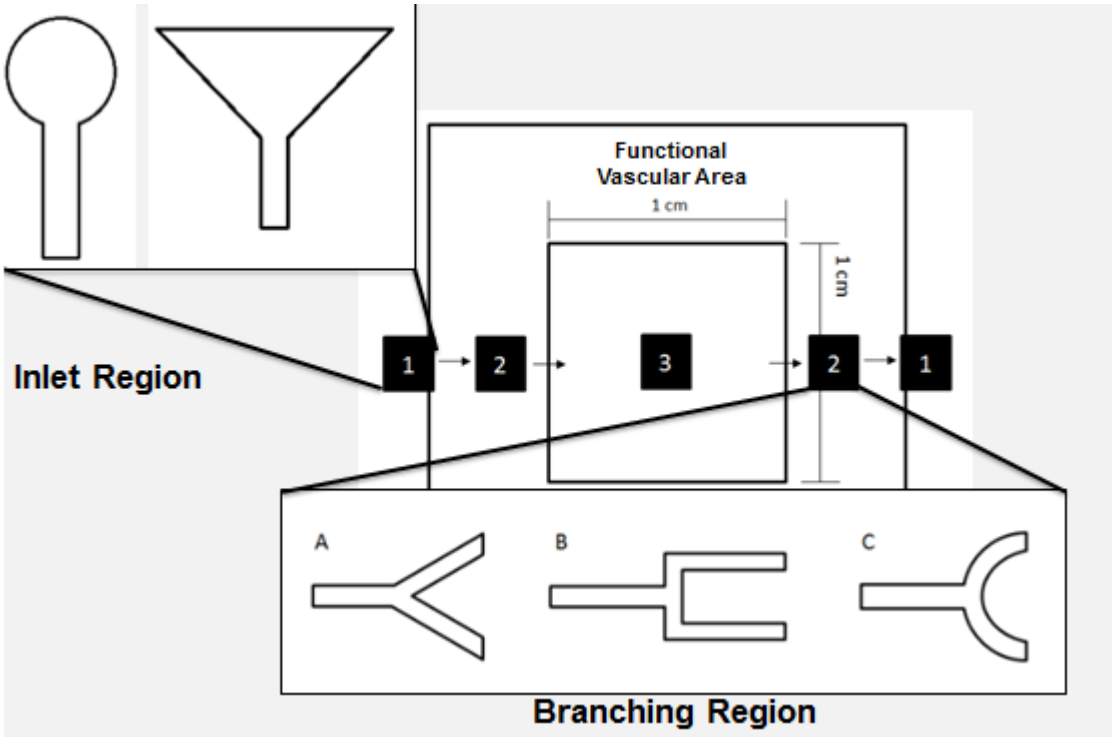

Figure 16: Schematic of the Three Regions of Microvascular Design. (1) Loading region, (2) branching region, (3) functional vascular area

As is suggested in this diagram, the flow enters the network through the loading region, before being split into the FVA by the branching region. After passing through the FVA, the flow is consolidated into a single outlet stream by the branching region, before being removed by the exit region, which is identical to the inlet region. Another noteworthy feature of this schematic is the size of the FVA; after discussion with the client and users, the team decided that the FVA should fulfill the 1x1cm criterion. Different design options for the design of each of these three regions are outlined below. Note that while flow progresses from the loading region to the branching region to the functional vascular region, the designs will be presented as loading region designs, followed by functional vascular area designs, followed by branching region designs. The rationale for this order is that not all of the FVAs considered require branching areas.

4.3.1 Loading Region

The loading region is the region of the network in which flow is directed into and out of the network. During brainstorming, two ideas for the loading region were brainstormed, a circular inlet and a fan inlet.

Circular Inlet

After a discussion with members of the Albrecht lab, Laura Aurilio and Dr. Dirk Albrecht, who use microfluidics extensively in their research which involves the development of an interdisciplinary set of skills in microfabrication, a 1mm circular inlet, similar to that seen in Figure 17 was proposed for the loading region of the network.

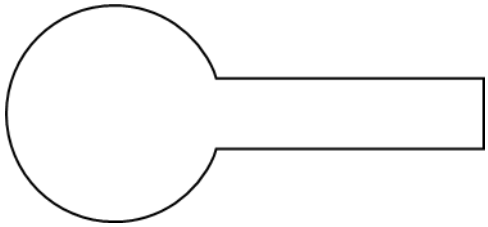

Figure 17: 1mm Circular Inlet

The Albrecht lab uses this inlet by first punching a 1mm hole in the substrate with a biopsy punch, at which point they connect PE-50 to a 23G needle stub and insert the needle stub into the hole. The pros and cons of applying this inlet to the fibrin-based microfluidic network is shown in Table 29.

Table 29: Top Loading Pros/Cons List

Pros	Cons
• Ideal for loading through the top • Small footprint	• Relies on a friction fit to prevent backflow • Small margin of error when cannulating

A second design alternative that was considered was a fan-shaped loading region. This pattern, similar to the schematic shown in Figure 18 consists of a triangular "fan" shape imprinted into the gel. It would have a wide edge near the edge of the gel and would funnel the flow into the channel at the start of the branching region.

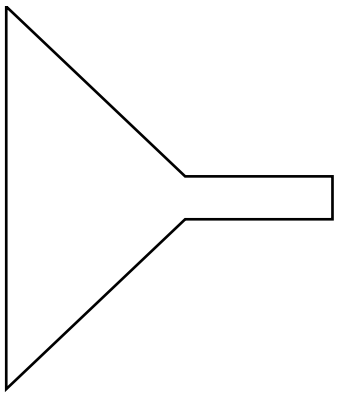

Figure 18: Fan-Shaped Loading Pattern

An analysis of the pros and cons of this loading mechanism can be seen in Table 30.

Table 30: Fan Shaped Loading Region Pros and Cons

Pros	Cons
• Ideal for loading through the side • Large margin of error • Should be able to cannulate with a variety of tips/needles, etc.	• Large footprint • Aspect ratio is a concern • Controlling backflow is a foreseeable issue

One immediate concern that the design team has was the aspect ratio of this feature. In many places, the width would be significantly larger than the height, which could lead to the top layer of the material dipping due to its own weight.

4.3.2 Functional Vascular Area

The FVA of the patch is the area in which sufficient nutrient supply was designed to occur. Unlike the loading region and branching region, the purpose of which is flow initiation and branching, respectively, the FVA is designed to act as an artificial capillary bed, having channels of sufficient size and density such that every region of the FVA is within 200 microns of a channel. After brainstorming, a number of different FVA's were considered. A large number of similar schematics were created; however, this discussion will focus only on the four simplest, most feasible designs, which can be seen in Figure 19. Most designs were adaptations of one of these designs.

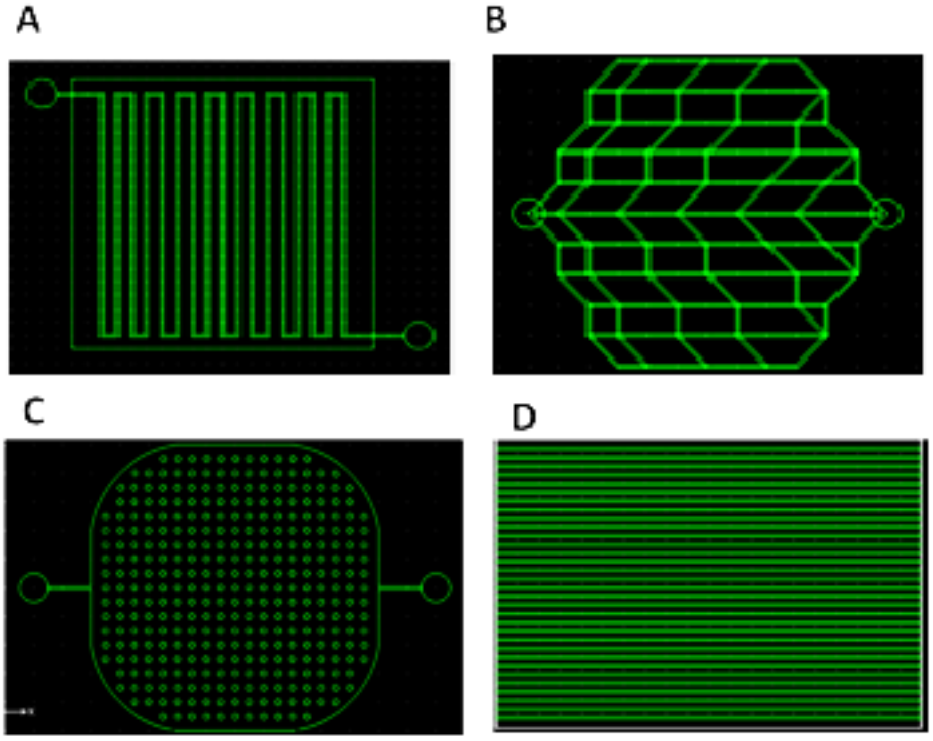

Figure 19: Images of 4 FVA regions. (A) A single, long channel. (B) A highly branched architecture. (C) Posts. (D) Parallel Channel Architecture.

Single Channel

One design considered by the team was the use of a single channel. Multiple variations of this single channel, including variation with curved bends and triangular bends, were considered. In each of these designs, perfusate would be injected through the inlet, travel through the single channel and would exit through the outlet. While style was fairly easy to design, and could theoretically deliver nutrients to each part of the FVA, the team did have a number of concerns with this design. The most obvious disadvantage to these designs is the failure to mimic physiological vasculature, as this FVA isn't comparable with any type of branching mechanism as seen in biological vasculature. Additionally, due to the presence of only a single channel, the perfusate would face tremendous resistance to flow. The driving pressure would need to be quite large, which could potentially disrupt the integrity of the channels. Another concern was in regards to the steady state diffusion assumptions with these channels. Since nutrient diffusion is from a constant source, the concentration of the perfusate could theoretically drop appreciably over time, leading to a decrease in concentration gradient as the fluid traveled farther through the channels.

Highly Branched Architecture

To more closely mimic physiologically relevant vasculature, including the high degree of bifurcations, the highly interconnected FVA, seen in Figure 19B, was created. This design would have one inlet and one outlet with multiple bifurcations, leading to a number of parallel channels between. While this design contains anastomoses like natural vessels, a major limitation readily becomes clear: flow would be very uneven. Perfusate would travel along the path of least resistance, namely the central straight channel (with the shortest total length and thus, the lowest resistance) and flow would be much slower along the outer-most channels. Another concern is the flow along different pathways

and the regions in which flows converged; preliminary examinations showed flow traveling back towards the inlet in some regions. Furthermore due to the branching mechanisms, there is also a potential for aggregation of particles in some corners of the channels; occlusion of channels by accumulations of small particles were seen in preliminary testing scenarios as well.

Posts

In Figure 19C, a post architecture is shown as a proposed functional vascular area. These posts serve to support the top layer of fibrin gel to keep it from dipping into the area of flow. While shown to have a single inlet and outlet, this FVA could conceivably have any number of inlets and outlets. A major advantage of this FVA design is that it allows for flow over nearly the entire 1x1 cm region that needs to be perfused, as only the regions where the posts are located are not being directly exposed to flow. Thus, this design has the largest area of FVA of any of the designs tested.

There are a number of drawbacks of this FVA design as well. Firstly, there is a concern over whether or not the posts will be sufficient to support the large cavity where flow occurs. The aspect ratio in question here borders on 100:1 width to height (1cm wide by 100µm tall), and as such, dipping of the top layer of fibrin would be highly probable. Additionally, it is questionable as to whether or not the posts would provide sufficient support to keep the channel open. A second concern with this design for an FVA is that the flow and in around the posts could lead to collision of fluid streamlines, which could induce turbulence. Finally, this FVA does not mimic natural vasculature, which is a design objective, thou it was ranked to be the least important design objective.

Parallel Channels

Another design alternative considered for the FVA was parallel channels. These were contemplated due to their potential low resistances (as compared to the single channels) and ability

to distribute nutrients around the entirety of the FVA, since channels could be spaced to guarantee sufficient delivery of nutrients to cells on top of the gel. While promising in their ability to provide total coverage nutrient diffusion to the patch, these channels would need a branching network such that all channels are perfused from a single inlet.

4.3.3 Branching Region

The parallel channel FVA design alternative, which the team considered to be the most flexible, needed a branching algorithm to divide flow from the single inlet to the multiple channels in the FVA. Overall, the team identified two parameters that were important to guiding the design of the vascular network: junction geometry and branching widths.

Junction Geometry

The team identified a number of junction geometries which could be used to aid in flow division. These ideas included a split branching geometry, a square branching geometry and a circular branching geometry. Schematics of these junction geometries can be seen in Figure 20.

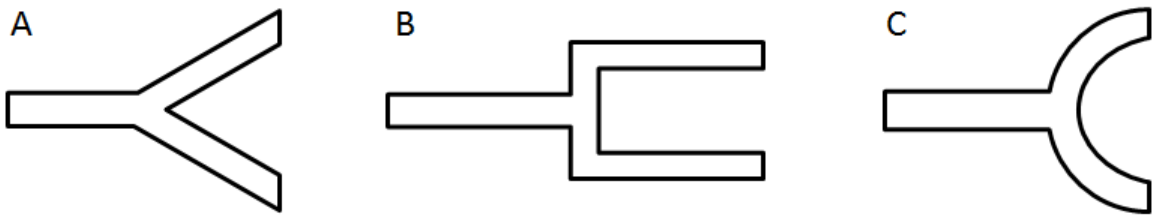

Figure 20: Examples of junction geometries. A) Split branching; B) Square branching; C) Circular branching

In order to ensure equal resistances and equal flow in all channels, the team limited each junction to two output channels. The team decided to move forward with all three of the designs, and

to use computational flow analysis (CFD) to assess the pros and cons of each junction geometry. This data will be presented later in Chapter 5.

Branching Widths

Another parameter which was important to the design of the branching region was the width relationship between the parent vessel width and daughter vessel width. After research and brainstorming, the team ultimately developed three potential options: fixed width, step-down and Murray's Law, which was described in Chapter 2. The fixed width branching relation is summarized by Equation 2.

$$Width_p = Width_D$$

Equation 2: Fixed Width Branching Relation, where $Width_p$ denotes the width of the preceding branch (parent width) and $Width_D$ denotes the width of the branch resulting from the previous bifurcation (daughter width)

Thus, with this branching geometry, the width of the parent vessels is equal to the width of daughter vessel. Intuitively, the team immediately realized that this width relationship was likely going to cause problems, as the volume that would be required to pump through the first channel would need to be very large in order to adequately supply appropriate volumes to each of the channels in the FVA. Pumping such a large volume through a single channel would require very high pressures.

Another branching width algorithm considered was the step-down branching algorithm. This branching relation is summarized by Equation 3.

$$Width_p = Width_D + c$$

Equation 3: Step-Down Branching Relation. Note that $Width_p$ denotes the width of the preceding branch (parent width), $Width_D$ denotes the width of the branch resulting from the previous bifurcation (daughter width), and c is a constant in the above equation

This branching strategy is a linear relation between the width of the parent and the width of the daughter vessel, in which each daughter vessel is a fixed width smaller than the parent vessel. For

example, if c was 100 µm and the width of the parent was 300 µm, then the width of each daughter channel would be 200 µm. This branching mechanism was considered due to the ease of computing parent-daughter widths and the understanding that the widths of daughter vessels should be smaller than the width of parent vessels.

A third branching width relationship explored was Murray's Law. While computationally the most time-consuming, this parent-daughter width relationship, by definition, is optimized to provide uniformity in flow velocity and shear stresses along a branching channel (Emerson et al., 2006; Painter et al., 2006). The relationship between parent and daughter vessel widths in this paradigm is summarized by Equation 4.

$$D_{parent}{}^{3} = \sum D_{daughter}{}^{3}$$

Equation 4: Generalized Murray's Law. Note that D_{parent} denotes the width of the preceding branch (parent width) and $D_{daughter}$ denotes the width of the branch resulting from the previous bifurcation (daughter width)

While the team intuitively had a feeling that Murray's law branching algorithm would produce the most uniform flow velocities and shear stresses within the branching patterns, they were not able to judge these properties for the other two patterns considered. As such, the team moved forward with algorithms of all three types. Each was analyzed using computational fluid dynamics to determine the different flow conditions of each branching width algorithm.

4.4 Continuous Perfusion

The fourth phase of the project entailed building a system that would be capable of continuous perfusion of the system. After brainstorming, a number of means of continuous perfusion of a system, as well as loading parameters, were considered. These are summarized in Table 31.

Table 31: Continuous Perfusion Function-Means Table

Function	Means						
Driving Force	Capillary Driven	Hydrostatic Pressure	Gravity & Pressure Driven	Syringe Pump Driven	Connect to Artery		
Loading Mechanism	Glass Capillary Tube	Hypodermic Needle	Needle Stub	Micropipette Tip	Droplet	Engineered Blood Vessel	Fibrin Tube

4.4.1 Driving Force

A number of different mechanism of driving the continuous perfusion were considered. Each of these methods is analyzed below.

Capillary Driven

Capillary driving force entails creating a small directionality of flow from the inlet to the outlet of the microfluidic channels utilizing capillary action to move fluid through the channels. Pipetting small volumes of fluid into the inlet well should lead to fluid uptake by the network. Pros and cons of using capillary action are discussed in Table 32.

Table 32: Pros and cons of using capillary action

Pros	Cons
• Easy • Simple design	• Must manually load medium • Flow rate dictated by capillary action • Once loaded, it is unclear as to whether or not fluid could be replaced

Hydrostatic Pressure

The team also considered using hydrostatic pressure to drive fluid through the vascular system. To accomplish this, all that would be needed would be a change in height between an environmentally exposed reservoir and the outlet of the system. The head pressure generated by the change in height of the medium level with the outlet would drive the fluid though the system. One downside with this system, however is that the pressure head will diminish as more medium is flown through the

channels, since the height of the fluid reservoir will decrease. This in turn causes a reduction of driving pressure and change in volumetric flowrate. Therefore the perfusion will never reach a steady volumetric flow rate- it will always be decreasing at a decreasing rate. The pros and cons of this system were further considered and are summarized in Table 33.

Table 33: Pros and Cons of Gravity

Pros	Cons
• Easy • Simple design	• Pressure changes with changing height (unless using an infinite diameter reservoir) • Occasional manual loading of medium • Flow rate varies with channel resistance

Gravity & Pressure Driven

In this perfusion method, a pressurized gravity fed system is used, such that the pressure head is constant. In just a gravity driven system, the pressure will change as the height of the inlet decreases during perfusion. This system takes the gravity system a step further by sealing the inlet container and maintaining a constant pressure within that chamber. This allows the pressure within the system to remain constant with a decrease inlet height. This allows for a constant pressure driving force to drive the system, leading to a constant flow state within the system. Pros and cons of using this method can be seen in Table 34.

Table 34: Pros and cons of a gravity and pressure driven device

Pros	Cons
• Maintains constant pressure in system • Simple design • Requires minimal adding of media	• Difficult to fit in incubator • Expensive • Flow velocity changes over time

Syringe Pump Driven

Another method of delivering media through the functional vascularized layer is to inject the media from a syringe via a loading inlet. Assuming a constant force is exerted on the syringe, the media is expected to flow through the vascular network at steady state flowrate. Due to the nature of a syringe pump, it will pump at a steady volumetric flowrate, therefore the pressure in the system is determined by the resistance in the system. If the resistance in the system increases due to channel collapse, the pressure in the system will also increase. Thus, while convenient to pump at a constant volumetric flow rate, this system is not as adaptive as other systems available. Pros and cons of using a syringe pump can be seen in Table 35.

Table 35: Pros and Cons of Syringe Pump

Pros	Cons
• Automatic • Constant flow rate	• Difficult to fit in incubator • Pressure changes with resistance in the channels • May cause vascular damage is resistance in channels increases.

Connect to Artery

A final method of sealing in which this microvascular network could be perfused is via connection to an artery. This would be the gold connection to an artery. This would be the gold standard in perfusion of the microvascular system, as it would provide the biomechanical it would provide the biomechanical cues necessary for proper endothelialization and vascular tissue development. More realistically, this not development. More realistically, this not an entirely feasible option given the time and budget constraints of this project, as well as the constraints of this project, as well as the relatively new nature of the technology. Pros and cons of using an artery connection as a means of an artery connection as a means of driving flow can be seen in

Table 36.

Table 36: Pros and cons of connecting to an artery

Pros	Cons
• Mimics *in vivo* environment • Naturally designed to feed liquid to microfluidic channels	• Availability of intact arteries • Expensive • Difficult to secure to fibrin gel

4.4.2 Loading Mechanism

While the loading direction (vertical vs. horizontal) was largely dictated by the chosen loading region pattern, the mechanism of interface between the perfusion source and the microvascular network was considered. A number of different loading mechanism were considered; an analysis of each idea is included below.

Glass Capillary Tube

A glass micro-tube is an option for the inlet and outlet component. This tube could be inserted into the loading region of microvascular network and could deliver fluids to the network fairly reliably, albeit at a slow rate. Further analysis of the pros and cons of using a capillary tube are displayed in Table 37.

Table 37: Pros and Cons of Glass micro-tube

Pros	Cons
• Low cost • Clear for visibility	• Difficulty adhering to fibrin for tight seal • Difficult interface with tube and fluid driving force • Large outer diameter to inner diameter ratio • Slow delivery rate

Hypodermic Needle

The hypodermic needle is another option that will allow for more precise location of tip because it comes to a sharp point rather than having a blunt end. This would allow for the easy

insertion through a gel without needing to punch any hole in the gel. Additionally, these needles come in a variety of sizes, so there would likely be a size that would address the perfusion needs of this scaffold. The pros and cons of using a hypodermic needle are discussed in Table 38.

Table 38: Pros and Cons of Hypodermic Needle

Pros	Cons
• Sharp point for interface with fibrin • Possible use for multilayered constructs	• Moderate cost • Difficult interaction with fibrin • Opaque

Additionally, the team believed that the use of a beveled needle could be used to perfuse media to multiple layers; the beveled tip would allow for each layer to independently seal to the bevel, thus generating discrete flow on multiple layers. This can be seen in Figure 21.

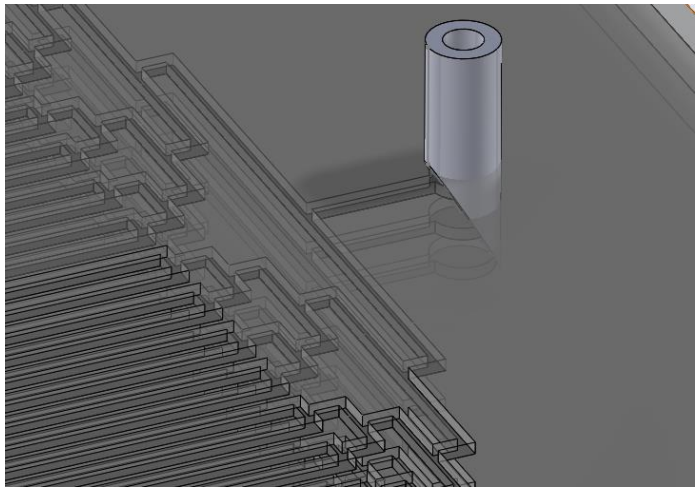

Figure 21: Top loading delivery of perfusate to multi-layered construct

Ideally, the steady fluid flow through the needle would establish laminar flow throughout the network, without rupturing the integrity of the pattern. Since the media is injected at the top layer, it can be assumed that the pressure of the syringe, aided by gravity, will drive flow of perfusate through the networks of the underlying layers. Because it is crucial that the media reaches all layers of the construct, it is required that the layers be aligned in a fashion that allows vertical flow to each layer.

Despite this advantage, this loading option poses difficulty in terms of stacking the layers. Top loading delivery of perfusate and depending on merely gravity as a means for driving perfusate throughout the construct is not a reliable method in terms of ensuring that media reaches the vascular networks of all layers.

Needle Stub

According to Albrecht lab, the blunt tip metal needle stub is typically used in PDMS microfluidic devices. The same vertical connection technique may also be used for our fibrin application, using a methodology quite similar to that discussed for use with hypodermic needles. The pros and cons of this strategy are examined in Table 39.

Table 39: Pros and Cons of Blunt Tip Metal Tube

Pros	Cons
• Low cost • Good outer diameter to inner diameter ratio	• Difficult to image within lumen because it is opaque • Biocompatibility unknown

Micropipette Tip

The micropipette tip is another potential option for this interface with the fibrin gel. It is hypothesized that a micropipette tip could be inserted into the inlet region of the system, much like a syringe. This would provide an accessible, low cost means of perfusion. Table 40 discusses additional pros and cons.

Table 40: Pros and Cons of Micropipette Tip

Pros	Cons
• Low cost • Clear • Sharp point • Interface with micropipette	• Low stiffness • Difficult interface with tubing • Unknown long-term biocompatibility

Droplet

The last alternative option for an inlet is the absence of any component interfacing with the gel. A small volume droplet of medium would be applied to the inlet location of the gel. Through capillary action, the media is expected to enter the vascular network, however continuous perfusion using this method is unattainable.

Table 41: Pros and Cons of Droplet

Pros	Cons
• No cost • No interface required with fibrin	• No containment of medium • Likely not confined to channels

Engineered Blood Vessel

Engineered blood vessels are large-scale synthetic vessels designed to replace failing vessels in the body (Koike et al., 2004; L'Heureux, Pâquet, Labbé, Germain, & Auger, 1998). Using an engineered blood vessel as inlet and outlet connections would provide a life-like model which would simulate connection to an artery *in vivo*. Pros and cons of using an engineered blood vessel can be seen in Table 42.

Table 42: Pros and cons of using an engineered blood vessel

Pros	Cons
• Closely matches *in vivo* models • Naturally designed to feed fluid to small channels	• Difficult to produce • Difficult to attach to inlet and outlet • Expensive and time consuming design required • Limited supply

Fibrin Tube

The team hypothesized that using a fibrin tube at the inlet and outlet might be useful in terms of adherence to the microfluidic hydrogel. A fibrin tube structure would be constructed by casting fibrin around a needle in a cylindrical mold, and then removing the needle after fibrin has completely

cast. The tube would then be removed from the mold, loaded into inlet and outlet ports and loaded with media using a tube or pipette. Pros and cons of using a fibrin tube can be seen in Table 43.

Table 43: Pros and Cons of using a Fibrin tube

Pros	Cons
• Biocompatible • Should integrate well with fibrin gel • Threads can be used to add support	• Difficult to produce • Requires added material and processing • Still requires sealing to inlet and outlet

4.5 Evaluation Of Design Alternatives

Each design alternative discussed above was assessed using a metric evaluation chart. In each case, a table was constructed which rated the various proposed mean in terms of their ability to satisfy the overall project objectives. To develop a sufficient scoring system, the objectives were ranked in pairwise comparison charts and objective scores were weighted based on ranking to determine an optimal design to accomplish the objectives.

4.5.1 Channel Fabrication Analysis

Table 44 displays an analysis of design alternatives for channel fabrication. Note that the metric designed addresses various objectives of the project which apply to channel fabrication. Points were awarded for rapid production, ability of the technique to be scaled to a batch process, potential patterning accuracy of each method, as well as the reproducibility of each method. The criteria for pattern resolution were assigned based on 10% and 25% of the ultimate goal of 100 µm. The criteria for the reproducibility criterion of the metric was established based on previous patterning experience using the coverslip method. This method yields approximately 4 usable gels for every 5 created, for a reproducibility of 80%.

Table 44: Metrics Evaluation for Channel Fabrication Methods

			Injection Molding	Sacrificial Layer	Pressure Stamp	Decellularized	3D Print	PDMS contact Imprint
Constraints								
Budget							X	
Objective								
Rapid Production	< 30 mins	4	4	0	4	2		4
	30 < X < 60 mins	2						
	> 60 mins	0						
Potential for Batch Processing	Indefinitely Scalable (6+ at once)	2	2	1	2	2		2
	Moderately Scalable (4+ at once)	1						
	Not Scalable	0						
High Resolution Patterning (Accuracy)	+/- 10 µm	6	6	3	0	0		6
	+/-25 µm	3						
	>25 µm	0						
Reproducible	>80%	8	8	4	4	0		8
	50-80%	4						
	<50%	0						
Total			20	8	10	4		20

The only constraint that limited design of fibrin gels was budgetary considerations. Due to MQP budget limitations, 3D printing was eliminated from contention. Although it may have produced feasible products, the budgetary requirements were beyond the resources of this project. In order to determine the value of the metric for each objective, their relative importance was used. As see in

Table 45, reproducible was ranked most important, followed by accuracy, rapid production, and finally batch processing.

Table 45: Fabrication Apparatus Weighted Metric Determination Table

	Rapid Production	Reproducible	Potential for Batch Processing	Accuracy	Totals
Rapid Production	x	0	1	0	1
Reproducible	1	x	1	1	3
Potential for Batch Processing	0	0	x	0	0
Accuracy	1	0	1	x	2

The ranking in Table 45 determined the ultimate ranking of points assigned to the metric for each objective, giving greater value to designs that met the most important objectives. The most important objective, reproducibility, was deemed to be important since these gels need to have consistent geometries such that diffusion and flow rates can be assumed consistent from gel to gel. Accuracy is almost as important, due to the fact that the ability to accurately produce the desired geometries will allow for simplification in quantifying diffusion. Rapid production is valued less than the previously two discussed objectives since a simple procedure was not as valued by the client as was an accurate and reproducible fabrication apparatus. Our client indicated that a difficult processing technique was acceptable as long as the production was consistent and reliable. Finally, the potential for batch processing was ranked a step below rapid production in terms of importance. Again, this is ranked low because an ability to produce an accurate and precise gel is more important to the client than producing it fast and in bulk quantities.

The method of decellularization was ranked lowest for two main reasons: it is not reproducible in any fashion and each iteration will produce different channel geometries. Although it has the ability

to be produced at high output and can be done relatively quickly, it is nowhere near as robust a fabrication method as the others.

The design alternatives involving the use of a sacrificial layer and pressure stamping were valued at 10 points. Although these processes may be able to produce fibrin gels quickly and in bulk fashion, it will be difficult to produce consistent fibrin gels, which is the most important objective. The top two alternative designs are the PDMS contact imprint and injection molding. These two processes are similar in the fact that both utilize PDMS molds to produce the proper channel geometries. Molding with PDMS produces high fidelity gels and can be done rapidly. The team ultimately decided to move forward with both of these strategies and to test to see which performed better.

4.5.2 Multi-Layer Construct Analysis

Table 46: Function/Means for Gel-Gel Adhesion

Function	Means							
Gel/Gel Adhesion	Surface Tension	$CaCl_2$	Thrombin Only	$CaCl_2$ & Thrombin	Fibrin Glue	Differential Casting	UV Crosslinking	Fibrinogen

With the objective of creating a multilayered tissue construct as well as creating sealed channels, the team determined several likely methods that could be used to accomplish this requirement. Due to a lack of sufficient existing literature on the topic bonding two polymerized fibrin gels together, the team moved chose to move forward and explore each of the identified methods. Each of the methods has various pros and cons that make them preferable over one another. Therefore they were assessed based on the analysis done below (Table 47) in order to establish an order in which they would be testing and how much focus would be directed toward each method. This list established a framework for the team to follow when systematically planning experiments in the laboratory.

Table 47: The following values were established based on estimates. The value of 4 best accomplishes the objective the team is looking for. The methods are compared and values were based relative to the others.

	Surface Tension	Fibrin Crosslinking	Fibrin Glue	Differential Casting	UV Crosslinking
Maintains Channel Geometry	4	3	2	3	4
Ease of Method	4	3	2	2	3
Available reagents and equipment	4	4	4	4	4
Adhesion Strength	1	2	2	2	2
Low time requirements	4	3	1	1	2
Allows for casting with cells	4	4	4	3	0
Low Cost	4	3	2	3	4
Preserves original material properties	4	4	4	4	0
Totals:	29	26	21	22	19

The team identified that the order in which the methods would be tested and the amount of time could be investing in each using the above table. This order was 1) Surface tension, 2) Fibrin crosslinking, 3) Differential Casting, 4) Fibrin Glue, 5) UV Crosslinking. The Fibrin Crosslinking category contains the various permutations of different ways the team would try to use the addition of reagents used during the standard casting protocol.

4.5.3 Microfluidic Network Analysis

Table 49 displays the evaluation of microfluidic design alternatives. These constraints were defined to eliminate design alternatives which were not feasible in the scope of this project. After the constraints were used to eliminate different design alternatives, the remaining objectives were

evaluated based upon their ability to satisfy the objectives. The objectives used for this metric were ranked based on their importance, as defined by the results in Table 48.

Table 48- Microfluidic Design Weighted Metric Determination Table

	Mimics Natural Vasculature	**Printable**	**Equal Flow**	**Equal distribution of nutrients**	**Totals**
Mimics Natural Vasculature	x	0	0	0	0
Printable	1	x	1	1	3
Equal Flow	1	0	x	0.5	1.5
Equal distribution of nutrients	1	0	0.5	x	1.5

Based on the evaluation of the objectives, the printability of the microfluidic design was deemed the most important objective with equal flow and distribution on nutrients tying for second. Mimicking physiological architecture was viewed as least important. We were able to weigh the scoring of objectives based on importance; therefore a high score in printability was more valuable than a high score in mimicry or physiological architectures.

Table 49: Metric Evaluations for Microfluidic Design

			Branching				Functional Vascular Area			
			Square Branching	**Circular Branching**	**Split Branching**		**Parallel Channels**	**H-Filter (Square)**	**Intersecting**	**Posts**
Constraints										
Inter-channel spacing cannot exceed 200 um										
Branching spacing > 100um										
1x1 Functional Vascular Area										
Branching Fits within 5 mm entrance range										
FVA- Channel Widths < 100um										x
Objectives										
Mimic biological architecture	Branching Mechanism	1	0	0	1					
	Murray's Law Potential	1	1	1	1		-	-	-	-
Repeatable/ Printable	Orthogonal Only	5	5	1	3		5	5	3	x
	Orthogonal & Diagonal	3								
	Orthogonal & Diagonal & Curved	1								
Total			6	2	5		5	5	4	0

In terms of branching, all three alternatives passed the constraints listed for microfluidic designs. Square branching scored highest for printability as the orthogonal layout of the designs would guarantee nearly exact printing, whereas the angles and curves in split and circular may pose challenges when it comes to fabrication.

The functional vascular area has been defined as the 1mm x 1mm area of the gel in which sufficient perfusion is available and cells are expected to remain alive. Eliminating designs that failed to meet the constraints, intersecting channels were eliminated from consideration since some of the diverging regions had inter-channel spacing exceeding 200 microns. Additionally, the post design failed the meet the constraint that all channels have widths less than 100 microns. In this design, there are not channels at all, which makes it nearly impossible to characterize flow, and can lead turbulence and dead spots of flow, both of which could induce clotting were blood to be perfused through.

Based on printability, orthogonal edges print the most accurately, followed closely by straight, diagonal lines. Curving edges do not always print well using photolithography, depending on the radius of curvature and the printing resolution. Based on this information, it was determined that parallel channels and the straight continuous channels would print nearly exactly, whereas the curved continuous design may have small defects due to rasterization of the non-orthogonal lines and non-straight edges.

4.5.4 Continuous Perfusion Analysis

Table 50: Metrics Evaluation for Perfusion Bioreactor Design

			Means				
			Capillary	**Hydrostatic**	**Gravity + pressure**	**Syringe Pump**	**Arterial Connection**
Constraints							
Available					X		X
Incubatable							
Objectives							
Long Term Flow	Flow for <24 hours	1	1	5		5	
	Flow for 24<X<48 hours	3					
	Flow for >72 hours	5					
Steady State	Uniform Flow Rate	4	2	3		4	
	Diminishing	3					
	Periodically Discontinuous	2					
	Random	1					
Easy to replenish medium	Open system	3	3	3		0	
	Closed System	0					
Total			6	11		9	

Table 50 displays an evaluation of the means, evaluated based on constraints and objectives of designing the continuous perfusion system. Two constraints are highlighted in designing a perfusion bioreactor. The first constraint is availability of the technology to the team, either in terms of budget or feasibility. A gravity and pressure controlled perfusion reactor is eliminated under this constraint due to the expense of having a pressure controlling device as part of the reactor. Arterial connection is eliminated from contention as well, as there is a lack of evidence supporting the implantation of this device at this point. Future testing of the device will certainly include studying this design alternative, however, there is no current need to surgically attach an artery to the fibrin gel to study perfusion. The other important constraint considered in our design was the ability to run the bioreactor within an incubator, which was be necessary once these devices became cellularized.

After considering the design constraints, the three main objectives were weighed according to their rank in Table 51.

Table 51: Perfusion Bioreactor Weighted Metric Determination Table

	Reliable	**Steady State**	**Easy to replenish medium**	**Totals**
Reliable	x	1	1	2
Steady State	0	x	1	1
Easy to replenish medium	0	0	x	0

Reliable was valued above steady state flow and ease of replenishing cell media the system needs to run continuously all the time. Any interruption of flow would lead to cell death. Steady state flow was valued above the ease of replenishing media since a steady supply of

nutrients is important for cellular growth and survival. Although ease of replenishment of media is important and will require serious consideration, the user has stated that functionality is preferable to ease. In this case, the other two objective were more important.

Using the weighted objective scoring, hydrostatic perfusion was ranked above capillary action and marginally better than a syringe pump. Hydrostatic perfusion was determined to be a better alternative than capillary action as it is capable of continuous perfusion for a longer time-frame than is capillary action. In comparison to the syringe pump, the hydrostatic system was ranked slightly higher due to its ease of medium replacement- medium can be replaced without stopping the perfusion. Ultimately, the team saw the potential in both solutions, but decided to move ahead with the hydrostatic system.

CHAPTER 5: DESIGN VERIFICATION

Throughout the duration of this project, the design process was used in order to achieve each of the objectives outlined in the revised problem statement. As presented in Chapter 3, a series of steps were identified to categorize the project into five major milestones, each of which accomplished different project objectives. These steps were: (1) Engineer a fibrin-based microvascular network (μVN), (2) Demonstrate μVN channel localization, (3) Design and optimize of microvascular architecture, (4) Establish continuous perfusion, and (5) Perform cellular validation. In this project, the first three milestones were accomplished via the creation of the novel, thin-film microvascular network. The design team fabricated a micropatterned fibrin gel, which consisted of a physiologically relevant vasculature architecture. The film was shown to have high pattern retention and it was shown that the vasculature network was able to contain perfusate. The architecture was then optimized using Comsol to minimize the fluidic stagnation zones and maximize the uniformity in flow velocity. The last two milestones, the validation of continuous perfusion and the cellular validation, were accomplished with the single channel perfusion system.

5.1 ENGINEERING A FIBRIN-BASED VASCULAR NETWORK

5.1.1 Microfluidic Network Preliminary Design

Patterning fibrin first required the design of a PDMS mold with a desired microfluidic architecture. The design team elected to test patterning with a square branching, 8 channel device in which the branching was a step-down version culminating in 200 μm channels. The

PDMS mold was printed to a height of 100 µm. This mold was selected due to its larger channel sizes (lower fluidic resistance) and its simple shape.

5.1.2 Photomask

The photomask, below, was printed and utilized during the microfabrication process to produce defined microfluidic patterns.

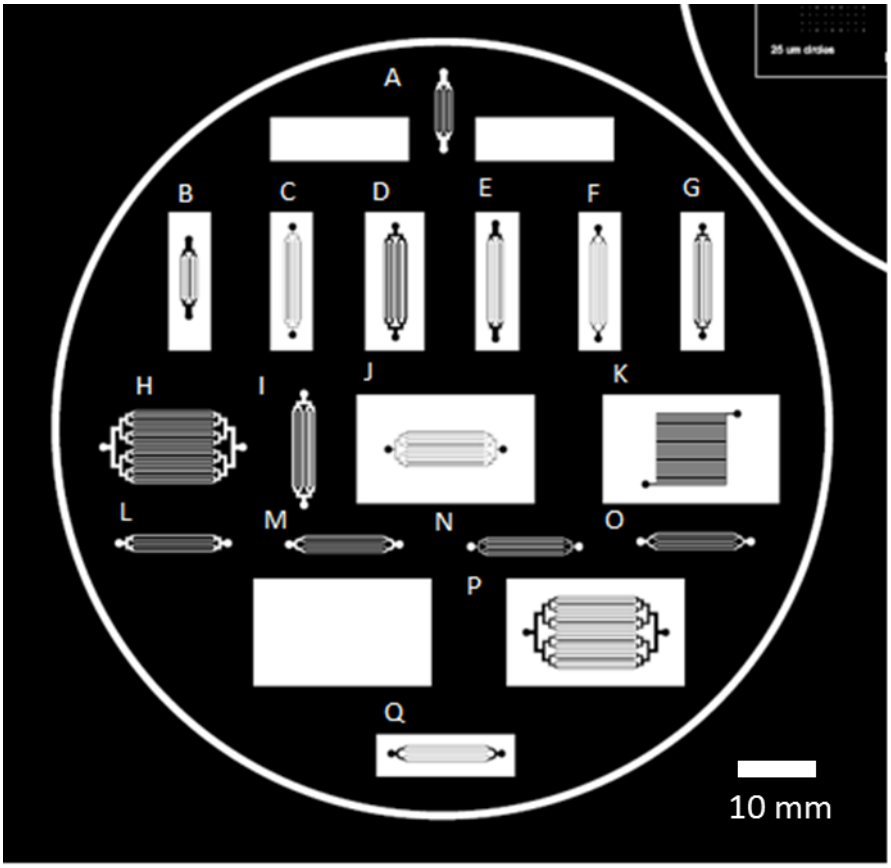

Figure 22: Image of first photomask printed

The designs included in the photomask submission above are outlined in the following table:

Table 52: Descriptions of designs from printed photomask in Figure 29. Note: Positive correlates to molds designed for imprinting fibrin and negative correlates to PDMS molds for testing flow characteristics.

Design	Number of Channels	Branching geometry	Branching mechanism	Negative/ Positive
A	8	Square	Murray's law	Positive
B	8	Square	Murray's law	Negative
C	8	Square	Uniform	Negative
D	8	Square	Step-down	Negative
E	8	Square	Murray's law	Negative
F	8	Split	Step-down	Negative
G	8	Square	Step-down	Negative
H	32	Square	Step-down	Positive
I	8	Square	Step-down	Positive
J	32	Square	Uniform	Negative
K	32	NA	NA	Negative
L	8	Square	Step-down	Positive
M	8	Circular	Step-down	Positive
N	8	Square	Uniform	Positive
O	8	Split	Step-down	Positive
P	32	Square	Step-down	Negative
Q	8	Circular	Step-down	Negative

Note that some squares have no design in them. The size of these squares correspond to the size of the squares around the fibrin molds, and were to be used to test the injection molding fabrication device, though this device was ultimately never tested, due to wafer imperfections in the patternless-squares.

These printed patterns consisted of various permutations in which the number of channels, branching geometry, and branching widths were altered, each producing a distinct design. Each of these microfluidic patterns was to be tested in order to determine the ideal design on the basis of pattern retention, even flow through channels, and adequate perfusion. Ultimately, pattern D, a step-down 200 µm channel was used to test the vast majority of

templating and perfusion attempts, due to its larger channel sizes, which were macroscopically visible and reduced the overall fluidic resistance of the device.

5.1.3 Fabrication of wafer

In order to transfer the final microfluidic designs onto a wafer, a standard procedure was conducted to achieve photolithographic fabrication of the wafer. During this process, the final microfluidic patterns were patterned in a 100 µm thick layer of photoresist spread on a crystalline silicon wafer by using UV light to transfer the geometric patterns of the photomask to the light-sensitive photoresist. A series of treatments following the UV light exposure dissolved away the un-exposed photoresist, leading to the fabrication of the microfluidic designs on the surface of the wafer. From this procedure, the team was able to develop a mold of the final microfluidic designs (Figure 23), enabling the casting of PDMS or fibrin to create constructs with embedded microfluidic networks. The complete procedure for the photolithography can be seen in Appendices A and B.

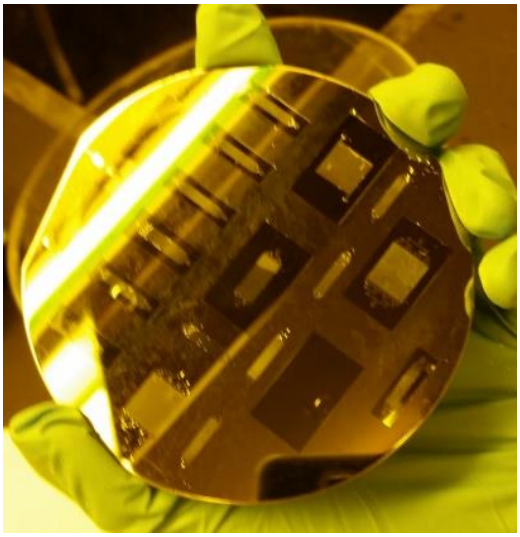

Figure 23: Printed Silicon Wafer

Ultimately, the finalized silicon wafer was fabricated, as can be seen in Figure 23. PDMS was then cast over this wafer, not only to protect the wafer from dust, but more importantly, to develop molded PDMS which would ultimately be use for patterning the fibrin hydrogels.

5.1.4 PDMS Mold Dimensions

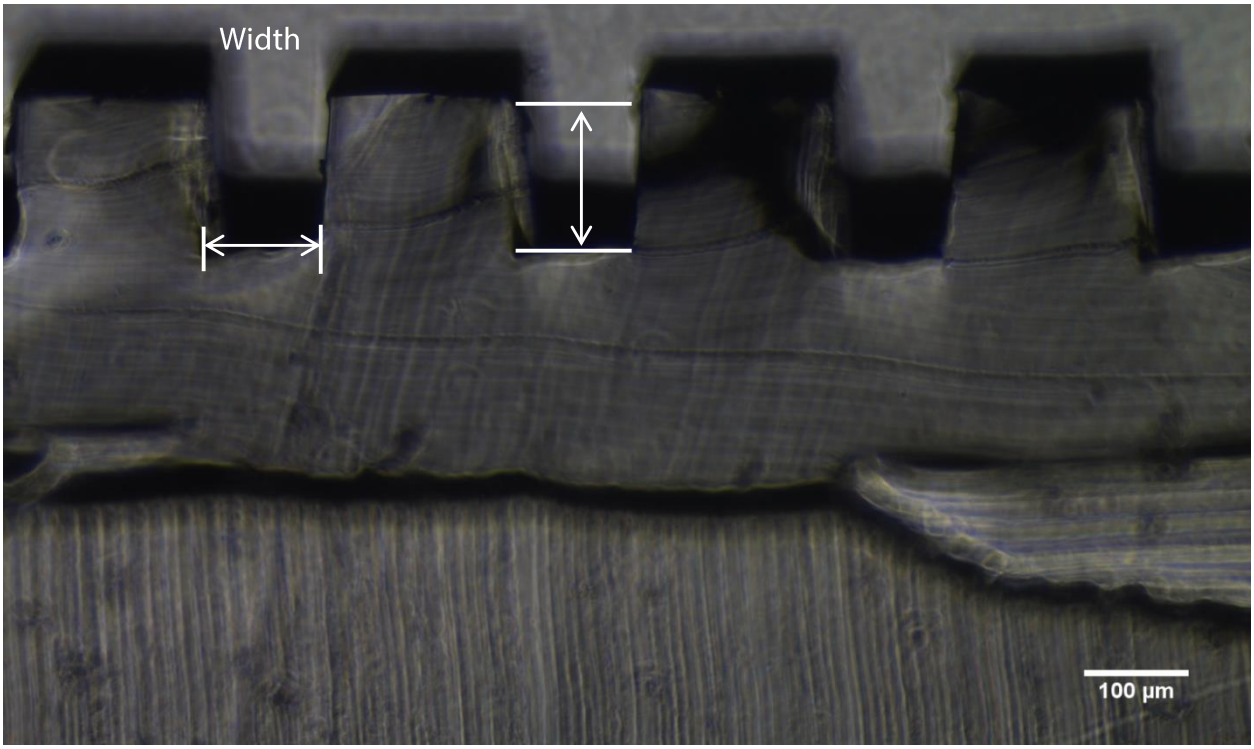

Figure 24: PDMS mold dimension verification. Note that the height was measured to be approximately 128 µm and the width was measured to be an average of 152µm.

Once the PDMS was successfully cured and removed from the silicon wafer, small sections were sliced in order to verify the dimensions imprinted from the wafer. The PDMS was thinly sliced using a scalpel and imaged using the Upright/BF microscope (Nikon, Tokyo). As designed, the cross section of the channels in the FVA was 100 µm wide by 100 µm deep. Measuring the cross-sectional dimensions shown in, the actual dimensions were characterized and are presented in Table 53.

Table 53: PDMS mold verification

Depth Verification	Width Verification
• Ideal: 100 µm • Actual: 128.586 $\pm$ 8.171 µm (n=4)	• Ideal: 100 µm • Actual: 152.007 $\pm$ 13.732 µm (n=4)

As is shown in Table 53, the channels are significantly larger than expected and have fairly large standard deviations, suggesting a large amount of variability resulting from the microfabrication process. It is highly likely that this variability resulted from relative user inexperience with the microfabrication process, thus generating a non-uniform thickness of photoresist, thus skewing the height of the channels. The large width deviation was somewhat confusing as well, as photolithography typically generates fairly accurate molds in PDMS.

The PDMS molds were also analyzed in the branching regions to assess overall channel geometries of the silicon wafer. Images were taking using the Upright/BF microscope and channel widths were validated using ImageJ software. Figure 25 below displays an image of the branching region of a 200µm FVA gel, with the different branch levels labelled. Table 54 below displays the ideal (as designed in DraftSight) and actual measurements for the width of branching regions in PDMS.

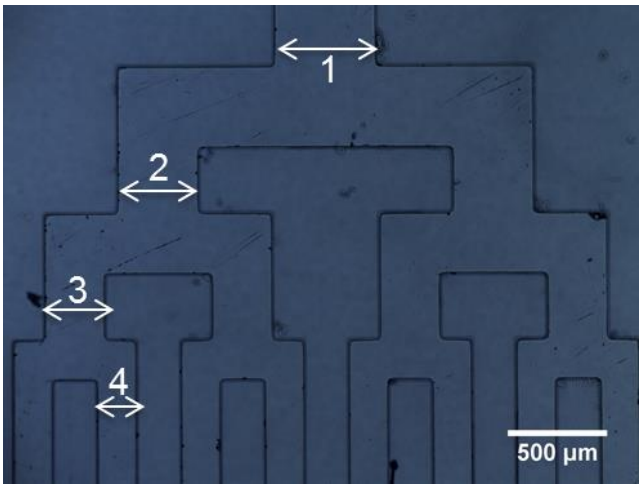

Figure 25: PDMS mold branching area of a Step down, square branching mechanism ending with 200 µm wide channels. A) Ideal = 200 µm. B) Ideal = 300 µm. C) Ideal = 400 µm. D) Ideal = 500 µm

Table 54: PDMS mold verification measurements based off Figure 25

Width Verification			
4	• Ideal: 200 µm • Actual: 180.7 $\pm$ 3.7 µm (n=8) • Deviation: 9.65%	3	• Ideal: 300 µm • Actual: 285.4 $\pm$ 4.7 µm (n=4) • Deviation: 4.87%
2	• Ideal: 400 µm • Actual: 398.7 $\pm$ 2.1 µm (n=2) • Deviation: 0.32%	1	• Ideal: 500 µm • Actual: 506.3 µm • Deviation: 1.26%

5.1.5 Fibrin Gel Preparation

To make fibrin gels, 670 µL of fibrinogen (MP Bio, 30mg/mL in HBS) was mixed with 150 µL of $CaCl_2$ (40mM) and 80 µL of PBS (1x) in an Eppendorf tube. PDMS molds were soaked in a 1% solution of PEO-PPO-PEO (E:P-3:1, PolySciences) for 30 minutes before being allowed to air dry. Vellum paper rings cut to an inner diameter of 0.75 inches with a slightly larger outer diameter were then placed around the PDMS molds. A 100 µL thrombin solution (2.35 U/mL) was then added to the fibrinogen solution and the resultant solution was triturated. 150 µL of

the combined solution was then pipetted onto each of the molds within the Vellum paper rings. The solution was then manually spread to cover the entire area of the vellum paper ring using a micropipette tip. Figure 26 below displays fibrin gels setting prior to sealing.

Figure 26: Fibrin Gels crosslinking in vellum rings on PDMS (microvascular layer) and Dacron (flat gel)

Fibrin gels were crosslinked for 30 minutes on the benchtop, before being submerged in DI water for 10 minutes. At this point, the vellum paper ring containing the imprinted fibrin gel was carefully removed from the PDMS mold, ensuring that the gel remained submerged the entire time. Gels were then placed on PDMS coated glass slides and imaged for quality assurance. Figure 27 below displays a complete graphic for preparation of a sealed fibrin gel.

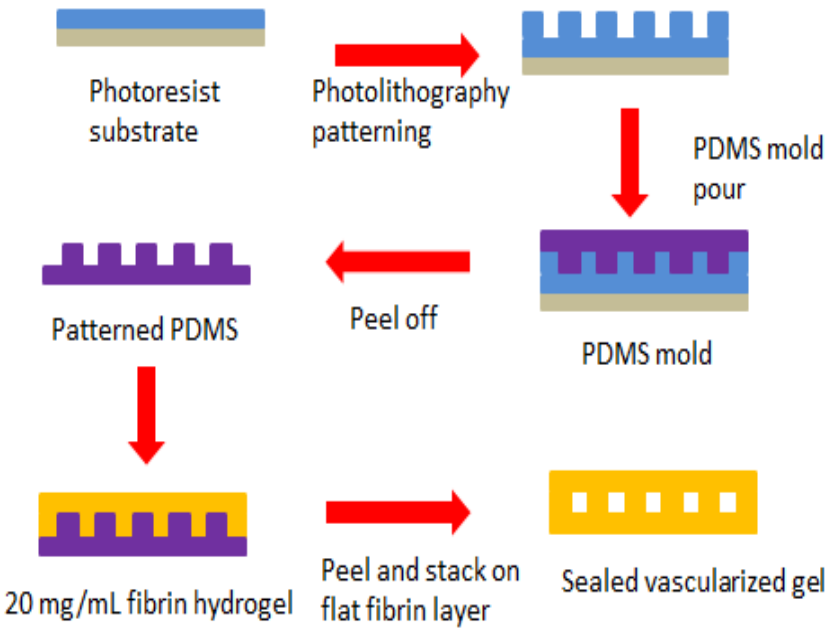

Figure 27: Procedural preparation of fibrin gel from photolithography to gel sealing

5.1.6 Fibrin Dimension Verification

In order to determine the fidelity of fibrin, branching dimensions were examined in fibrin gel and compared to the PDMS mold from which it was cast. The design used for verification was the 8 channel, square branching step-down design with 200 µm parallel channels for the FVA, as this was the most often utilized pattern. Figure 28 displays both the PDMS and fibrin images of the same branching region. If the fidelity of fibrin were perfect, it would be expected that fibrin dimensions should match the PDMS dimensions. ImageJ was used to measure the width dimensions in fibrin and those measurements were compared to the dimensions obtained from Figure 25. Figure 29 displays a comparison of PDMS and fibrin for branching geometries.

PDMS

Fibrin

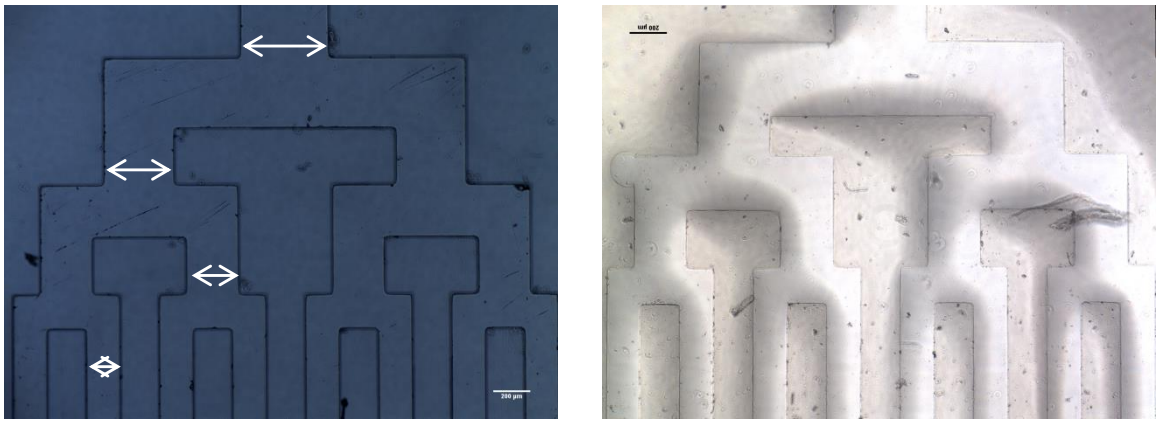

Figure 28: PDMS mold and Fibrin gel branching images for dimension verification. 1) PDMS Mold. 2) Fibrin Hydrogel

For each of the four branching levels, the average width of channel(s) was calculated in both the PDMS mold as well as the fibrin hydrogel. The first level consisted of one branch; the second level consisted of two branches; the third level consisted of four branches; the fourth level consisted of eight branches. The following chart shows a comparison between the expected widths (based on the width of the PDMS mold) and the actual width of fibrin at each branching level. As shown in Figure 29, the expected and actual widths, while statistically different at the third and fourth branch level are relatively close.

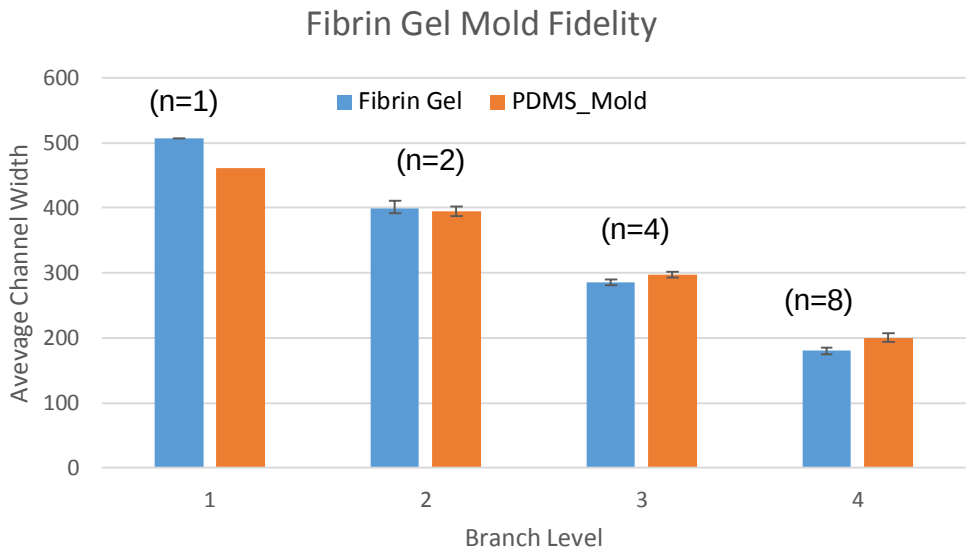

Figure 29: PDMS and Fibrin dimension comparison. See appendix D for data.

5.2 Demonstrate Channel Localization

The next phase of the project was to demonstrate the localization of fluids to the channels. This was necessary in order to demonstrate that the channels acted as a conduit for flow and expedited fluidic delivery throughout the patch, over bulk diffusion alone.

5.2.1 Fibrin to Fibrin Adhesion

Based on the client's desire to utilize microfluidics for microvasculature, the most promising approach was deemed to be the layering of fibrin gels to form channels within the gel construct. To guarantee that flow remained in the channels and did not leak between layers, a strong seal between fibrin gels was needed. One of the design alternatives proposed was the use of calcium chloride, thrombin and a combination of the two, as it was proposed that they might activate a secondary polymerization reaction which could be used to seal two fabricated gels together.

Figure 30 displays the results of using $CaCl_2$ and a mixture of $CaCl_2$ and thrombin to seal gels to each other. As shown, all three techniques were successful, in that the gels remained adhered while no shear forces were applied.

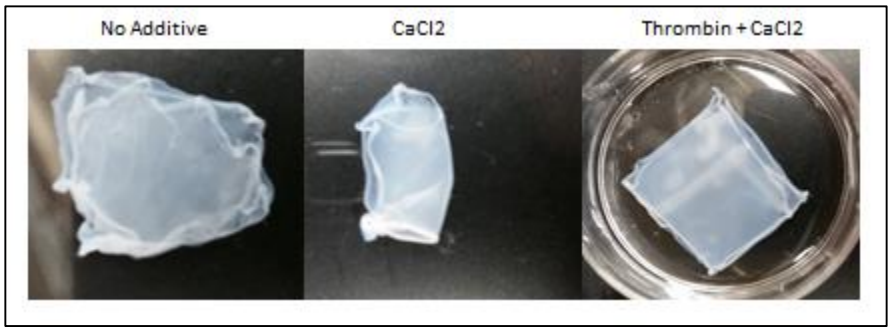

Figure 30: Gel to Gel adhesion testing using no additive (left), $CaCl_2$ only (middle) and activated thrombin (right).

Although they maintained adhered, it was clear that the bonding was not particularly strong. After 24 hours, the gels could be manually pulled apart, indicating that the stacking was not sufficiently bonded. Were these gels patterned gels, it is highly unlikely that they would have adhered sufficiently to localize flow. Of note, the thrombin/$CaCl_2$ bonded fibrin gels were slightly more difficult to separate than the other two stacks, though they were separable. This indicates that a small degree of crosslinking might have occurred between the gels.

Further testing investigated using activated fibrin as a "glue" to seal layers together. Figure 31 displays the use of the fibrin "glue" technique described earlier. In this experiment, five gels were layered on top of each other with no additives. To layer the five gels, the first gel was removed from solution, dabbed of excess moisture, and a second layer was placed on top. The layer and substrate was then re-submerged and another layer was added to the top. This process was continued until five gels had been stacked. Extra fibrin was produced and then pipetted around the edges of the five gel stack.

Figure 31: Preliminary Gel Stacking; Image on right shows gel out of solution holding a square shape

The fibrin set-up around the edges of the stack was successfully in holding all five gels together. The far right image of Figure 31 displays the five gel construct pulled out of solution and held with tweezers. The gel construct maintained rigidity, unlike unsealed fibrin gels, which form a tear-drop shape (due to surface tension) when removed from solution.

After testing the use of fibrin gel ingredients as sealants, it was hypothesized that layering gels atop one another before they were fully set could help enhance the inter-gel polymerization, thus enhancing the adhesion. This process, called differential sealing, is further explained in Chapter 4. Various times between application of the cast gel to the developing gel were investigated. Times of 10, 20, and 30 minutes were attempted, and it was found that a window of 10 to 20 minutes was optimal for sealing two gels together. However, due to the nature and variability with which fibrin polymerizes from batch to batch, it was difficult to optimize this process to ensure that the gels sealed but the fibrin was polymerized enough so as not to fill in the channels, blocking flow. Various tests suggested that the channels were either filled and non-perfusable or the gels were non-adherent to one another.

5.2.2 Channel Loading

Successful loading of channels would provide evidence that continuous perfusion should be possible in a microvascularized fibrin gel. All attempts to load the channels utilized capillary action in order to draw fluid into the channels. Prior to sealing gels together, the microvascularized gel inlet and outlet circles were punched with a 1 mm biopsy punch, as is shown in Figure 32 .

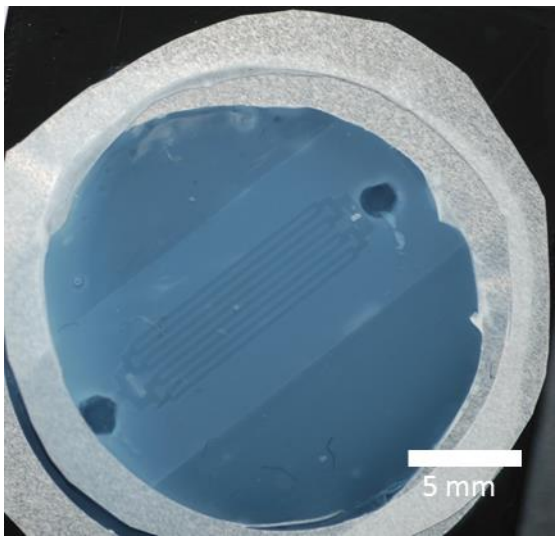

Figure 32: Unloaded fibrin channel with holes punched at inlet and outlet

Gels were then loaded by micropipetting 1.7 µL of 1µm diameter blue latex beads (Polyscience Inc. Warrington) on the inlet and gently tilting the gel. The microbead solution was observed to wick through the channels, though in some instances, some channels did not fully fill. This could potentially be caused by increased resistances or a channel blockage. Figure 33, Figure 34, and Figure 35, below display successful loading of a single engineered fibrin microvascular network and successful loading of two stacked and discretely perfusable microvascular networks layered atop one another.

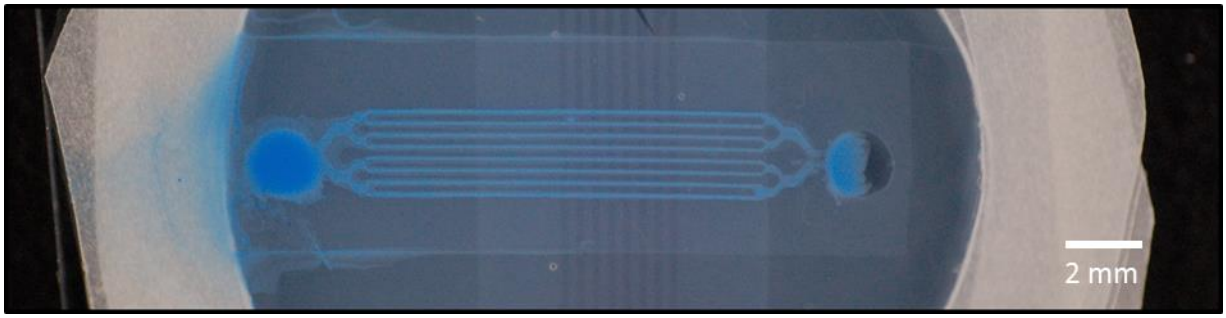

Figure 33: Successfully loaded Fibrin microfluidic network

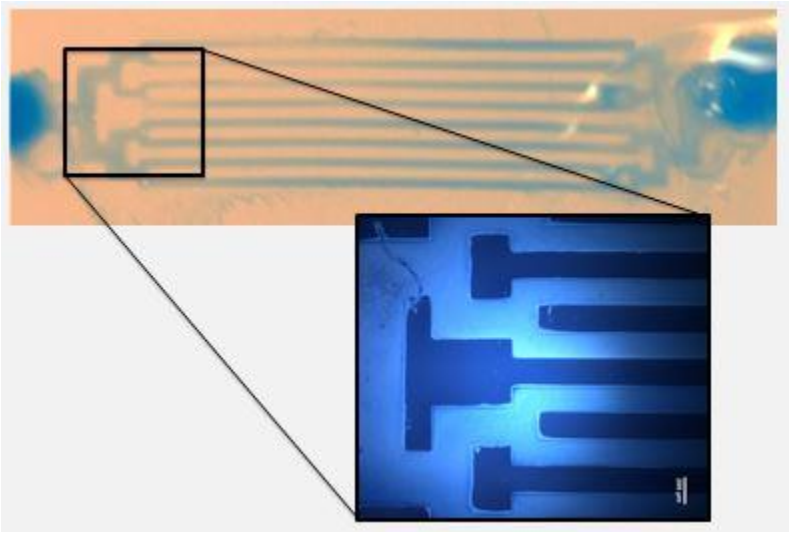

Figure 34: Macro and Microscopic images of a loaded microfluidic network

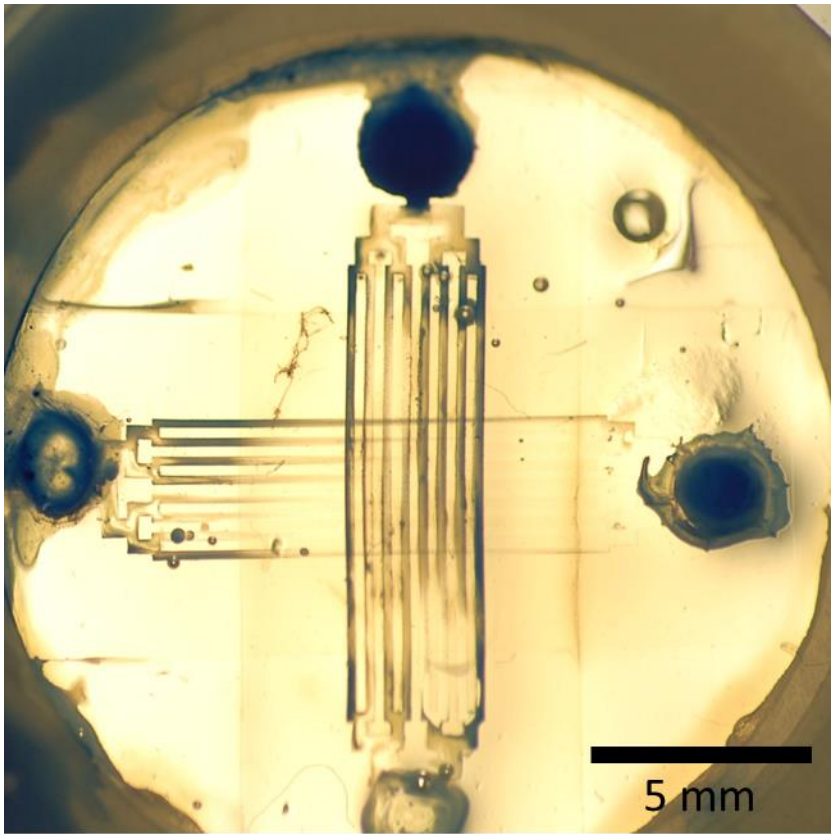

Figure 35: Multiple Fibrin microfluidic networks layered and individually loaded with micro-bead solution

5.3 Microfluidic Design Optimization

In order to determine which of the design alternatives were most effective in generating uniform flows with a minimization of low-flow "dead zones," computational fluid dynamics (CFD) was performed on each of the designs (Comsol Multiphysics, Burlington). While a complete procedural overview can be found in Chapter 7, briefly, CAD drawings (Solidworks, Waltham) were perfused at a physiologic flow rate (300 μm/sec flow velocity) assuming a steady-state laminar flow profile for well-developed flow. The results of this analysis will be presented in the remainder of this section.

The first parameter to be tested using a CFD model was the branching architecture of the system. During brainstorming, three design alternatives were generated: Constant Width, in which the width of the channels was constant throughout; Stepping Width, in which the width of the channels decreased by a fixed rate for each increase in branching level; and Murray's Law, in which the channel widths obeyed Murray's Law, which is outlined in Chapter 2 and Chapter 4. The velocity profile generated by a theoretical 300μm/sec flow rate in each of the 8 channels of the FVA can be seen in Figure 36 .

Notice that the constant width branching profile generated very high flow rates near the inlet and outlet (on the order of 5 mm/sec), and very low flow rates (~100 μm/sec) in the channels. Thus, this design is not a viable biomimetic vasculature. In contrast, the stepping-width profile showed promising results in terms of similarity of flow conditions from one branch to the next. Flow in the center of the larger channels appears to be similar in velocity to the flow in the FVA. However, this flow is exceptionally fast, reaching approximately 600 μm/sec, a flow velocity of nearly double what was calculated. Additionally, these CFD results suggest that a Murray's Law width pattern does generate nearly uniform flow conditions throughout all branches of the system. This model shows very little variation in center-channel flow velocity between branch levels. Note however, that the velocity predicted is nearly double the velocity of physiologic conditions, despite the optimization of velocity for the channel.

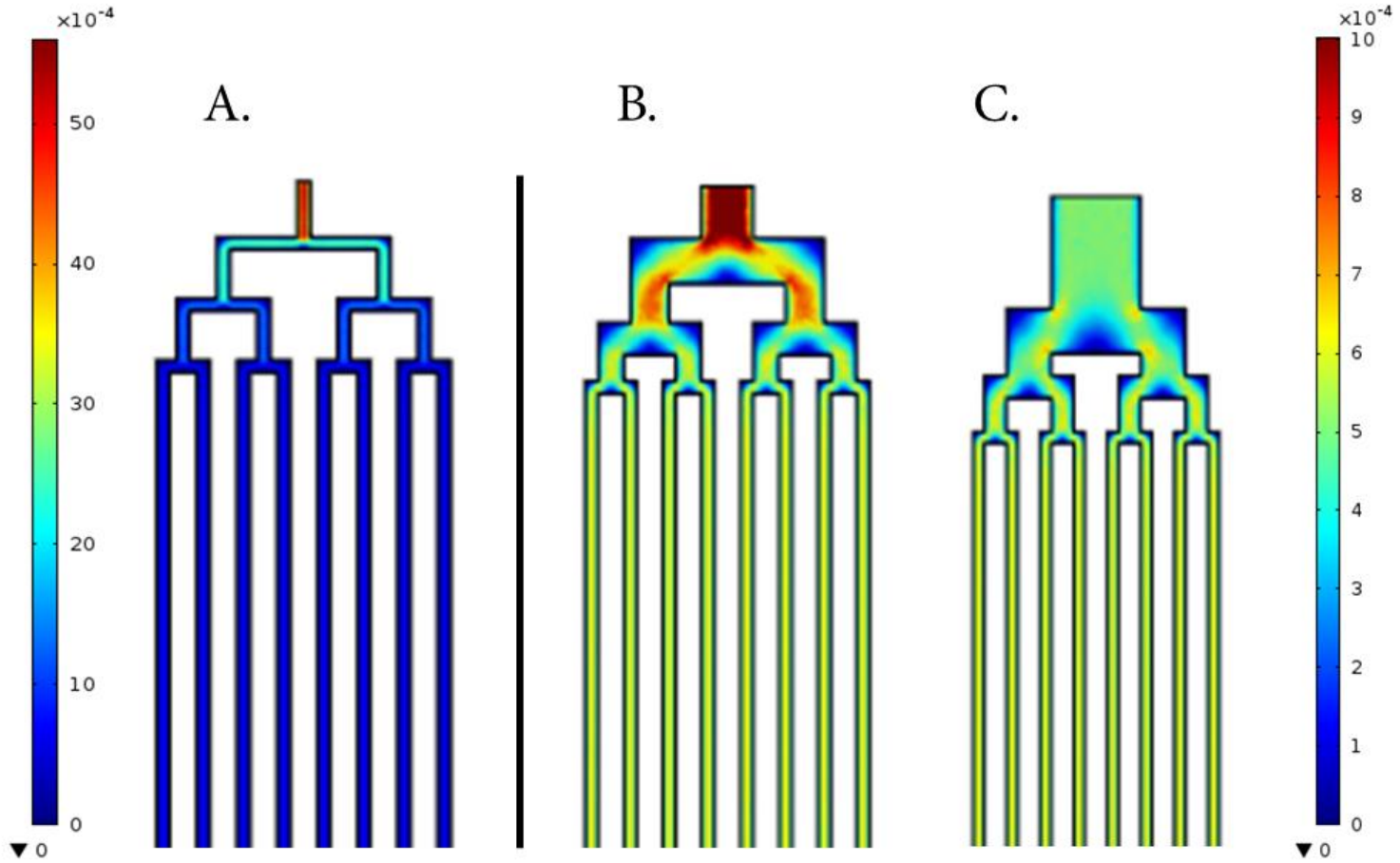

Figure 36: Velocity Profiles for a 24 nKg/sec mass flow inlet. (A) Constant Width. Note that flow velocity throughout the channels is minimal with very high inlet velocities, which rapidly dissapate. (B) Stepping Width. Note that flow velocity through the channel is approximately twice the flow rate expected for the given flow rate. (C) Murray's Law. Note that the flow rates in the channels are comparable to those of the step function, however, this branching architecture generates the most highly uniform flow profile throughout.

CFD modeling was also used to examine the pressure drops that occurred in each of these channels. It was determined that large pressure drops should occur over the length of the channels and not within the branching region, as high pressure drops in the branching region were deemed to indicate severe resistance to flow, a trait indicating inefficient branching. Additionally, natural capillaries use the pressure gradient within a channel to force fluid into the extracellular space, a technique which would greatly increase the efficacy of nutrient diffusion into the surrounding tissue (Marieb & Hoehn, 2013). The pressure predicted at different points within the network can be found in Figure 37.

Figure 37A displays pressure as a function of flow path for the constant width design. Notice how the pressure required driving the system is 24 Pa, 9.5 Pa of this driving force is lost in the branching region of the vasculature, indicating poor, inefficient flow. Figure 37B shows the stepping function model. Note that the driving pressure of the system is much smaller (11.3 Pa) and that the pressure lost over the branching region of the channels was approximately 1.5 Pa. Finally, Figure 37C shows the pressure of perfusate at various points in the system. Notice that the pressure required to drive flow in this system was the smallest of the three, 11 Pa, and the pressure drop seen across the branching network is 0.8 Pa, indicating that this branching width minimizes the pressure drop in the branching region, thus maximizing the pressure gradient within the channels. This data is summarized in Table 55.

Table 55: Summary of Driving Pressure and Pressure Drop across Branches for Various Width Profiles. Note that the constant width system had the largest drive pressure and drop, while Murray's law had the lowest driving pressure and pressure drop across channels.

	Drive Pressure (Pa)	Approximate Pressure Drop Across Branches (Pa)
Constant Width	24	9.5
Stepping Width	11.3	1.5
Murray's Law	1	0.8

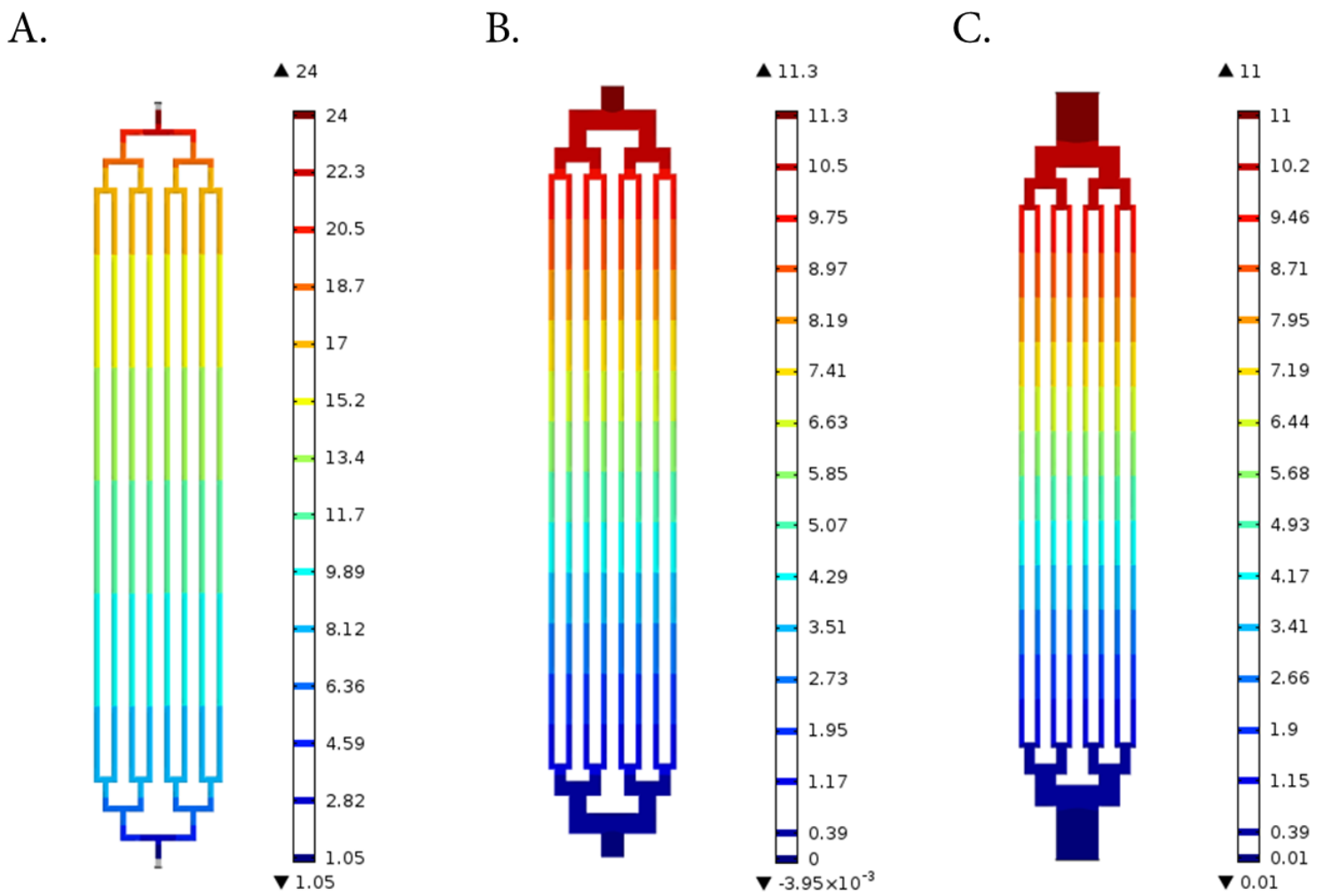

Figure 37: Pressure Drop in Various Branch Width Profiles. (A) Constant Width, (B) Stepping Width, (C) Murray's Law. Note that the constant width profile has a large pressure drop within the branching architecture and that the

Note that while the Murray's law model generated the most consistent flow rates and the lowest pressure drop, calculation of the widths of each channel (especially when having a non-circular cross-section) is computationally expensive and, given the height of the channels, the equation cannot be solved after the third branch, as the solution yields a negative value. Additionally, Murray's Law (in solvable systems) begins increasing more and more rapidly at the higher branches, and the requisite channel width become a significant portion of the area available. Since stepping widths produced a similar flow profile and had a comparably low branch pressure drop, this model was deemed to be the best option for use in the microvascular array.

Once the models of branching widths had finished running, CFD models of the different branching architectures were analyzed using CFD. During brainstorming, the team identified three different branching geometries which could be used for a microvascular network: square branches, circular branches and triangular branches. In order to determine which of the branches was able to generate the most uniform and physiologic relevant flow, each model was examined using COMSOL. Each branching pattern was examined for regions of low flow, which, physiologically, can induce regions of less-well developed endothelialization and clotting. Velocity profiles were also judged on overall uniformity of flow. The velocity profile for each of the branching mechanisms can be seen in Figure 38.

Note that the corners of the square branching vasculature, seen in Figure 38A, appeared to be low-flow, "dead-zones", in which fluid velocity was fairly low. Additionally, note that the regions on the flat wall opposite flow inlet to a junction have semi-circular "dead-zones" in which minimal flow velocity was observed. The circular branching architecture displayed in

Figure 38B shows an absence of corner-related “dead-zones”. The only “dead-zones” observed in this model were the regions directly opposite a junction inlet. The third branching alternative modelled was the split branching. Figure 38C shows the absence of “dead-zones” across from inlets to junctions, a trait not seen in the square or circular branching. There are, however still corners in which some (minimal) flow stagnation can occur.

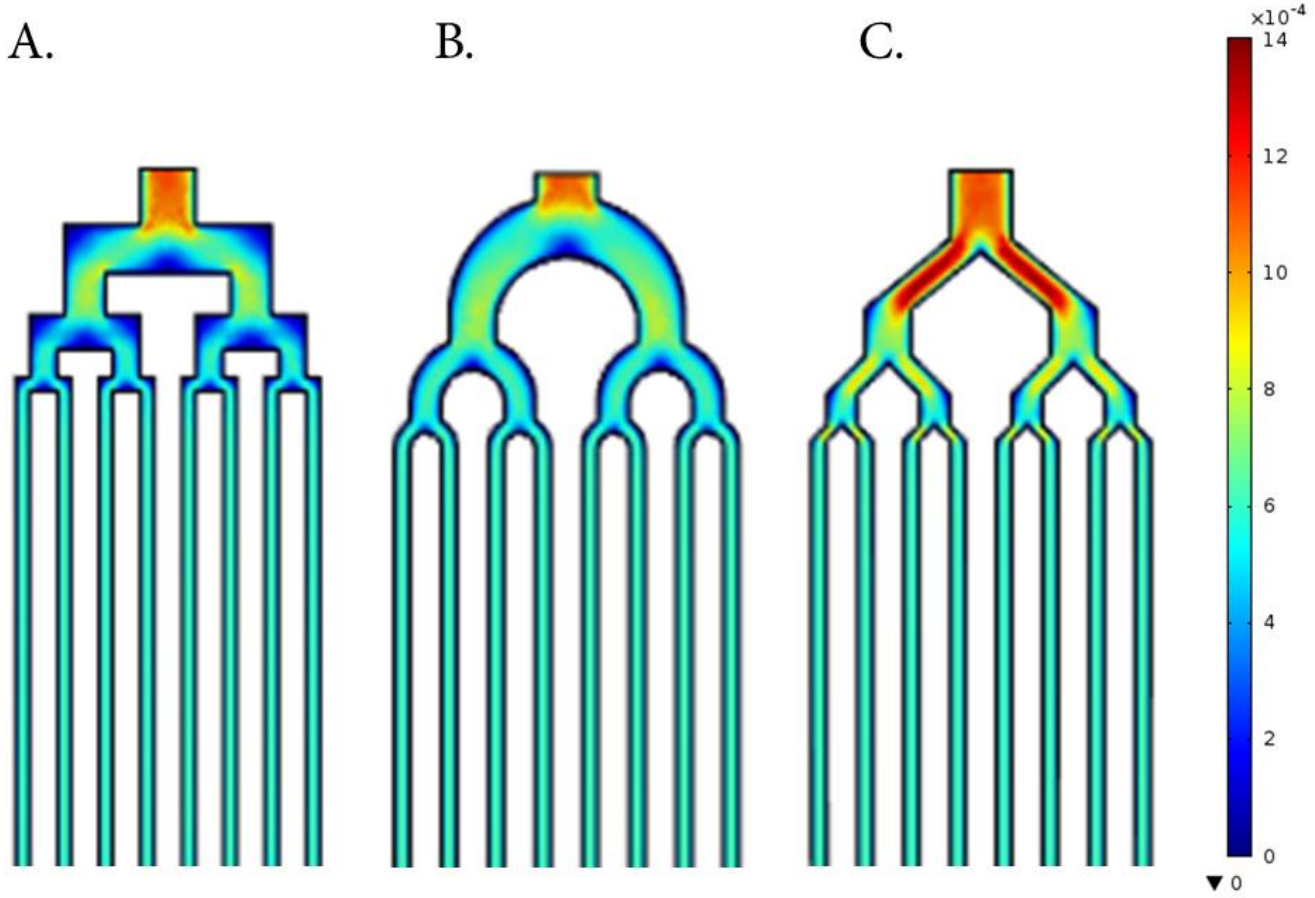

Figure 38: Comparison of Flow Velocities for Various Junction Geometries. (A) Square Branching. (B) Circular Branching. (C) Split Branching. Note that the circular branching algorithm reduce the flow stagnation in corners, while the split branching reduced the wall-stagnation opposite the junction inlet.

Additionally, the triangular branching algorithm shows apparent flow acceleration through the two exit channels of a bifurcation, a trait not seen in natural vasculature. Overall, flow modelling with various branching parameters revealed that a square branching pattern, despite its compactness, generates the most non-homogenous flow patterns, while the circular and split branching patterns generated more homogenous flow with fewer dead zones.

Another concern with branching algorithms is the pressure drop. If the pressure drop across the branching network is too high it suggests large branching resistances, which can generate non-physiologic shears on the walls. Ultimately, as described previously, the largest pressure drop should occur in the FVA and not in the branching region. The results of the CFD pressure analysis of each system can be found in Figure 39.

Note that the drive pressure of the square stepping branching algorithm was the lowest, measured to be 11.3 Pa, and the pressure drop across the channels was approximately 1.5 Pa. The circular branching had a fairly low driving pressure as well, calculated to be 11.4 Pa, with a pressure drop of 1.6 Pa across the branches. Finally, the pressure needed to drive the split branching geometry at physiologic flow rates was 12.7 Pa, with a pressure drop of approximately 2.5 Pa across the branching region of the network. This information is summarized in Table 56.

Table 56: Summary of Driving Pressure and Pressure Drop across Branching Region for Various Junction Geometries.

	Drive Pressure (Pa)	**Approximate Pressure Drop Across Branches (Pa)**
Square Branching	11.3	1.5
Circular Branching	11.4	1.6
Split Branching	12.7	2.5

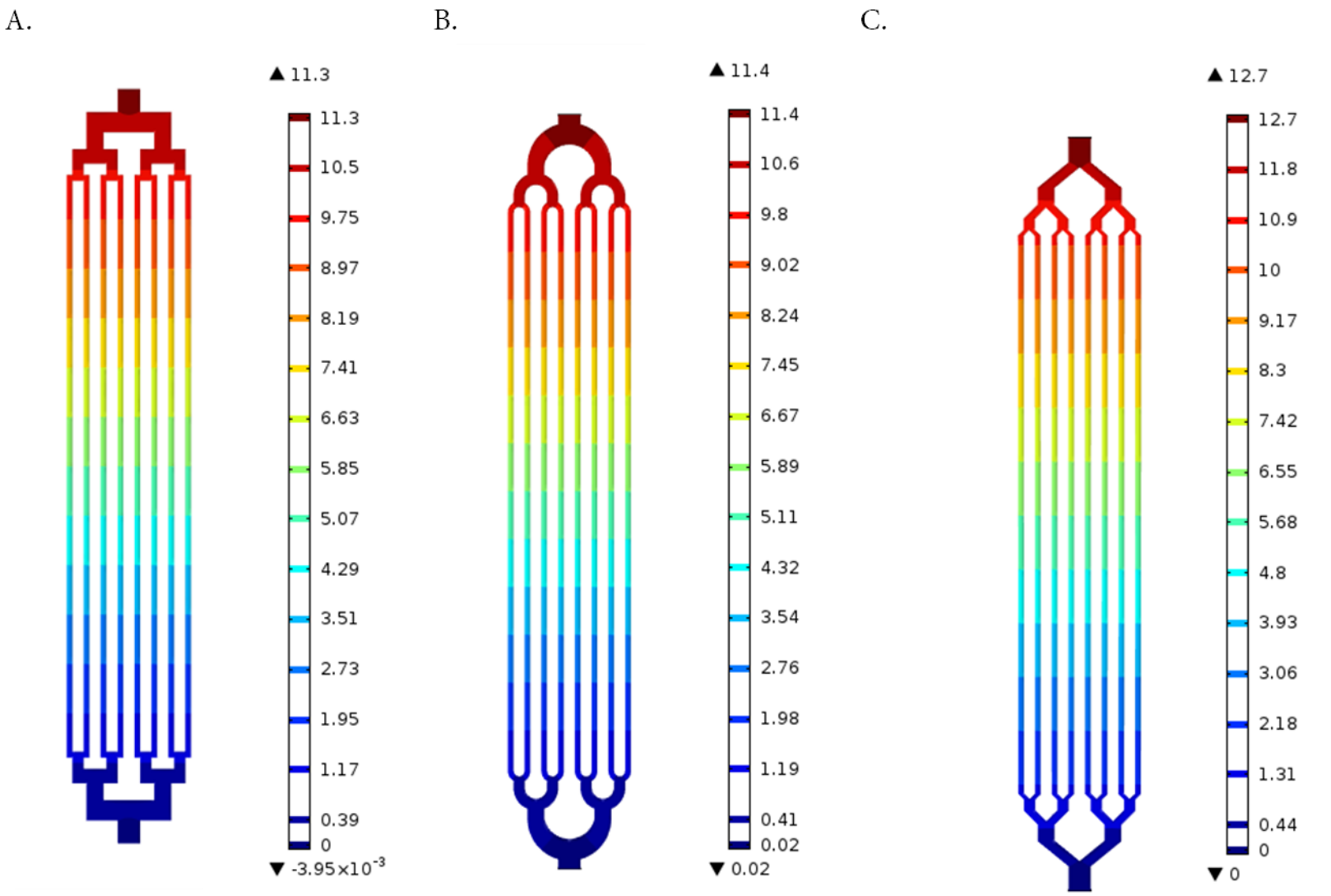

Figure 39: Pressure Profiles for Various Junction Geometries. (A) Square Branching. (B) Circular Branching. (C) Split Branching.

The information obtained from these simulations of both width and junction geometry provided important information to the team, who were able to optimize the design of the microfluidic system. Ultimately, the team produced a hybrid design, which used a Murray's Law width algorithm with a hybrid junction geometry that utilized a minimum number of corners to limit velocity "dead zones" and used a semi-circular flow divider to enhance flow division, minimizing the flow stagnation that was seen across from the junction inlet. Both the flow velocity and pressure analysis of this hybrid geometry can be seen in Figure 40.

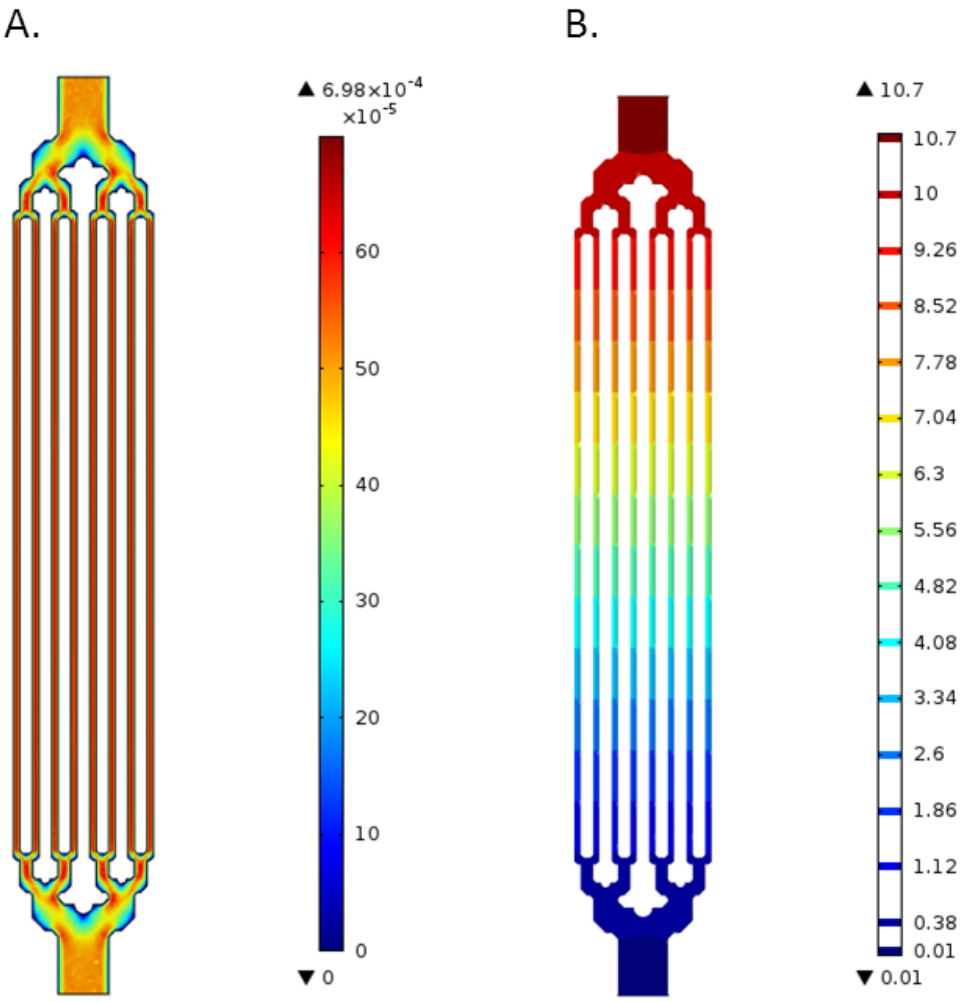

Figure 40: Optimized Microvascular Network. (A) Velocity Profile. (B) Pressure Profile.

This system shows highly uniform flow velocity at each level of branching, with no major "dead zones." Additionally, the pressure profile suggests that this hybrid system outperforms all of the other systems modeled; the driving pressure for this entire network was 10.7 Pa, and the pressure drop over the branching region was 0.6 Pa.

Unfortunately, due to budgetary and time constraints, this optimized architecture was not able to be validated, as this would require the fabrication of an entirely new wafer, which was not just in the eyes of the team.

5.4 Continuous Perfusion

After optimizing the microfluidic architecture, the team then progressed on to develop a continuously perfused system, as would be needed in order to deliver a constant stream of nutrients to cells loaded on the microvascular layer.

5.4.1 Continuous Perfusion through the Engineered Microvascular Layer

Following the experimental success in demonstrating discrete loading of microbeads into the channels of the designed microvascular network, the design team set out to achieve continuous perfusion through the system. The following experiments required additional trouble shooting and brainstorming in order to develop a technique that would continuously perfuse liquid through the microvascular channels. The design team developed and implemented various techniques in an attempt to demonstrate that the construct is able to contain discrete flow of medium through the channels without leaking in a bulk flow manner. Just as in the experiments that demonstrated that discrete loading of the channels is possible,

latex microbeads in solution were utilized as flow medium in all of the techniques used to induce continuous perfusion through the construct.

The design team worked through several iterations of experimental methods and techniques to continuously perfuse liquid through the construct with sustained flow. The various techniques included using a 30 gauge hypodermic needle to precisely flow liquid into the designed inlet of the microvascular network. The most promising orientation for the needle was horizontally placed between a patterned layer and a flat layer of fibrin. This technique can be seen in Figure 41.

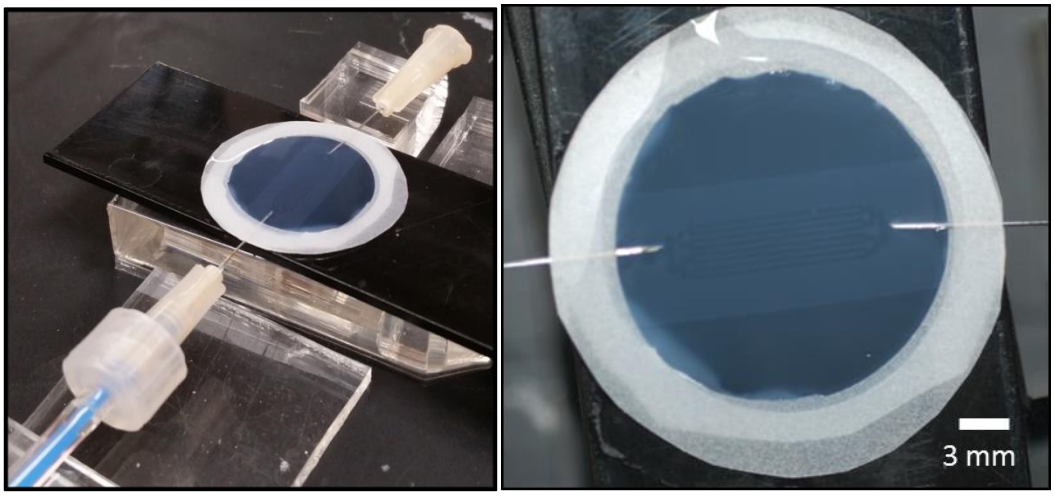

Figure 41: One patterned fibrin layer placed atop of a flat fibrin layer with hypodermic needles extending from the inlet and outlet

The design team attempted to drive liquid through the channels using this method with each of the fibrin to fibrin gel sealing methods discussed above in Section 5.2.1 Fibrin to Fibrin Adhesion. With each of the methods, the team encountered a challenge that limited progress forward with continuous perfusion through the patterned layer. The fibrin to fibrin sealing methods that showed promise in previous experiments were unable to facilitate flow of liquid

through the system. Each attempt resulted in a similar result, exampled in Figure 42. With weak fibrin to fibrin adhesion, the perfused fluid always escaped the gels from where the needle was inserted. The backflow of fluid through the needle occurred as the perfusate followed the path of least resistance, which was the space along the needle, as seen in Figure 42, below. In a best case scenario, some of the channels were perfused, however, backflow still occurred, as seen in Figure 43.

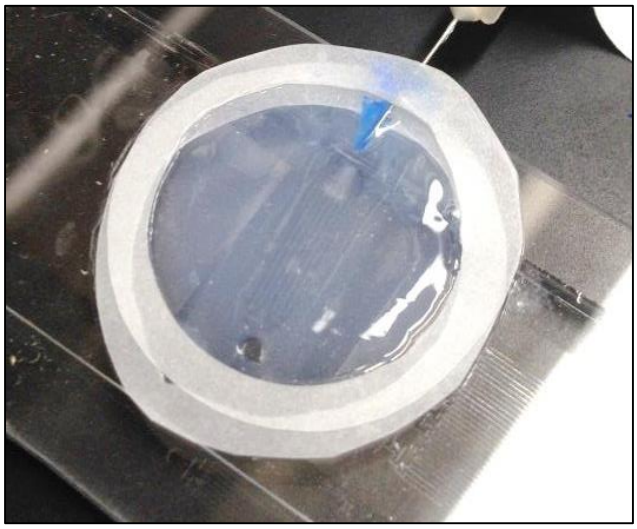

Figure 42: Back flow of microbeads in solution along the side of the hypodermic needle

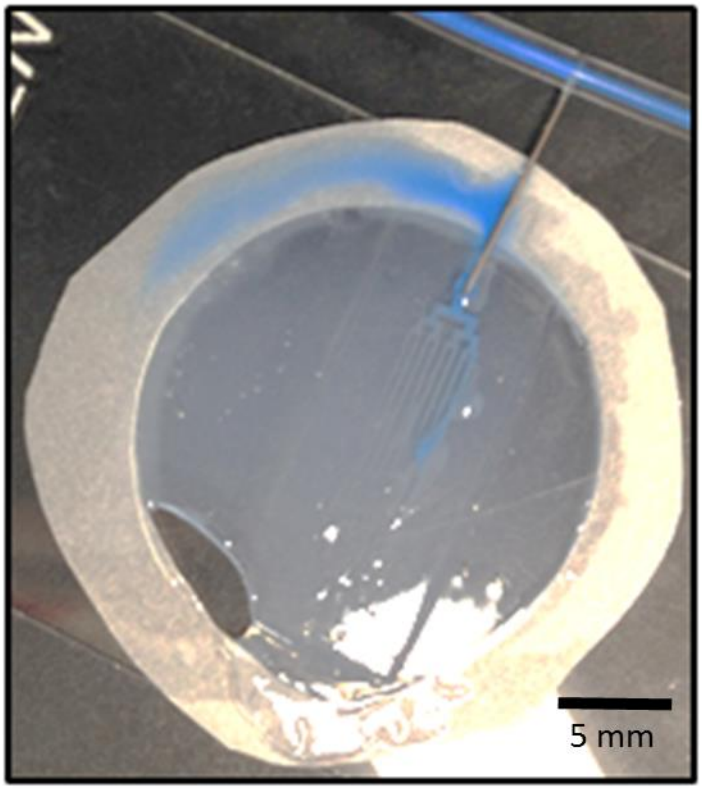

Figure 43: Semi-successful continuous perfusion

With the consistent limitation of backflow, the team was unable to successfully obtain sustained continuous perfusion through the engineered microvasculature. Although continuous perfusion was achieved in rare but unrepeatable cases, the design team decided to alter the microfluidic design in fibrin gels to continue validation of fibrin as a proper scaffold.

5.4.2 Need for a Model to Demonstrate Properties of Fibrin

Without reproducible continuous perfusion through the fibrin construct, the team set out to develop a model which could validate fibrin as a viable scaffold. This would allow for the proof of concept that fibrin is capable of containing a perfusate without leakage. This model required a different technique for creating a stronger inlet-fibrin interface to prevent backflow.

The simplest of models that demonstrates this is a single channel system that removes the complexity of creating a branched network.

5.5 Single Channel Continuous Perfusion

As discussed above, it was found that continuous perfusion in the vascular network designed to mimic physiological architecture was unachievable due the challenges associated with adequate sealing between adjacent fibrin layers. In an effort to demonstrate continuous perfusion in an engineered fibrin vascular system, the team designed a means for creating a single channel fibrin hydrogel, eliminating the need adhere two individual fibrin layers to form this channel. Not only was the channel itself designed, but the means for creating this channel through the use of a bioreactor was also designed.

5.5.1 Single Channel Bioreactor

The following device was created to demonstrate continuous perfusion through a fibrin channel. Figure 44 displays a robust single channel system that allows for continuous perfusion of liquid and further experimentation to better characterize fibrin as a biomaterial for use in a microfluidic based vascularized construct. The bioreactors displayed below are composed of a PDMS frame that has an inlet and outlet needle that are both secured in place when the fibrin is cast into the center well. There is a needle that is initially nested through the inlet and outlet that is removed after the fibrin hydrogel has fully polymerized, leaving a hollow single channel through the center of the gel.

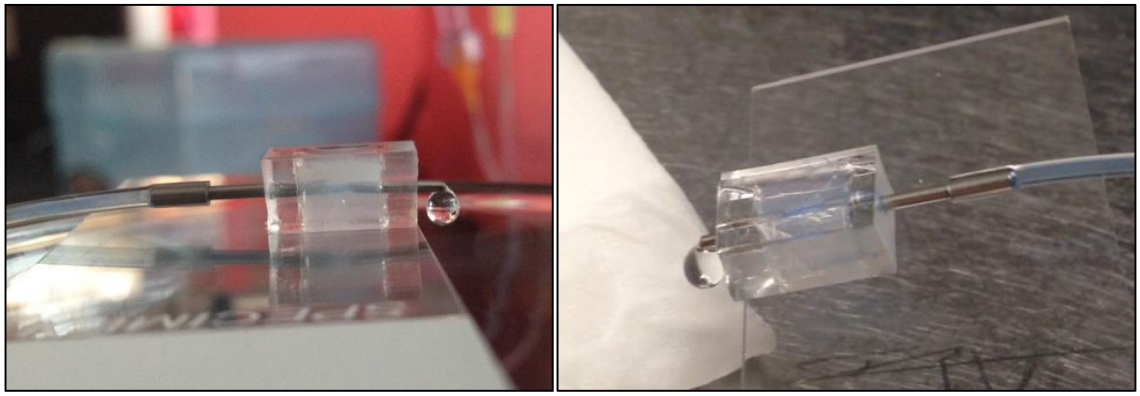

Figure 44: Single Channel Perfusion proof of concept with PDMS

Once these single channel bioreactors showed promising results, they were next tested using FITC to show both contained perfusion and the diffusion characteristics of the fibrin. In order to increase alignment of the inlet and outlet needles and decrease channel diameter to 300 µm, single channel frames were printed on a high resolution 3D printer. With the smaller more precise devices, the team flowed a 36 µg/mL solution of fluorescein isothiocynate (FITC) through while observing on a fluorescent microscope. Macroscopic images of this experiment are displayed below in Figure 45.

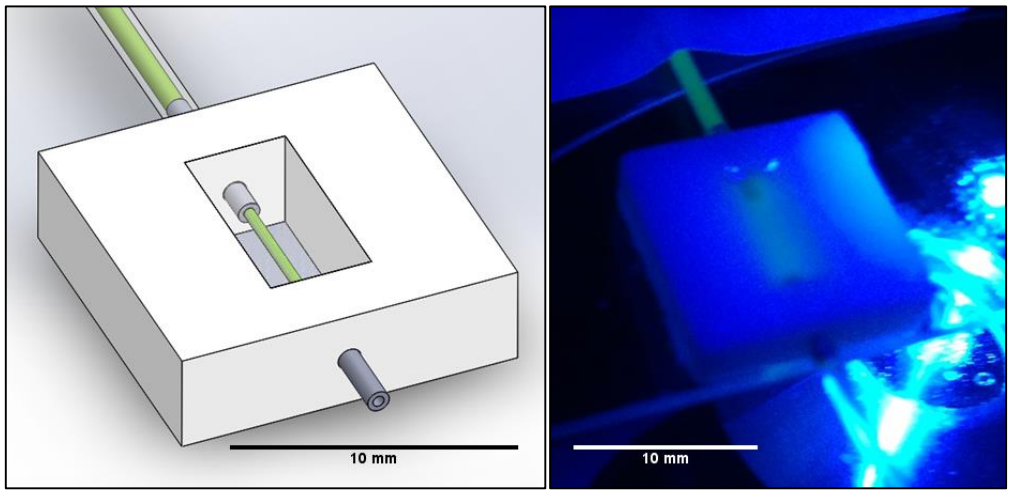

Figure 45: Single Channel Perfusion of FITC

5.5.2 Diffusion Assay with FITC

Flow and diffusion of FITC in the fibrin channel indicated that there was no bulk flow leakage of the perfusate and that the diffusion was observed to be at a constant rate that can be characterized. Both qualitative and quantitative data from this experiment is displayed below. The duration of this experiment was visualized at a magnification of 5X.

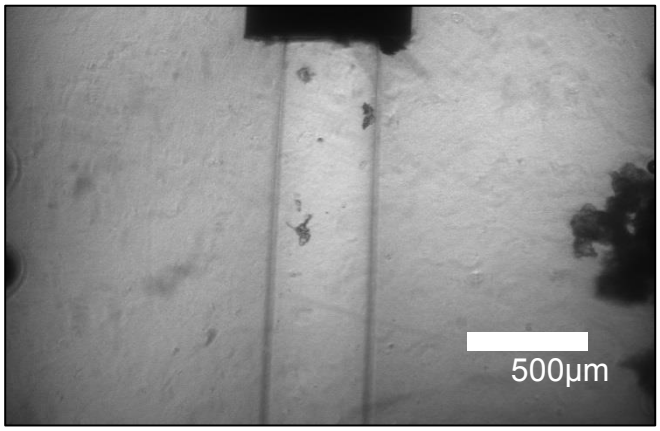

Figure 46: Bright field image of a single channel within fibrin gel with the inlet needle at the bottom of the image

The FITC solution was driven through the single channel for a duration of 14 minutes at a flow rate of 82 µL/hr. The channel was imaged in 1 minute intervals in order to both visualize and quantify the consistent increase in diffusion over time.

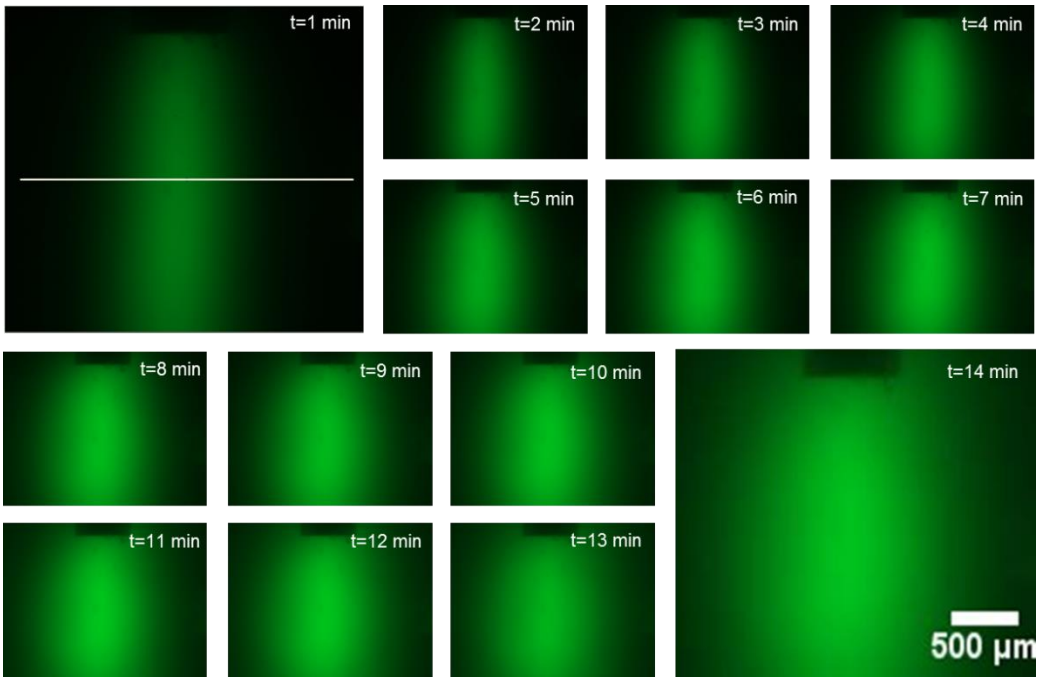

Figure 47: Diffusion of FITC from the channel into the surrounding fibrin through 14 minutes.

At each time point, the horizontal spread (as seen by the line in Figure 47, T=1 min) of the FITC intensity was quantified, providing a distance of diffusion over time. Figure 48, below, provides an intensity profile for each time point. Due to the saturation threshold of FITC, the intensity profile for each time point was restricted to a maximum intensity reading of 253.

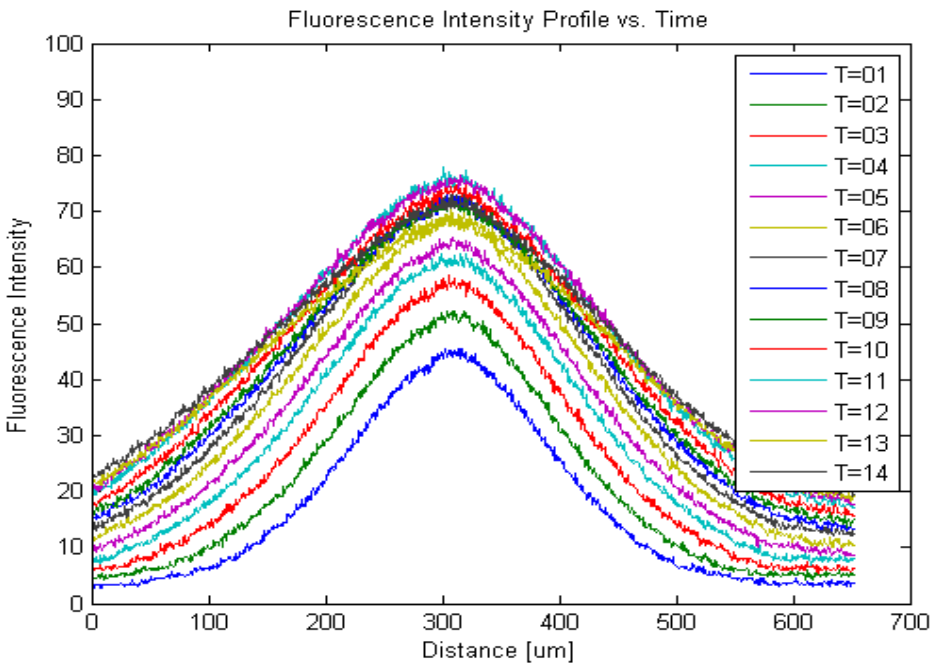

Figure 48: Quantization of intensity profile of FITC diffusion over change in time.

In Figure 48 above, the distance of diffusion spread with the corresponding fluorescent intensity creates a Gaussian distribution for each time point. This distribution indicates consistent diffusion of FITC through the gel, on both sides of the channel. Each time point shows an increase in intensity, indicating that diffusion through fibrin occurs at a constant rate. In order to adequately portray this consistency, the following graph was created, showing the Full Width at Half the Maximum (FWHM). In other words, for each time point, the distance of the width at half of the maximum intensity was plotted.

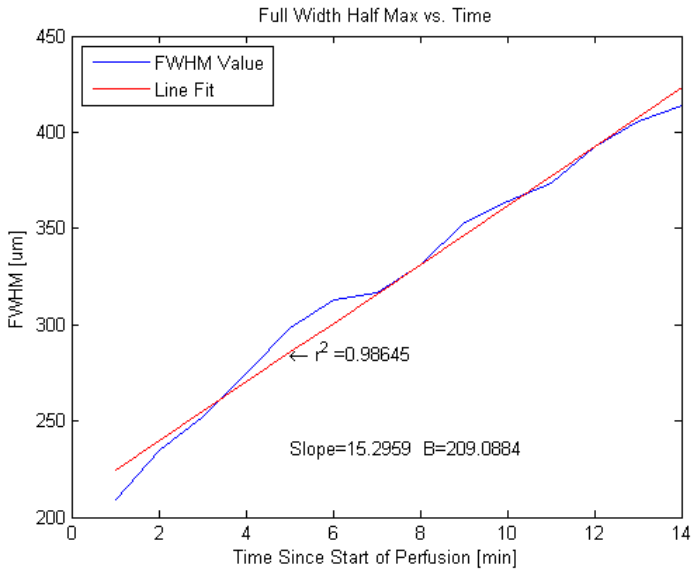

Figure 49: The diffusion of FITC through fibrin over time

As shown in Figure 49, the relationship between the FWHM and time creates a linear line. The linearity of this relationship further indicates that FITC diffuses through fibrin at a constant rate. This suggests that smaller molecules, such as oxygen (32 Da) and Glucose (180 Da), can likewise diffuse through fibrin at a similar rate, potentially reaching cells on the surface of the gel.

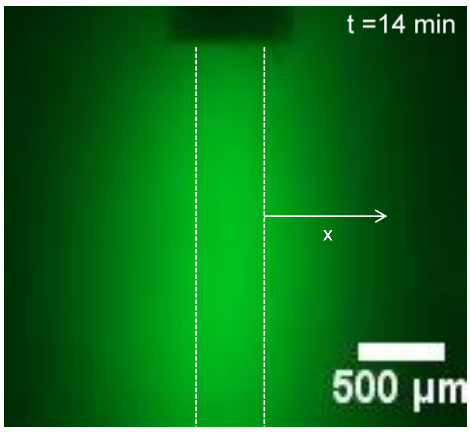

Figure 50: Diffusion schematic for calculations.

Figure 50 shows the direction of and where the following diffusion calculation were based on.

$$\frac{\partial N_{Ax}}{\partial x} + \frac{\partial N_{Ay}}{\partial y} + \frac{\partial N_{Az}}{\partial z} + \frac{\partial C_t}{\partial t} - R_A = 0$$

Equation 5: Rectangular Coordinates Mass Transfer Equation

$$N = flux; C = concentration; t = time; R = reaction$$

$$Assumptions:$$

$$No\ reaction\ between\ the\ fibrin\ and\ FITC$$

$$No\ Bulk\ Flow\ of\ FITC\ through\ the\ Fibrin$$

$$Non - steady\ state\ system$$

$$No\ diffusion\ in\ the\ y\ and\ z\ axis$$

$$\frac{\partial N_{Ax}}{\partial x} + \frac{\partial C_t}{\partial t} = 0$$

Equation 6: Simplified Rectangular Coordinates Mass Transfer Equation Based on Assumptions

$$N_{Ax} = -D_{AB}\frac{\partial C_A}{\partial x} + (Bulk\ Flow)$$

$$D = diffusivity$$

$$\frac{\partial}{\partial x}\left(-D_{AB}\frac{\partial C_A}{\partial x}\right) + \frac{\partial C_A}{\partial x} = 0$$

$$C_{AB}\frac{\partial^2 C_A}{\partial x^2} = \frac{\partial C_A}{\partial t}$$

$$\boldsymbol{\Psi = \frac{C_A + C_{A0}}{C_{AS} + C_{A0}}}$$

Equation 7: Dimensionless Concentration Equation

$$C_A = concentration\ at\ the\ value\ x;$$

$$C_{AS} = concentration\ at\ the\ surface\ of\ the\ channel;$$

$$C_{A0} = Concentration\ of\ FITC\ at\ time\ zero;$$

$$\Psi = dimensionless\ variable\ representing\ concetration;$$

$$C_A = \Psi(C_{AS} - C_{A0}) + C_{A0}$$

$$\partial C_A = \partial\Psi(C_{AS} - C_{A0})$$

$$\partial^2 C_A = \partial^2\Psi(C_{AS} - C_{A0})$$

$$D_{AB}\frac{\partial^2\Psi}{\partial x^2}(C_{AS} - C_{A0}) = \frac{\partial\Psi}{\partial t}(C_{AS} - C_{A0})$$

$$D_{AB}\frac{\partial^2\Psi}{\partial x^2} = \frac{\partial\Psi}{\partial t}$$

$$\frac{\partial^2\Psi}{\partial\eta^2} = 2\eta\frac{\partial\Psi}{\partial\eta};\ \eta = \frac{x}{2\sqrt{D_{AB}t}}$$

$$\boldsymbol{\frac{C_A + C_{A0}}{C_{AS} + C_{A0}} = \Psi = 1 - \mathrm{erf}\left(\frac{x}{2\sqrt{D_{AB}t}}\right)}$$

Equation 8: Error function in Relation to Ψ

$$Boundary\ Conditions:$$

$$z = 0;\ C_A = C_{AS};\ \Psi = 1$$

$$z = \infty;\ C_A = C_{A0};\ \Psi = 0$$

$$t = 0;\ C_A = C_{A0};\ \Psi = 0$$

$$t = \infty;\ C_A = C_{AS};\ \Psi = 1$$

Example Calculation:

$$\frac{C_A + C_{A0}}{C_{AS} + C_{A0}} = 1 - \text{erf}\left(\frac{x}{2\sqrt{D_{AB}t}}\right)$$

$$At\ t = 60\ [sec]\ and\ z = 0.01\ [cm]$$

$$C_A = 4.667\ [Intensity]$$

$$C_{A0} = 3.0\ [Intensity]$$

$$C_{AS} = 12.407\ [Intensity]$$

$$\therefore 1 - \frac{4.667 - 3}{12.407 - 3} = \text{erf}\left(\frac{0.01}{2\sqrt{60D_{AB}}}\right)$$

$$0.823 = \text{erf}\left(\frac{0.01}{2\sqrt{60D_{AB}}}\right)$$

$$0.96 = \left(\frac{0.01}{2\sqrt{60D_{AB}}}\right)$$

$$\frac{\left(\frac{0.01}{2(0.96)}\right)^2}{60} = D_{AB}\ \left[\frac{cm^2}{s}\right]$$

$$\boldsymbol{D_{AB} = 4.52x10^{-7}\left[\frac{cm^2}{s}\right]\ at\ t = 60[sec];\ x = 0.01[cm]}$$

In our first calculation we see that the diffusivity is equal to 4.52 x 10^{-7} cm^2/s. This calculation was then done for all of the time points at the same distance (0.01cm) from the channel. The below table displays all of these values and the average diffusivity of the system.

Table 57: Diffusivity Calculations with Respect to Time

Time [min]	Diffusivity
1	4.52112E-07
2	5.26028E-07
3	6.51042E-07
4	9.01096E-07
5	1.15741E-06
6	1.19697E-06
7	1.48333E-06
8	1.54093E-06
9	1.80845E-06
10	1.66667E-06
11	1.96912E-06
12	2.36206E-06
13	2.25347E-06
14	2.8855E-06

$$D_{avg} = 1.5\ x\ 10^{-7}\ \left[\frac{cm^2}{s}\right]$$

Based on this data, the diffusivity of FITC through 20 mg/ml fibrin hydrogel is 1.5 x 10^{-7}. This diffusivity value does not account for the cumulative intensity due to the 3D nature of the fibrin hydrogel and the imaging technique. The imaging technique is part of the reason why the diffusivity changes over time. Figure 51 shows the change of intensity over time at the point x=0.01 cm from the edge of the channel.

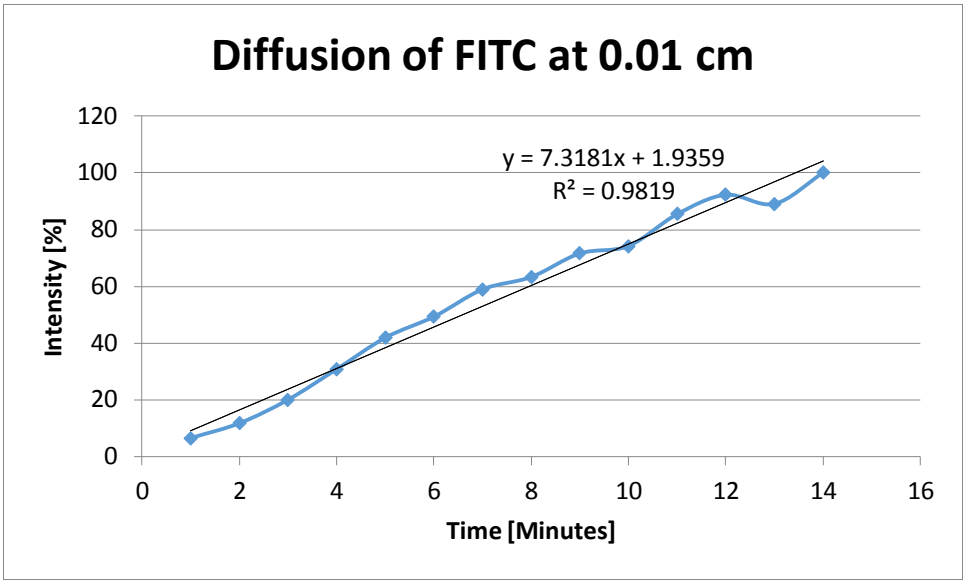

Figure 51: FITC Diffusion over time for a fixed (x,y,z)

5.5.3 Multiple Channel Perfusion

Given the success in achieving perfusion through a single channel, using the method discussed above, the ability to flow perfusate through multiple channels was assessed. FITC solution was perfused through the center fibrin channel while a counter current of 1xPBS was perfused through the outside two channels. This multi-channel system demonstrates that it is possible to create a construct with 300 µm diameter channels that are within 450 um from each other edge to edge. Therefore, the potential for creating a functional vascular area, consisting of multiple individual channels, is conceivable.

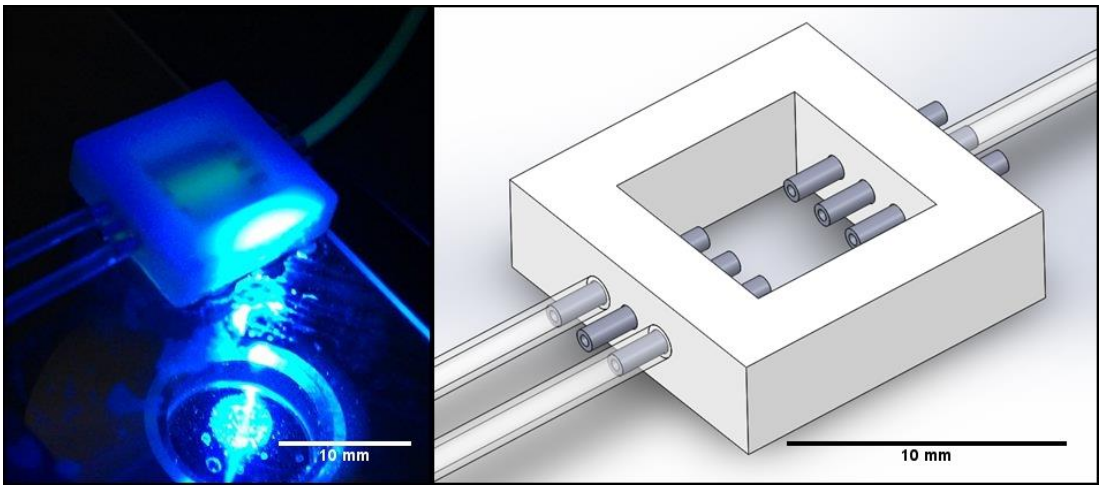

Figure 52: Counter current multi-channel perfusion through fibrin

5.5.4 Cellular Viability

The cellular viability study performed produced very promising results. After fibrin gels were cast in the 3-D rapid prototype parts, seen in Figure 53, 100,000 cells were seeded in media on top of the gel. After 4 hours, cells were imaged to verify successful attachment to the gel and the media was removed and replaced with DPBS. The channel was then perfused with either DMEM culture media (experimental condition) or 1X DPBS, which was the control. Each solution was perfused at 82 µL/hour (flow rate calculated assuming a 300 µm/sec flow velocity and using the observed channel diameter) through the single channel, with 1X DPBS covering the cells to maintain hydration of both the hydrogel scaffold and the cells.

It was hypothesized that medium would diffuse out of the channel and travel to the layer of the cells cultured on the surface, supplying them with the necessary nutrients to keep them alive. A simplified schematic of this process can be seen in Figure 54.

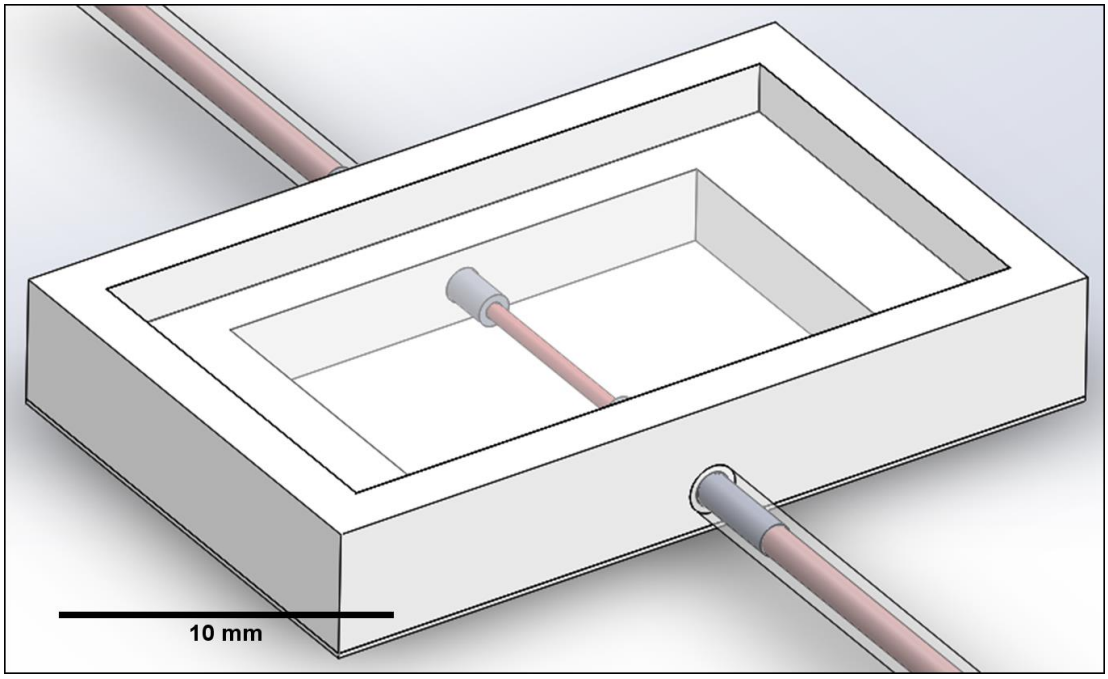

Figure 53: SolidWorks model of final design

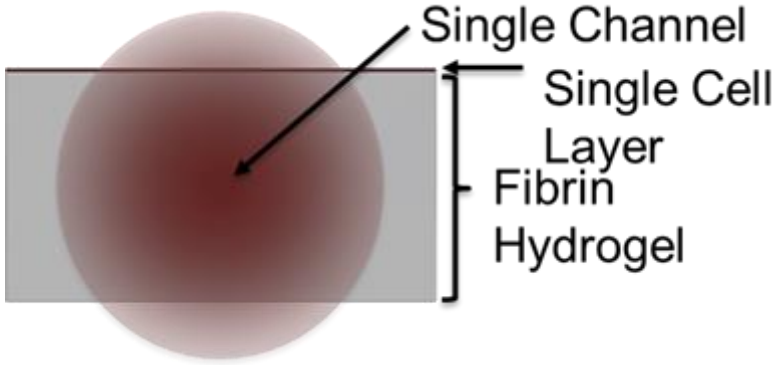

Figure 54: Illustration of Single Channel Diffusion to Cellular Monolayer

24 hours following the initiation of perfusion, the gels were stained with Calcein AM, Ethidium-dimer and Hoechst 33342 in order to stain for living, dead and all cells, respectively.

The cells were then imaged on a Leica inverted fluorescent microscope. Representative images from the DMEM and DPBS perfused channels can be found in Figure 55.

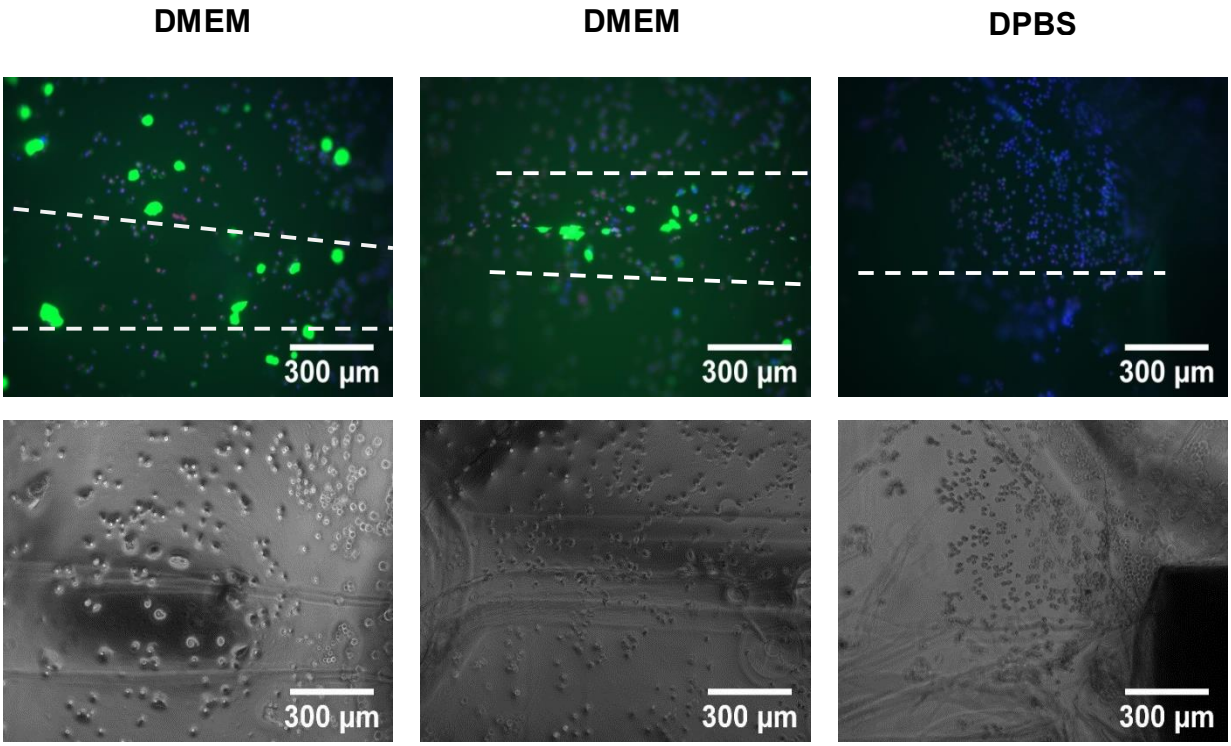

Figure 55: Cellular viability results with single channel perfusion

Based on this figure, it appears that the single channel system perfused with media enhances overall cellular viability. In the medium perfused channels, living cells are clearly seen atop the scaffold. In contrast, in the DPBS perfused channels, all cells were found to be dead. This suggests that the nutrients perfused through the channel have diffused through the scaffold and are able to provide moderate support to cells cultured on the surface. Although both treatment groups were seeded under media initially, the control scaffold shows that this medium provided no overall enhancement to cellular outcome.

CHAPTER 6: DISCUSSION

The purpose of this project was to design and develop a fibrin-based scaffold that incorporates a micro-fluidics-based vasculature that allows for the perfusion and diffusion of nutrients to all regions of a multi-layered construct. As outlined previously in this report, thorough analysis of the original problem statement alongside comprehensive interviews with the clients and users led to the formation of five top-tier objectives: mimic physiological architecture, able to be perfused, maintain cellular viability, easy to handle, easy to produce. In order to accomplish these objectives, a series of functions were identified. The most important functions include: harness high pattern fidelity, permit oxygen diffusion, encourage cell adhesion, consist of physiological interchannel spacing, and sustain continuous perfusion. Throughout the duration of this project, each of these functions were achieved and thus, all top-tier objectives were accomplished.

The subsequent sections provide a succession of milestones through analysis of results presented in Chapter 5: Design Verification. As each milestone was subsequently completed, it was deemed that the original microfluidic system was difficult to continuously reproduce, ultimately leading to the development of two related perfusion systems: (1) a thin construct with an embedded micro-vascular network and (2) a thick construct with a single channel capable of continuous perfusion. Although the team encountered the challenge in terms of integrating all design components into one device, the team successfully demonstrated each objective and function, motivating the potential for designing a fibrin- based construct having a microvascular network that is capable of undergoing continuous perfusion in the foreseeable future.

6.1 PROJECT MILESTONES

6.1.1 Engineer Microvascular Network

The design of microvascular network was accomplished through the preliminary design of a bifurcated network utilizing a step-down branching mechanism of square shaped branching geometries, having a functional vascular area of 8 channels. After this design was transferred from a fabricated silicon wafer onto PDMS, fibrin gel was produced and casted directly onto the microfluidic pattern, which were encompassed by Vellum paper rings. Sizes of PDMS molds were verified as seen in Figure 24 and Figure 25. These results showed that photo and soft lithography procedures were performed relatively accurately.

After allowing development in distilled water, the gels were able to be manually removed from the PDMS template. After removal from the PDMS, it was found that fibrin expressed high pattern fidelity. Figure 28 shows a qualitative analysis of the PDMS mold and fibrin gel. It is obvious from a visual perspective that the two materials appear nearly identical, indicating a high pattern fidelity in fibrin. Furthermore, Figure 29 displays quantitative analysis of dimensions, showing that dimensions are very similar, with a maximum deviation of 8% in size, which is seen in the first level of branching. This can potentially be attributed to the fact there is an n of 1 for this measurement.

The ability to create a microfluidic network within an implantable biomaterial served as an extremely promising result in terms of future cardiac tissue engineering prospects. Furthermore, the ability to prove maneuverability of these gels is critical with regard to

transporting individual gel layers and/or orientating them to produce multi-layered constructs. Ultimately, the proficiency in developing a microvascular network in fibrin was a huge milestone that needed to be achieved in order to address the perfusion and channel localization of perfusate.

6.1.2 Demonstrate Channel Localization

A major milestone in developing a construct with an engineered microvascular network was demonstrating that a perfusate solution remained localized within the channels and did not leak between the layers. In order to achieve a sealed, localized channel, the design team aimed to seal fibrin gels to each other. Showed in Figure 30 and Figure 31, gels were not easily sealed. When directly casting a gel on top of a premade gel, the two layers will seal, however this strategy would disrupt microfluidic channels in a fibrin gel as the channels would likely be filled with non-polymerized fibrin gel. The most successful layering of two gels to achieve contained loading of channels was found to simply be layering two casted gels on top of each other.

Microfluidic channels were loaded with a microparticle solution via capillary action. The gels were hole-punched at inlet and outlet to allow capillary action to be the driving force of discontinuous perfusion. Figure 32 displays an example of a prepared gel, which can be loaded with microparticles to verify no leakage occurs within the gel. Figure 33 and Figure 34 provide qualitative proof that these channels can be successfully loaded and will not leak into the bulk of the gel or between layers. Given that the channels were able to contain microparticles without causing leakage of particles or damage to interchannel fibrin walls, the potential for

achieving continuous perfusion through a microvascular network within a fibrin-based construct was next verified.

6.1.3 Design and Optimize Microvascular Architecture

The design of the microvascular architecture was optimized through the use of computational modeling. Figure 36 and Figure 37 examined flow velocities and pressure drops across square branching systems which varied in width profiles. From the modeling, it was clear that a constant width branching was the worst case scenario. A stepping width geometry was much improved, however, a Murray's law branching width slightly outperformed the stepping width branching algorithm. Subsequently, the design team examined branching geometries in terms of the type of branch. Figure 38 and Figure 39 examine these branching geometries and were used to mainly examine dead zones within a branching network. By examining these dead spaces, an understanding of how to eliminate them was developed.

Because each parameter was isolated by holding the remaining parameters constant and only altering one parameter, the optimal condition for each parameter was determined, as shown in Figure 40. The results obtained from these simulations allowed for the design of a microfluidic network that consists of a combination of these optimal conditions. The resulting hybrid design is presumed to generate ideal conditions upon being fabricated and essentially patterned into a fibrin gel, creating even distributions of velocity and pressure through the channels while minimizing the amount of dead space within the channels.

6.1.4 Establish Continuous Perfusion

The team made many attempts to drive fluid through the engineered network (examples in Figure 41); however, due to inadequate sealing between layers, the fluid took the path of least resistance, which was backwards along the inlet needle (Figure 42). The design team was able to accomplish semi-continuous perfusion is minimal cases (Figure 43), however, it was deemed important to create a simpler system in order to validate continuous perfusion and cellular viability. Although continuous perfusion was found to be not reproducible in the microvascular network system, it was proven that a channel within fibrin is capable of facilitating continuous perfusion for an extended period of time as seen in Figure 44. The design and development of a method for creating a single channel within fibrin omitted the need for establishing a seal between two discrete fibrin layers. By confirming the ability of fibrin to contain the flow of perfusate, the use of fibrin as a biomaterial in the development of an engineered cardiac construct was validated.

To further validate continuous flow as well as characterize diffusion within a fibrin gel, FITC flow analysis was performed. From Figure 47, the design team qualitatively was able to demonstrate that fibrin controlled the rate of diffusion. FITC was not able to immediately diffuse through the gel and was shown to slowly diffuse at an apparent constant rate. Using these images, Figure 48 was constructed to quantitatively display the diffusion of nutrients. Consequently, a Full-Width Half-Max graph seen in Figure 49 was created to display a nearly constant increase in intensity of FITC over time. Furthermore, using the data obtained from Figure 48, a diffusion coefficient of 1.5×10^{-7} cm^2/second was calculated. Due to the novelty of using a 20 mg/mL fibrin hydrogel as a perfusable construct, there is no published data on

diffusivity values of FITC. However, this diffusivity value is on the same order of magnitude as small molecules diffusing through a solid (Bergman, 2011). This diffusion coefficient for FITC in fibrin is useful to understand that smaller molecules such as glucose or oxygen will theoretically have a greater diffusion coefficient.

6.1.5 Perform Cellular Validation

Cellular validation was performed through the design of an experiment that confirmed vascularization as the source of cell survival. Most discernable from Figure 55, the account of cellular survival on the surface of the construct in response to continuous perfusion of cell media indicates the proficiency of fibrin as a material in terms of fostering diffusion across the thickness of the layer. The evidence suggests that perfusion of media vs 1X DPBS has a significant impact on cellular survival. No cells had survived on all four control experiments. In imaging three successfully perfused channels with media, all contained cells alive above the channel. The distance from the top of the channel to the top of the gel is 600 μm. In each experimental construct, cells were at a minimum alive directly above the channel. In some cases as seen in the top left image of Figure 55, cells had survived much farther than the solely above the channel. Therefore it is possible that a diffusion limit of media through a fibrin gel exists and is between 600 μm and approximately 1 mm.

Not only did this experiment indicate the potential for cellular survival and proliferation in/on fibrin, but it also confirmed the importance of a vascularization source. By creating an experiment that compared the effect of flowing cell media through the single channel system with that of flowing PBS through the channel, the team was able to confirm the necessity of a vascularization source in producing an engineered tissue construct. Because cells survived after

being seeded on the surface of the construct consisting of continuous flow of media, as opposed to PBS, the presence of a vascularization source was proven as a vital component to a tissue construct.

6.2 Comparison to Existing Constructs

As discussed previously, in Chapter 2, the current strategies currently being researched to regenerate cardiac tissue include injectable hydrogels and myocardial tissue element (MTE). The use of injectable hydrogels involves the insertion of a cell-laden hydrogel directly into the region where the myocardial infarction occurred. The MTE strategy consists of the development of a functional myocardium layer in vitro, which is later implanted into the region of the infarction.

6.2.1 Advantages

Both the strategies mentioned above are similar in that they lack vascularization, limiting the thickness of the construct due to the distance of oxygen diffusion. Without vascularization, the current strategies will fail to reach physiologically relevant thicknesses. In contrast, the components of this project, including both the bifurcated system as well as the single channel system, consisted of a source of vascularization, permitting the flow of cell culture media through the construct.

6.2.2 Disadvantages

If the construct developed during this project were to be utilized clinically, the procedure involved in implanting this construct is extremely invasive, in comparison to the use of an injectable hydrogel, for example. In a clinical application, the inlet and outlet ports of this

construct would need to be sutured into the arterioles and veins, respectively. Upon connection to the patient's circulatory system, the surgeon would then need to verify that perfusion of blood reaches all layers of the construct. In comparison to more simple approaches, the discrete layer system presents more uncertainty in terms of facilitating perfusion through multiple engineered, vascular layers. The level of precision and difficulty in performing this procedure is a major disadvantage, especially in comparison to the comparatively user friendly nature of the other strategies mentioned. In addition, the surgeon would need to delicately customize the dimensions of the construct, prior to implantation, as each patient will suffer from varying degrees of necrosis following a myocardial infarction. On the other hand, the properties of an injectable hydrogel allow for the hydrogel to conform to the specific region of necrosis upon injection.

Lastly, the proficiency of endothelialization of the construct is unknown at this point. Given that cells survive in fibrin due a continuously perfused vascular layer, it can be assumed that cells would eventually create a vessel from the initial patterned network. As the fibrin degrades, it can be assumed that cells will gradually replace fibrin, creating lumens and essentially blood vessels. However, if this endothelialization process fails to occur then the construct would be clinically irrelevant. Without the formation of an endothelialized lumen, platelets normally present in blood plasma will naturally adhere to the fibrin, creating clots in the vascular network. With the fact that endothelialization of the vascular network has yet to be observed, this uncertainty presents a major disadvantage with regard to clinical considerations.

6.3 Future Impacts and Implications

Since the results of this project will likely be used by the client, and potentially others in the future, it is important to consider the impacts and implications of this product. This product will be analyzed in terms of economy, society, environmental, political ramifications, ethical concerns, health and safety issues, manufacturability, and sustainability.

6.3.1 Economy

Due to the use of fibrin-based, tissue engineered cardiac constructs is currently limited to research in vitro, this device has little impact on the economy in the foreseeable future. Although the components of this project, the design of a microvascular network and a model for demonstrating continuous perfusion, have the potential to address current issues associated with tissue engineering, such as lack of vascularization, there are no considerations of animal or human clinical trials in the near future. This is due to both the high costs associated with clinical trials, and the limited research data which is currently available. Before this device can have any significant economic impact, much more research must be performed with fibrin-based, vascularized constructs. If a fibrin-based, vascularized cardiac construct was to be optimized in the future and implanted in humans as a treatment for myocardial infarction, then the device would have some economic impact as a controlled source of producing fibrin in mass amounts would need to be established. In addition, the cost of hospital resources, including the implantation procedure itself and all post-operational costs (food, any supplemental medications, living quarters, etc.) would need to be considered if this device were to be perfected and administered to humans.

6.3.2 Society

If the results of this project were to become applicable in vivo, which is infeasible in the near future given the need for further research, this project may eventually pose a substantial impact on society. For instance, if fibrin-based cardiac constructs were deemed effective in regenerating cardiac tissue, the quality of life of the average person will be greatly improved. The potential availability of a reliable treatment option for cardiac tissue death would eliminate the need for a heart transplant or the implantation of a LVAD device in some cases. This option would offer a dependable cure for heart failure, creating a happier, less stressed atmosphere in the case of heart failure. In addition, if the results of this project were to be perfected in the future, the use of fibrin as a scaffold material would most likely extend to other tissue engineering applications, calling for an increase in productivity and efficiency of laboratory research.

6.3.3 Environmental

Since the components designed during this project are still limited to the research phase and will not be advanced to the clinical trial phase of development for some time, there are no environmental impacts directly associated with the results of this project. If the design of an engineered, micro-vascularized cardiac construct was to be perfected and the potential for in vivo implantation into a human was attainable, then the construct would have the potential for posing environmental consequences. If this construct was perfected and deemed successful in terms of regenerating cardiac tissue, the means for production of this construct need to become more efficient and would be scaled up to meet the clinical demand. This would increase the demand for fibrin components, such as fibrinogen and thrombin.

Since both fibrinogen and thrombin are derived from bovine sources, the increase in demand for these proteins may lead to an increase in source populations, which will increase the demand for a number of resources needed to house cattle. These resources include land, housing facilities, food, waste management, and increased labor force to maintain the source population. Any increase in energy needed to raise and maintain cattle as well as the waste produced may significantly impact the environment. For instance, ample land and water must be allotted as living space for the increased number of bovine sources. This additional need for space may involve clearing trees and dredging, severely impacting the area's natural environment. Obtaining food sources, in order to sustain the cattle, also require additional land allocation, further contributing to the overall environmental impact. Furthermore, the facilities needed to house the bovine sources will require electrical energy, requiring an increased use of limited natural fuel resources. Additionally, the increased cattle population would lead to an increase in methane production, one of the most potent contributors to global warming.

The increase in source population could have some positive environmental impacts as well. If properly regulated, environmentally beneficial actions could be taken, such as the use of renewable energy sources or converting waste from sources into fertilizer. Through proper management, the impact of an increased fibrinogen and thrombin source population can have minimal effects on the environment, while still meeting the growing medical demands.

6.3.4 Political Ramifications

The results of this project currently have minimal political ramifications. Because the production of micro-engineered tissue constructs is very much in the research and initial development stages, the results produced during this project has little effect on the

commercial or industrial market. If this results of this project were to be incorporated into a functional, successful cardiac patch the efficiency and production of fibrin-based tissue scaffolds would be likely enhanced, but mostly in a research and development setting. Although there are multiple research laboratories in various countries who would find the results of this project useful, however, bovine sourced materials such as fibrin cannot be used in the European Union. Until the engineered, microvascularized construct becomes commercialized or the results of this project are adapted and developed to create tissue engineered scaffolds on a commercial scale, there would be little effect on the international market and thus, major political impacts are unforeseeable.

6.3.5 Ethical Concerns

There are minimal ethical concerns associated with the results of this project. The effort to engineer a fibrin-based, microvascular layer is designed to aid in regenerating necrotic cardiac tissue following a myocardial infarction. Because the components designed during this project could eventually be used in tissue regeneration technologies, which would improve the quality of life for patients suffering from heart failure, there are no direct ethical concerns associated with this project. Ultimately the tissue scaffold will rely on adult stem cells from the patient, therefore, it does not raise any ethical concerns. The only ethical concern that could be raised is with the materials that are used in this device. For instance, fibrinogen and thrombin, components used in the formation of fibrin gel, are derived from bovine sources. Some potential users may feel uncomfortable using materials from an animal source, even though the manner in which the materials were obtained was ethical.

6.3.6 Health and Safety Issues

The results gathered from this project have the potential to greatly improve the health of patients suffering from heart failure, in the future. By providing a treatment option for heart failure patients, alternative to the dangerous procedures associated with heart transplants and LVAD implantations, the future ramifications of this project pose substantial effects on the quality of life of a large portion of the human population. Following initial development of this device, assuming that continuous perfusion through a bifurcated, microvascular network is eventually achieved, extensive tests will be necessary to verify the construct's safety, reliability, and reproducibility. Once these tests are completed and the product is approved by the FDA, it will be considered safe for the majority of the population. However, the inevitable danger associated with the use of fibrin in clinical applications will continue to be apparent; since fibrin naturally exist in the body as a clotting agent, the mere presence of fibrin in the heart will not cease to be a risk. The way in which this device is implanted in the body would most likely be perfected in a way that minimizes this risk.

6.3.7 Manufacturability

The device created by the design team was intended to be as straightforward and easy to use and as reproduce as possible. Initially, the design team sought to design a single system that incorporated both a microvascular network and a continuous system. Although the team ended up designing two distinct components of the project, which separately addressed all objectives originally outlined by the client and users, the manufacturing process utilized for the production of both systems were relatively simple in that they did not require complicated machinery or expensive materials.

It was found that after fabricating the template devices, needed to produce the fibrin-based layers themselves, the production of the actual fibrin constructs is relatively simple and cost effective. The fabrication of the silicon wafer, used as a template for the production of the PDMS mold, requires an extensive manufacturing process in order to produce the micro-patterned features with high accuracy. After the PDMS mold is acquired, the production of the fibrin constructs is very repeatable assuming that the protocol for fibrin production and casting is followed, in order to produce patterned fibrin layers. Likewise, for the continuous perfusion system, the manufacturing procedure needed to fabricate the template device required complex machinery while the fabrication of the fibrin constructs themselves remained relatively simple. After the bioreactor, containment device was 3-D printed with precise dimensions and features, in order to secure all components during the creation of the single channel, this same device can be reused in the production of future single channel systems. After thorough training is provided to the user, enabling proficiency in creating single channels in fibrin, the production of the fibrin system is cost effective, requires no complicated machinery, and is repeatable (assuming thorough training has been provided).

6.3.8 Sustainability

This device itself is composed entirely of fibrin, which requires some energy to produce, often from a bovine source. In contrast, the material used for the mold in creating patterned fibrin is PDMS, which cures at room temperature and requires very minimal energy to produce. Although the materials used in the device itself are relatively sustainable, the steps and materials utilized throughout the process of developing the final device requires more energy. For instance, the template utilized for the production of the PDMS mold must undergo an

extensive fabrication procedure, consisting of several energy sources and chemical sources, producing the silicon wafer with imbedded microfluidic patterns. Indeed, this step requires a substantial amount of energy and therefore is not very sustainable. However, because this fabrication process is necessary to only produce the template, this process is seldom undergone, assuming that the template is used with care and doesn't endure damage thus requiring the fabrication of a replacement template. As a disclaimer, any future developments with regard to this project will likely omit this complicated template fabrication process since this component of the project led to several challenges. Instead, channels will be created in fibrin using a method that is less energy costly. In addition, the use of the results of this project, if they were to be eventually enhanced and operational in vivo models, would pose no major effects on the ecological world, as the device itself is entirely composed of fibrin and naturally degrades.

CHAPTER 7: FINAL DESIGN AND VALIDATION

Using the results and discussion, it can be shown that the team accomplished each of the five milestones proposed, to varying degrees of success. This section outlines these accomplishments.

7.1 ENGINEERED FIBRIN MICROVASCULAR NETWORK

The main goal in engineering a fibrin microvascular network was to produce 200 micron thick channels in a thin-film fibrin hydrogel. This process needed to retain pattern fidelity and be easily reproducible. Furthermore, the gels needed to be maneuverable so that channel retention was retained during movement of the device, enabling the alignment of gels and essentially the potential for production of a multi-layered construct.

Fibrin gels were successfully patterned with a thickness of 200 microns and pattern retention in the fibrin was validated by comparing dimensions to those of PDMS molds. Using the PDMS molds as a template, patterned fibrin gels were easily produced, with a high degree of repeatability. The gels were cast inside paper vellum rings, creating a light-weight, versatile material to hold and maneuver the fibrin microvascular network. Fibrin dimensions were verified and compared to those of the PDMS template through imaging, using bright field microscopy and imageJ (in order to measure dimensions of the network patterned in fibrin). This allowed for the comparison between the resulting images of patterned fibrin to the known dimensions of the corresponding PDMS molds. The results stated previously show that the dimensions of fibrin microvascular networks very closely mimicked their PDMS mold counterparts. In producing fibrin gels, successful patterning was well above 90%, as most

products were produced with no issues. Qualitatively, it was observed that the vellum paper ring provided excellent support to the fibrin microvascular networks. They could be easily picked up and moved with a high confidence that the networks would not be damaged. Figure 56 below displays a successfully produced fibrin microvascular network.

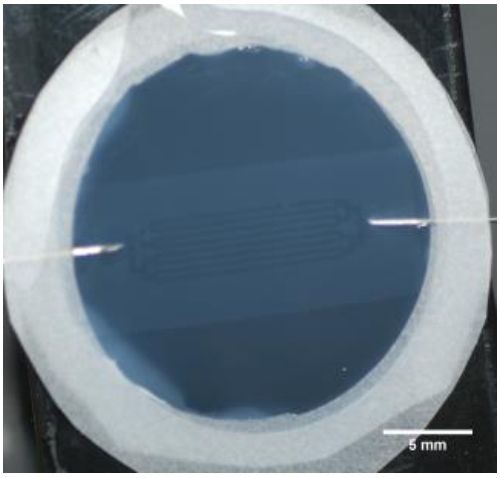

Figure 56: Engineered Fibrin Microvascular Network

7.1.1 Design Drafting

To design a fibrin microvascular network, the team first created various network designs in DraftSight, a free, two-dimensional drafting program. Various designs were created so that the design team could determine optimal channel designs in terms of branching, channel widths, and overall size limits. Once designs were drafted, they were printed onto a photomask. The photomask is used during a photolithography process to create a silicon wafer.

7.1.2 Silicon Wafer Preparation

A 4 inch diameter silicon wafer (University Wafer) was dehydrated on a hot plate for 5 minutes, before being spin-coated with SU-8 2035 (MicroChem, Newton, MA) at a speed of 1250 rpm. The coated wafer was then pre-baked at 65°C for 5 minutes, before being baked

for 15 minutes at 95°C. The photomask was then placed atop the wafer and the combination was exposed to 365 nm UV light for 14 seconds at an intensity of 23.4 mW/cm^2. The wafer was then baked at 65°C for 5 minutes, 95°C for 9 minutes, and finally 65°C for 3 more minutes. Next, the photoresist was developed in the developer solution with gentle agitation for approximately 8 minutes. The resultant wafer can be seen in Figure 572.

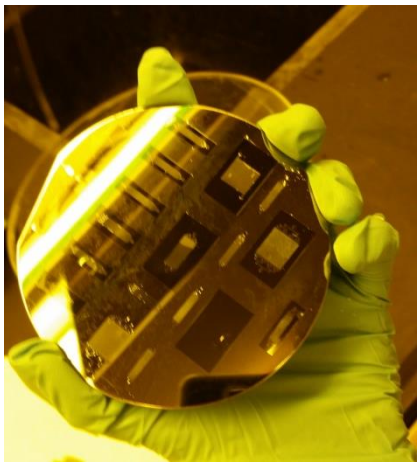

Figure 57: Wafer Post Development

7.1.3 Soft Lithography Protocol

Once the silicon wafer was fabricated, it was prepared to be used as a mold for the elastomeric polymer PDMS. The first step was the fluorination of the surface, in which the silicon surface was treated with Tridecafluoro-1,1,2,2-tetrahydrooctyl)trichlorosilane (TFOCS), which binds to the surface, making it hydrophobic. To coat the surface with TFOCS, the wafer was placed in a vacuum chamber with 40 µL of TFOCS for 1 hour. 110 grams of SYLGARD 184 (Dow Corning, Midland) was created by mixing 100 g of elastomer base with 10 g of the elastomer curing agent. This mixture was poured over the TFOCS-treated wafer and cured in an over at 65°C for four hours. The central region of PDMS, the region above the wafer, was

then excised using a scalpel and 49.5 g of PDMS (45 g base, 4.5 g curing agent) was added to the void and cured, such that no dust would settle on the wafer.

7.1.4 Fibrin mixing and casting

To make fibrin gels, 670 µL of fibrinogen (MP Bio, 30mg/mL in HBS) was mixed with 150 µL of $CaCl_2$ (40mM) and 80 µL of PBS (1x) in an Eppendorf tube. PDMS molds were soaked in a 1% solution of PEO-PPO-PEO (E:P-3:1, PolySciences) for 30 minutes before being allowed to air dry. Vellum paper rings cut to an inner diameter of 0.75 in with a slightly larger outer diameter were then placed around the PDMS molds. A 100 µL thrombin solution (2.35 U/mL) was then added to the fibrinogen solution, and the resultant solution was triturated. 150 µL of the combined solution was then pipetted onto each of the molds within the Vellum paper rings. The solution was then manually spread to cover the entire area of the vellum paper ring using a micropipette tip.

Fibrin gels were cross-linked for 10 minutes on the benchtop, before being submerged in DI water for 10 minutes. At this point, the vellum paper ring containing the imprinted fibrin gel was carefully removed from the PDMS mold, ensuring that the gel remained submerged the entire time. Gels were then placed on PDMS coated glass slides and imaged for quality assurance. Figure 583 below displays a complete graphic for preparation of a sealed fibrin gel.

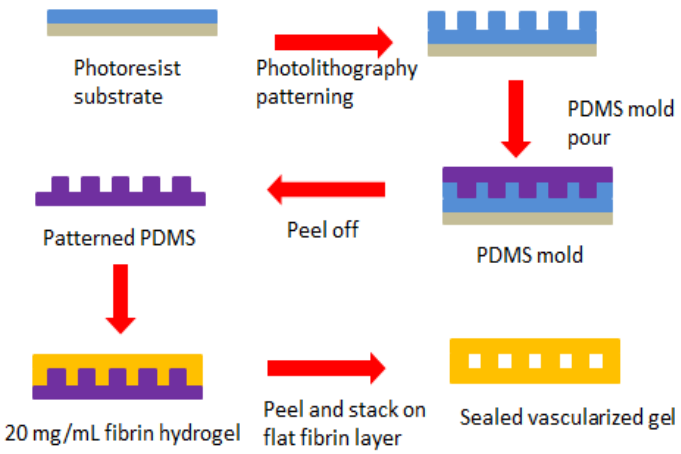

Figure 58: Procedural preparation of fibrin gel from photolithography to gel sealing

7.2 DISCRETELY LOADED MICROFLUIDIC NETWORK

In discretely loading the engineered microvascular network, the design team needed to confirm that the network could contain perfusate, prevent leakages outside individual channels, and evenly distribute perfusate from the inlet to outlet. Successful perfusate loading of an engineered fibrin microvascular network comprised of flowing a perfusate into the inlet of the network and observing fluid movement through the network. Success was measured through observation of the network macroscopically and microscopically. Figure 59 displays an example of a successfully loaded fibrin microvascular network both macroscopically and microscopically.

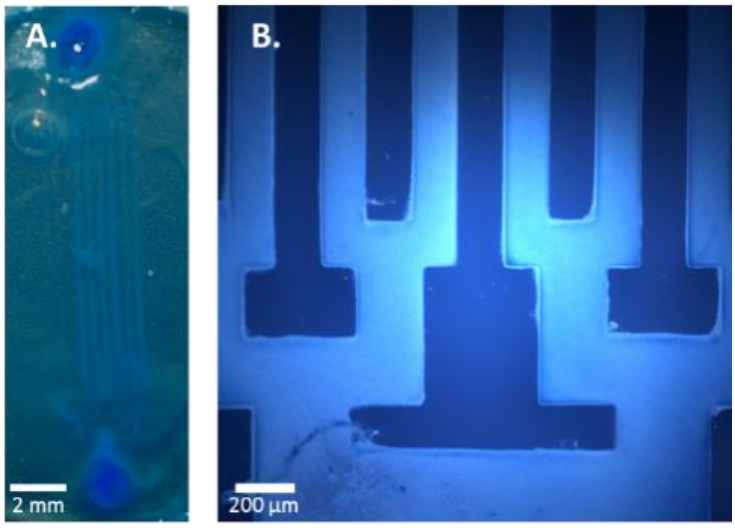

Figure 59: Perfusion of channels. (A) Macroscopic examination suggested flow containment, which was confirmed with optical microscopy (B).

7.2.1 Inlet & Outlet creation and Capillary Action Loading

Engineered fibrin microvascular networks were successfully loaded through capillary action. Inlet and outlet holes in the molded fibrin gel were punched with a 1 mm biopsy punch and then layered on top of a flat fibrin gel. Using a micropipette, approximately 1.5 µL of 1 µm blue latex beads were loaded into the inlet, and capillary action was utilized to pull the beads through the microfluidic channel.

Macroscopically, flow could only be seen as initial flow filled the network. The gels were then imaged and examined under dark field microscopy and individual particles could be visualized moving from the inlet to the outlet, flowing through the network. The edges of channels were also observed to examine any leakages from channels. Channels slightly bulged and trace amounts of particles could be seen just outside the network, however bulk flow remained within the network and severe leakages were not visible.

7.3 OPTIMIZATION OF MICROFLUIDIC NETWORK

The goal of optimizing a microfluidic network was to eliminate any potential dead zones or unutilized space within the microfluidic network. It was anticipated that changes in pressure over the channel would affect flow; therefore, it was desired to reduce the pressure change through the system at a physiological flow rate. The reduction of pressure within the functional vascular area would minimize the resistance to flow, ensuring that the path of least resistance is through the network. By eliminating low-flow zones and reducing the pressure drop, an optimized network would be easily perfused and fresh medium for cells could be guaranteed for all areas of the microvascular network.

The optimized branching model consisted of a combination of ideal conditions for each parameter. The overall design consisted of the square branching pattern; the outer edges of the branching network were chamfered and circular inner edges were inserted as well. In studying each branching pattern, it was noted that square branching reduced pressure because it was the shortest branching network. Triangular branching was excellent in reducing low flow areas along the outer edges of each branch. Circular branching produced similar results as triangular branching, however, the most effective reduction was seen on the inside edge of each channel. In combining the three positive characteristics, an optimal branching geometry was achieved. Consequently, the width of these channels was determined to be optimal for Murray's Law. It most closely mimics native vasculature and reduces the accumulation of pressure within the vascular network. However, the step down branching was only slightly worse in terms of reducing pressure, indicating that it is possible to use this branching mechanism as well for a slightly less effective model. Figure 60 below displays the

COMSOL model of the optimized microvascular network. Note that the other half of the network is a mirrored image of Figure 60.

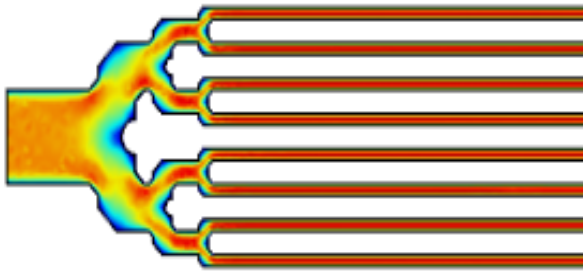

Figure 60: COMSOL model of inlet side of the optimal micro-fluidic design with minimized dead zones and reduced pressure drop

7.3.1 COMSOL Modeling and Optimization

Various iterations of the variables in the design of the network were designed in DraftSight. These iterations of the branching network consisted of different geometries and widths in the branching region of the microvascular network. Branching geometries of square, triangular, and circular bifurcation were selected to further investigate. Branching channel widths were also evaluated to determine how width would affect pressure changes through the system. The three studied branching channel widths were: constant width, step down, and Murray's Law. COMSOL allowed for robust testing of the various parameters, while maintaining constant conditions for other parameters. Each model was flowed at a volumetric flow rate of 300 µL, simulating an approximate flow rate seen in blood vessels of similar size.

Through qualitative and quantitative analysis of COMSOL models, low flow zones were highlighted and pressure drops were calculated. In examining all three branching geometries, characteristics of each were combined to produce an optimized geometry. In studying pressure

drops, each width size produced different pressure changes for the same branching geometry. In order of lowest pressure change, Murray's Law performed best, followed by step down and then constant width. By adding the optimized branching geometry to a Murray's Law width network, and running this model through COMSOL, an even lower pressure change and reduction in low flow spaces was observed. This final model outperformed any other model tested in COMSOL and should theoretically allow for optimal flow through the engineered fibrin microvascular network.

7.4 Successful Continuous Perfusion

Successful continuous perfusion was required in order to confirm the ability of this scaffold to sustain cellular viability. Continuous perfusion through the engineered network needed to occur without leakage from the channel, while allowing for controlled flow rate as well as easy collection of used medium. Ideally, the perfusion apparatus needed to be maneuverable and allow for imaging under microscopy, enabling the imaging of cells once seeded on the single channel gel system.

Continuous perfusion through the engineered network was accomplished, first in a PDMS prototype mold, and then through gel secured in perfusion apparatuses, which were 3D printed using an Objet printer with MED610. The 3D printed apparatus allowed for continuous perfusion as the channels were fully sealed around an inlet and outlet, avoiding the obstacle of inadequate sealing between layers. Perfusate traveled through the gel, and could be completely collected from the outlet tubing, with no visible leakages. This perfusion system allows for various perfusate driving systems, including gravity fed and syringe pump systems. Gels were perfused for 24 hours using both gravity fed and syringe pump systems and no

visible leakages occurred. Using a gravity pressure driving system, gels were perfused at varying flow rates to qualitatively assess the robust nature of the gel. Gels were able to handle significantly higher volumetric flow rates than the desired 82 µL/hour. Figure 61 below displays the PDMS preliminary device and a 3D rendering of the perfusion apparatus.

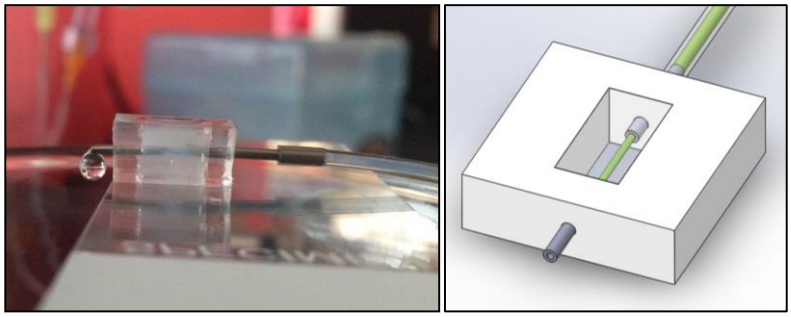

Figure 61: Single Channel Perfusion proof of concept with PDMS and SolidWorks model of rapid prototyped apparatus

7.4.1 Single channel production

In order to create a single channel gel, 23 gauge needles stubs were to be inserted into the holes of the rapid prototyped frame. A 30 gauge needle would then be loaded across the center of the well, suspended within the 23 gauge needles. A fibrin gel would be cast over this needle, and once polymerized, the needle would be removed, leaving a void that spanned the distance between the needle stubs. With this gel production method in mind, SolidWorks was used to develop a perfusion apparatus for 3D printing. After modelling, this system was mocked-up using PDMS prior to rapid prototyping a finalized perfusion apparatus. In the PDMS system, the fibrin was able to be perfused continuously via syringe pump with PBS, and fluid was observed to drip out the other side of the mold. This verification of design allowed for confidence in printing rapid prototyped perfusion apparatuses.

The 3D printed apparatuses were printed using an Objet printer loaded with MED610, a biocompatible polymer compatible for printing with the Objet. Channels in these gels were constructed in the same manner as described earlier and perfused to verify no leakages occurred at the inlet, outlet, or through the bulk of the gel.

7.4.2 FITC diffusion

Once perfusion was qualitatively accomplished in the rapid prototyped part, FITC diffusion analysis was used to verify that the gels were not losing fluid in a bulk flow manner. Using the single channel system, FITC (Sigma, St. Louis) (36 ug/ml in PBS) was perfused through the channel at a flow rate of 82 µL/hr for 15 minutes to assess the diffusivity of the fibrin gel. Diffusion was characterized by imaging FITC diffusion in the channel with an epifluorescent microscope and analyzing the diffusion profile in MATLAB (Mathworks, Natick). This flow analysis verified that bulk flow through the gel does not occur and that fibrin retains the bulk fluid within the channel.

7.5 CELLULAR VALIDATION

Cellular validation of the single channel system was required to provide evidence that this system could potentially support the survival of a cardiomyocyte seeded hydrogel adjacent to the single channel engineered gel. This system needed to provide evidence that cells could survive topically and also provide a distance from the channel in which survival of cells is no longer viable, validating the diffusion limit of fibrin and then need for a vascularization source.

Cellular survival was validated in a single channel perfused system after 24 and 48 hours of perfusion. Leakage did not occur in the channels and cells were fluorescently imaged to

display which cells survived topically. Living cells were observed directly above the channel, and a gradient of living cells decreased as distance increased from the channel. The presence of living cells in close proximity to the vascularization source further emphasized the necessity of vascularization in providing nutrients to cells. Figure 7

7.5.1 Cellular Viability Study

In this experiment there were 100,000 C_2C_{12} cells, cultured at 37°C and 5% CO_2 with a C_2C_{12} modified DMEM nutrient source, were seeded on top of each single channel system. After allowing the cells to attach for four hours in media, the media was removed and replaced with PBS. Then cell culture medium (experiment) or PBS (control) was perfused through the single channel for 24 hours at a flow rate of 82 µL/hr. To verify the diffusion of medium through the gel, the cells were stained with CFDA and ethidium bromide (Life Technologies, Grand Island). Using fluorescent microscopy, each gel was imaged in order to observe cell activity on the gel. It was observed that gels perfused with media had living cells above the channel, while PBS perfused gels had no living cells.

CHAPTER 8: CONCLUSIONS AND RECOMMENDATIONS

This chapter provides a conclusion to the accomplishments of the project and a summary of the potential global impacts that will result from the successful completion of the thin-film microvascular hydrogel. It also discusses the author's recommendations for the project and suggested future directions that the design team believes will be most advantageous to the realization of the original goal.

8.1 GLOBAL PROJECT CONCLUSIONS AND IMPACTS

The design team initially intended to accomplish the goal of designing and developing an engineered micro-vascularized tissue construct to be used in a layer-by-layer constructed tissue scaffold with a clinically applicable thickness. Theoretically, this strategy would allow tissue engineers to bypass the fundamental limitation of engineered tissue constructs, which is the minimal diffusion of oxygen and nutrient through cellularized tissue. Without an intact vascular network, the tissue construct is limited to the thickness through which oxygen and nutrients can diffuse in sufficient concentrations to support growth and proliferation of cells. The team was successful in accomplishing all five of the milestones discussed throughout this report, with varying degrees of success. The first three milestones were achieved using a micropatterned, thin film fibrin vasculature, while the final two milestones were achieved using a single-channel, continuous perfusion system. Ultimately, these two systems need to be combined before the thin-film perfusion system can be integrated into a layer-by-layer fabricated tissue construct.

8.1.1 Microengineered Vascular Network

For the design and creation of an engineered microvascular network, the design team was able to successfully pattern fibrin with a high fidelity, demonstrate fluid localization in the engineered vasculature, and design an optimized vascular network based on system flow and pressure drop. However, the team was unable to accomplish contained continuous perfusion in the thin vascularized hydrogel layer.

8.1.2 Continuous Contained Perfusion through Fibrin and Cellular Validation

Upon successful creation of an engineered microvascularized construct, the team proceeded to demonstrate, using a single-channel system, that continuous perfusion of nutrient rich medium could be contained within a low-density fibrin hydrogel without leakage in a bulk flow fashion. Additionally, the team demonstrated that fluid remains within the channel and diffuses out in a deterministic, first order Fickean manner**.** This diffusion was then harnessed to show that perfusion of the channel with nutrient laden medium was capable of supporting cells located over 600 µm away, demonstrating the robust nature of this platform.

8.2 PLATFORM TECHNOLOGY

The creation of a thin vascularized tissue construct has many applications in the field of tissue engineering. Nearly all tissues in the body require a high degree of vascularization in order to provide adequate oxygen and nutrients for cellular function. Thus, the authors view the results of this MQP as a platform technology which could be integrated into any layer-by-layer fabricated tissue construct to support cellular growth and function. In addition to the cardiac tissue constructs, other highly vascularized tissues that this technology could be part

of include hepatic or splenic tissue constructs, just to name a few. This technology could theoretically be used to incorporate vascularization in any soft-tissue (non-osseous) construct. Such a mechanism of vascularization has enormous ramifications for the world of tissue engineering, as effective vascularization of tissue constructs is one of the most limiting steps in the creation of engineered tissue constructs of physiologically relevant size. This platform technology has the potential to revolutionize tissue engineering in a translational sense, bringing *in vitro* cultured, patient-specific tissues one step closer to becoming a clinical reality.

8.3 Future Directions and Recommendations

The results of the two discrete systems created, the thin film patterned hydrogel and the single channel continuously perfusable system, suggest that the premise of this MQP, the creation of a thin-film engineered microvascular network in a fibrin gel, is indeed feasible. The real challenge for future work focuses on the unification of these two discrete systems into a single, harmonious system (i.e., a continuously perfusable, micropatterened thin-film hydrogel). As has been suggested throughout this report, this task is far more difficult than it would initially seem. Having studied this problem for several months, the authors have brainstormed a number of solutions to this problem, which, were it not for time and budgetary restrictions, would have been further explored.

All authors unanimously agree that the limiting factor in the single channel perfusion system is the sealing of the inlet to the gels. In all pressure driven systems, the failure (backflow) occurred around the needle, due to inadequate sealing of the fibrin gel to the needle. In the single-channel system, in which the gel was cast around the needle stubs, adequate sealing occurred, suggesting that fibrin can seal to metals during its polymerization process. The

authors propose that insertion of the needle prior to full casting of the patterned gel could yield promising results. Another potential strategy would be the fabrication of a sacrificial gel layer, which could be cannulated with the perfusion ports prior to gel casting. Similar to that done in Golden et al., the sacrificial layer could be melted away and flushed prior to channel perfusion, leaving a hollow vascular network having the architecture of the sacrificial element. A third potential strategy to remedy the sealing challenge would be the coating of the perfusion port with a thin coating of fibrin, which might seal to the fibrin layers better than the metal port alone. Any method that could be used to generate a more permanent seal between the perfusion port and the gels would benefit the integration of the thin-film technology with continuous perfusion system.

Another vein of research not fully developed by the team was the sealing of layers to one another. While perfusion via capillary action showed high localization using only surface tension to seal the patterned layer to the flat layer, the pressures exerted by this loading mechanism were quite small. It is unknown whether surface tension is a sufficient sealing mechanism for the higher pressures associated with continuous perfusion of the channels. Thus, adequate sealing of adjacent layers is another line of research which must be fully developed prior to implementation of the continuously perfused thin-film system. While sealing was preliminary attempted using UV crosslinking, much better results are expected with cross-linking agents which could be locally applied to the surfaces of the gels to be cross-linked, such as 1-Ethyl-3-(3-dimethylaminopropyl)carbodiimide (EDC) or a more natural cross-linking agent, such as genepin.

In addition to the thin-film, continuously perfusable vascular layer, the team recommends that the single channel perfusion system created be further explored. Due to its ability to be perfused at physiologically relevant flow rates, it holds promise in creating an *in vitro* model of endothelialization of arterioles. Not only is the system capable of supporting pulsatile flow that would allow for the mechanical stimulation of endothelial cells and therefore create a more robust vessel wall, but the potential for multiple discrete channels allows for a whole host of flexibility. Imaging, for example, a single endothelialized channel surround on both sides by channels perfused with VEGF, which would generate a cytokine gradient between the endothelialized channel and the VEGF sources. Vascular sprouting towards the VEGF sources could be monitored and further explored. The flexibility afforded with this set-up, which could be used as a model system for examining clotting mechanisms or neutrophil adhesion and migration or the efficacy of drug eluting stents on prohibiting restenosis, is nearly limitless.

Overall, this MQP validated the idea that a thin-film, engineered microvasculature fibrin hydrogel for integration into a layer-by-layer constructed tissue element is indeed feasible, though future work and refinement of the idea is needed.

CHAPTER 9: REFERENCES

A Trial of the Beta-Blocker Bucindolol in Patients with Advanced Chronic Heart Failure. (2001). *New England Journal of Medicine, 344*(22), 1659-1667. doi: 10.1056/NEJM200105313442202

Ahmed, T. A., Dare, E. V., & Hincke, M. (2008). Fibrin: a versatile scaffold for tissue engineering applications. *Tissue Engineering Part B: Reviews, 14*(2), 199-215.

Alberts, B., Bray, D., Hopkin, K., Johnson, A., Lewis, J., Raff, M., . . . Walter, P. (2013). *Essential cell biology*: Garland Science.

Auger, F. A., Gibot, L., & Lacroix, D. (2013). The pivotal role of vascularization in tissue engineering. *Annu Rev Biomed Eng, 15*, 177-200. doi: 10.1146/annurev-bioeng-071812-152428

Badylak, S. F., Taylor, D., & Uygun, K. (2011). Whole-Organ Tissue Engineering: Decellularization and Recellularization of Three-Dimensional Matrix Scaffolds. *Annual Review of Biomedical Engineering, 13*(1), 27-53. doi: 10.1146/annurev-bioeng-071910-124743

Bakris, G. L., Weir, M. R., DeQuattro, V., & McMahon, F. G. (1998). Effects of an ACE inhibitor/calcium antagonist combination on proteinuria in diabetic nephropathy. *Kidney Int, 54*(4), 1283-1289.

Beltrami, C. A., Finato, N., Rocco, M., Feruglio, G. A., Puricelli, C., Cigola, E., . . . Anversa, P. (1994). Structural basis of end-stage failure in ischemic cardiomyopathy in humans. *Circulation, 89*(1), 151-163.

Bergman, T. L. (2011). Fundamentals of Heat and Mass Transfer (7th ed.): John Wiley and Sons.

Berthier, E., Young, E. W. K., & Beebe, D. (2012). Engineers are from PDMS-land, Biologists are from Polystyrenia. *Lab on a Chip, 12*(7), 1224-1237.

Bick, A., Gomez, E., Shin, H., Brigham, M., Vu, M., & Khademhosseini, A. (2009). *Fabrication of microchannels in methacrylated hyaluronic acid hydrogels*.

Boersma, E., Mercado, N., Poldermans, D., Gardien, M., Vos, J., & Simoons, M. L. (2003). Acute myocardial infarction. *Lancet, 361*(9360), 847-858. doi: 10.1016/s0140-6736(03)12712-2

Bolooki, M. H. (2010). Acute Myocardial Infarction: Cleveland Clinic.

Borenstein, J. T., Terai, H., King, K. R., Weinberg, E. J., Kaazempur-Mofrad, M. R., & Vacanti, J. P. (2002). Microfabrication technology for vascularized tissue engineering. *Biomedical Microdevices, 4*(3), 167-175.

Borenstein, J. T., & Vunjak-Novakovic, G. (2011). Engineering tissue with BioMEMS. *IEEE Pulse, 2*(6), 28-34. doi: 10.1109/MPUL.2011.942764

Carmeliet, P., & Jain, R. K. (2000). Angiogenesis in cancer and other diseases. *Nature, 407*(6801), 249-257. doi: 10.1038/35025220

Chen, X., Aledia, A. S., Popson, S. A., Him, L., Hughes, C. C., & George, S. C. (2010). Rapid anastomosis of endothelial progenitor cell-derived vessels with host vasculature is promoted by a high density of cotransplanted fibroblasts. *Tissue Eng Part A, 16*(2), 585-594. doi: 10.1089/ten.TEA.2009.0491

Choi, N. W., Cabodi, M., Held, B., Gleghorn, J. P., Bonassar, L. J., & Stroock, A. D. (2007). Microfluidic scaffolds for tissue engineering. *Nature materials, 6*(11), 908-915.

Cornwell, K. G., & Pins, G. D. (2007). Discrete crosslinked fibrin microthread scaffolds for tissue regeneration. *J Biomed Mater Res A, 82*(1), 104-112. doi: 10.1002/jbm.a.31057

Cowger, J., Pagani, F. D., Haft, J. W., Romano, M. A., Aaronson, K. D., & Kolias, T. J. (2010). The development of aortic insufficiency in left ventricular assist device-supported patients. *Circ Heart Fail, 3*(6), 668-674. doi: 10.1161/circheartfailure.109.917765

Cowie, M. R., Mosterd, A., Wood, D. A., Deckers, J. W., Poole-Wilson, P. A., Sutton, G. C., & Grobbee, D. (1997). The epidemiology of heart failure. *European heart journal, 18*(2), 208-225.

Crapo, P. M., Gilbert, T. W., & Badylak, S. F. (2011). An overview of tissue and whole organ decellularization processes. *Biomaterials, 32*(12), 3233-3243.

Cui, X., & Boland, T. (2009). Human microvasculature fabrication using thermal inkjet printing technology. *Biomaterials, 30*(31), 6221-6227.

Dickstein, K., Cohen-Solal, A., Filippatos, G., McMurray, J. J. V., Ponikowski, P., Poole-Wilson, P. A., . . . Hoes, A. W. (2008). ESC Guidelines for the diagnosis and treatment of acute and chronic heart failure 2008‡. *European journal of heart failure, 10*(10), 933-989.

Dvir, T., Kedem, A., Ruvinov, E., Levy, O., Freeman, I., Landa, N., . . . Cohen, S. (2009). Prevascularization of cardiac patch on the omentum improves its therapeutic outcome. *Proc Natl Acad Sci U S A, 106*(35), 14990-14995. doi: 10.1073/pnas.0812242106

Dym, C. L., Little, P., Orwin, E. J., & Spjut, E. E. (2009). *Engineering Design: A Project Based Introduction* (3 ed.). Hoboken: John Wiley & Sons, Inc.

Elsasser, A., Suzuki, K., Lorenz-Meyer, S., Bode, C., & Schaper, J. (2001). The role of apoptosis in myocardial ischemia: a critical appraisal. *Basic Res Cardiol, 96*(3), 219-226.

Emerson, D. R., Cieslicki, K., Gu, X., & Barber, R. W. (2006). Biomimetic design of microfluidic manifolds based on a generalised Murray's law. *Lab Chip, 6*(3), 447-454. doi: 10.1039/b516975e

Ertl, G., & Frantz, S. (2005). Healing after myocardial infarction. *Cardiovascular Research, 66*(1), 22-32.

Fidkowski, C., Kaazempur-Mofrad, M. R., Borenstein, J., Vacanti, J. P., Langer, R., & Wang, Y. (2005). Endothelialized microvasculature based on a biodegradable elastomer. *Tissue Eng, 11*(1-2), 302-309. doi: 10.1089/ten.2005.11.302

Flather, M. D., Yusuf, S., Køber, L., Pfeffer, M., Hall, A., Murray, G., . . . Moyé, L. (2000). Long-term ACE-inhibitor therapy in patients with heart failure or left-ventricular dysfunction: a systematic overview of data from individual patients. *The Lancet, 355*(9215), 1575-1581.

Godier, A., Maidhof, R., Marsano, A., Martens, T. P., Radisic, M., Tandon, N., & Vunjak-Novakovic, G. (2010). Challenges in cardiac tissue engineering. *Tissue Engineering, Part B: Reviews, 16*, 169+.

Golden, A. P., & Tien, J. (2007). Fabrication of microfluidic hydrogels using molded gelatin as a sacrificial element. *Lab Chip, 7*(6), 720-725. doi: 10.1039/b618409j

Green, J. V., Kniazeva, T., Abedi, M., Sokhey, D. S., Taslim, M. E., & Murthy, S. K. (2009). Effect of channel geometry on cell adhesion in microfluidic devices. *Lab Chip, 9*(5), 677-685. doi: 10.1039/b813516a

Hegen, A., Blois, A., Tiron, C. E., Hellesøy, M., Micklem, D. R., Nör, J. E., . . . Lorens, J. B. (2011). Efficient in vivo vascularization of tissue-engineering scaffolds. *Journal of Tissue Engineering and Regenerative Medicine, 5*(4), e52-e62. doi: 10.1002/term.336

Holley, C. T., Harvey, L., & John, R. (2014). Left ventricular assist devices as a bridge to cardiac transplantation. *J Thorac Dis, 6*(8), 1110-1119. doi: 10.3978/j.issn.2072-1439.2014.06.46

Hunt, S. A., & Haddad, F. (2008). The Changing Face of Heart Transplantation. *Journal of the American College of Cardiology, 52*(8), 587-598. doi: http://dx.doi.org/10.1016/j.jacc.2008.05.020

Isenberg, B. C., Williams, C., & Tranquillo, R. T. (2006). Endothelialization and flow conditioning of fibrin-based media-equivalents. *Annals of biomedical engineering, 34*(6), 971-985.

Janakiraman, V., Kienitz, B. L., & Baskaran, H. (2007). Lithography Technique for Topographical Micropatterning of Collagen-Glycosaminoglycan Membranes for Tissue Engineering Applications. *Journal of medical devices, 1*(3), 233-237. doi: 10.1115/1.2775937

Jentzer, J. C., Hickey, G. W., & Khandhar, S. J. (2014). Transplant coronary heart disease: challenges and solutions. *Transplant Research and Risk Management, 6*, 117-127.

Jung, S.-H., Kim, J. J., Choo, S. J., Yun, T.-J., Chung, C. H., & Lee, J. W. (2011). Long-term Mortality in Adult Orthotopic Heart Transplant Recipients. *Journal of Korean Medical Science, 26*(5), 599-603. doi: 10.3346/jkms.2011.26.5.599

Kaihara, S., Borenstein, J., Koka, R., Lalan, S., Ochoa, E. R., Ravens, M., . . . Vacanti, J. P. (2000). Silicon micromachining to tissue engineer branched vascular channels for liver fabrication. *Tissue engineering, 6*(2), 105-117.

Koike, N., Fukumura, D., Gralla, O., Au, P., Schechner, J. S., & Jain, R. K. (2004). Tissue engineering: creation of long-lasting blood vessels. *Nature, 428*(6979), 138-139.

Kolesky, D. B., Truby, R. L., Gladman, A., Busbee, T. A., Homan, K. A., & Lewis, J. A. (2014). 3D bioprinting of vascularized, heterogeneous cell-laden tissue constructs. *Advanced Materials, 26*(19), 3124-3130.

L'Heureux, N., Pâquet, S., Labbé, R., Germain, L., & Auger, F. A. (1998). A completely biological tissue-engineered human blood vessel. *The FASEB Journal, 12*(1), 47-56.

Langer, R., & Vacanti, J. P. (1993). Tissue engineering. *Science, 260*(5110), 920-926.

Less, J. R., Skalak, T. C., Sevick, E. M., & Jain, R. K. (1991). Microvascular architecture in a mammary carcinoma: branching patterns and vessel dimensions. *Cancer research, 51*(1), 265-273.

Lichtenberg, A., Cebotari S Fau - Tudorache, I., Tudorache I Fau - Sturz, G., Sturz G Fau - Winterhalter, M., Winterhalter M Fau - Hilfiker, A., Hilfiker A Fau - Haverich, A., & Haverich, A. Flow-dependent re-endothelialization of tissue-engineered heart valves. (0966-8519 (Print)).

Lindenfeld, J., Miller, G. G., Shakar, S. F., Zolty, R., Lowes, B. D., Wolfel, E. E., . . . Kobashigawa, J. (2004). Drug Therapy in the Heart Transplant Recipient: Part II: Immunosuppressive Drugs. *Circulation, 110*(25), 3858-3865.

Ling, Y., Rubin, J., Deng, Y., Huang, C., Demirci, U., Karp, J. M., & Khademhosseini, A. (2007). A cell-laden microfluidic hydrogel. *Lab on a Chip, 7*(6), 756-762.

Lund, L. H., Edwards, L. B., Kucheryavaya, A. Y., Dipchand, A. I., Benden, C., Christie, J. D., . . . Yusen, R. D. (2013). The Registry of the International Society for Heart and Lung Transplantation: thirtieth official adult heart transplant report—2013; focus theme: age. *The Journal of Heart and Lung Transplantation, 32*(10), 951-964.

Marieb, E., & Hoehn, K. (2013). *Human Anatomy & Physiology* (9 ed.). Boston: Pearson.

Marsano, A., Maidhof, R., Luo, J., Fujikara, K., Konofagou, E. E., Banfi, A., & Vunjak-Novakovic, G. (2013). The effect of controlled expression of VEGF by transduced myoblasts in a cardiac patch on vascularization in a mouse model of myocardial infarction. *Biomaterials, 34*(2), 393-401. doi: 10.1016/j.biomaterials.2012.09.038

Masuda, S., Shimizu, T., Yamato, M., & Okano, T. (2008). Cell sheet engineering for heart tissue repair. *Adv Drug Deliv Rev, 60*(2), 277-285. doi: http://dx.doi.org/10.1016/j.addr.2007.08.031

McMurray, J. J. V., Adamopoulos, S., Anker, S. D., Auricchio, A., Böhm, M., Dickstein, K., . . . Gomez-Sanchez, M. A. (2012). ESC Guidelines for the diagnosis and treatment of acute and chronic heart failure 2012. *European journal of heart failure, 14*(8), 803-869.

Miller, J. S., Stevens, K. R., Yang, M. T., Baker, B. M., Nguyen, D.-H. T., Cohen, D. M., . . . Chen, C. S. (2012). Rapid casting of patterned vascular networks for perfusable engineered 3D tissues. *Nature materials, 11*(9), 768-774. doi: 10.1038/nmat3357

Montgomery, M., Zhang, B., & Radisic, M. (2014). Cardiac Tissue Vascularization From Angiogenesis to Microfluidic Blood Vessels. *Journal of cardiovascular pharmacology and therapeutics*, 1074248414528576.

Mozaffarian, D., Benjamin, E. J., Go, A. S., Arnett, D. K., Blaha, M. J., Cushman, M., . . . Turner, M. B. (2015). Heart Disease and Stroke Statistics—2015 Update: A Report From the American Heart Association. *Circulation, 131*(4), e29-e322.

Mulloy, D. P., Bhamidipati, C. M., Stone, M. L., Ailawadi, G., Kron, I. L., & Kern, J. A. (2013). Orthotopic heart transplant versus left ventricular assist device: A national comparison of cost and survival. *The Journal of Thoracic and Cardiovascular Surgery, 145*(2), 566-574. doi: http://dx.doi.org/10.1016/j.jtcvs.2012.10.034

Murray, C. D. (1926). <THE PHYSIOLOGICAL PRINCIPLE OF MINIMUM WORK APPLIED TO THE ANGLE OF BRANCHING OF ARTERIES.pdf>. *J Gen Physiol, 9*(6), 835-841.

Novosel, E. C., Kleinhans, C., & Kluger, P. J. (2011). Vascularization is the key challenge in tissue engineering. *Adv Drug Deliv Rev, 63*(4-5), 300-311. doi: 10.1016/j.addr.2011.03.004

Ott, H. C., Matthiesen, T. S., Goh, S.-K., Black, L. D., Kren, S. M., Netoff, T. I., & Taylor, D. A. (2008). Perfusion-decellularized matrix: using nature's platform to engineer a bioartificial heart. *Nat Med, 14*(2), 213-221. doi: http://www.nature.com/nm/journal/v14/n2/suppinfo/nm1684_S1.html

Painter, P., Eden, P., & Bengtsson, H.-U. (2006). Pulsatile blood flow, shear force, energy dissipation and Murray's Law. *Theoretical Biology and Medical Modelling, 3*(1), 31.

Patan, S. Vasculogenesis and angiogenesis. (0927-3042 (Print)).

Phelps, E. A., & García, A. J. (2010). Engineering more than a cell: Vascularization Strategies in Tissue Engineering. *Curr Opin Biotechnol, 21*(5), 704-709. doi: 10.1016/j.copbio.2010.06.005

Pocock, S. J., Ariti, C. A., McMurray, J. J. V., Maggioni, A., Køber, L., Squire, I. B., . . . Doughty, R. N. (2013). Predicting survival in heart failure: a risk score based on 39 372 patients from 30 studies. *European heart journal, 34*(19), 1404-1413.

Radisic, M., & Christman, K. L. (2013). Materials science and tissue engineering: repairing the heart. *Mayo Clin Proc, 88*(8), 884-898. doi: 10.1016/j.mayocp.2013.05.003

Risau, W. (1997). Mechanisms of angiogenesis. *Nature, 386*(6626), 671-674. doi: 10.1038/386671a0

Risau, W., & Flamme, I. (1995). Vasculogenesis. *Annu Rev Cell Dev Biol, 11*, 73-91. doi: 10.1146/annurev.cb.11.110195.000445

Rose, E. A., Gelijns, A. C., Moskowitz, A. J., Heitjan, D. F., Stevenson, L. W., Dembitsky, W., . . . Levitan, R. G. (2001). Long-term use of a left ventricular assist device for end-stage heart failure. *New England Journal of Medicine, 345*(20), 1435-1443.

Sakaguchi, K., Shimizu, T., Horaguchi, S., Sekine, H., Yamato, M., Umezu, M., & Okano, T. (2013). In vitro engineering of vascularized tissue surrogates. *Sci Rep, 3*, 1316. doi: 10.1038/srep01316

Sasagawa, T., Shimizu, T., Sekiya, S., Haraguchi, Y., Yamato, M., Sawa, Y., & Okano, T. (2010). Design of prevascularized three-dimensional cell-dense tissues using a cell sheet stacking manipulation technology. *Biomaterials, 31*(7), 1646-1654. doi: http://dx.doi.org/10.1016/j.biomaterials.2009.11.036

Schaner, P. J., Martin, N. D., Tulenko, T. N., Shapiro, I. M., Tarola, N. A., Leichter, R. F., . . . DiMuzio, P. J. (2004). Decellularized vein as a potential scaffold for vascular tissue engineering. *Journal of Vascular Surgery, 40*(1), 146-153. doi: http://dx.doi.org/10.1016/j.jvs.2004.03.033

Sekine, H., Shimizu, T., Hobo, K., Sekiya, S., Yang, J., Yamato, M., . . . Okano, T. (2008). Endothelial cell coculture within tissue-engineered cardiomyocyte sheets enhances neovascularization and improves cardiac function of ischemic hearts. *Circulation, 118*(14 suppl 1), S145-S152.

Sekine, H., Shimizu, T., Sakaguchi, K., Dobashi, I., Wada, M., Yamato, M., . . . Okano, T. (2013). In vitro fabrication of functional three-dimensional tissues with perfusable blood vessels. *Nat Commun, 4*, 1399. doi: 10.1038/ncomms2406

Sherman, T. F. (1981). On connecting large vessels to small. The meaning of Murray's law. *The Journal of general physiology, 78*(4), 431-453.

Shimizu, T. (2011). *Myocardial Tissue Engineering*: INTECH Open Access Publisher.

Shin, M., Ishii, O., Sueda, T., & Vacanti, J. P. (2004). Contractile cardiac grafts using a novel nanofibrous mesh. *Biomaterials, 25*(17), 3717-3723. doi: http://dx.doi.org/10.1016/j.biomaterials.2003.10.055

Singelyn, J. M., & Christman, K. L. (2010). Injectable materials for the treatment of myocardial infarction and heart failure: the promise of decellularized matrices. *J Cardiovasc Transl Res, 3*(5), 478-486.

Skalak, T. C., & Schmid-Schönbein, G. W. (1986). The microvasculature in skeletal muscle. IV. A model of the capillary network. *Microvascular Research, 32*(3), 333-347. doi: http://dx.doi.org/10.1016/0026-2862(86)90069-5

Slaughter, M. S., Rogers, J. G., Milano, C. A., Russell, S. D., Conte, J. V., Feldman, D., . . . Long, J. W. (2009). Advanced heart failure treated with continuous-flow left ventricular assist device. *New England Journal of Medicine, 361*(23), 2241-2251.

Stehlik, J., Edwards, L. B., Kucheryavaya, A. Y., Benden, C., Christie, J. D., Dobbels, F., . . . Hertz, M. I. (2011). The Registry of the International Society for Heart and Lung Transplantation: Twenty-eighth Adult Heart Transplant Report—2011. *The Journal of Heart and Lung Transplantation, 30*(10), 1078-1094. doi: http://dx.doi.org/10.1016/j.healun.2011.08.003

Stern, D. R., Kazam, J., Edwards, P., Maybaum, S., Bello, R. A., D'Alessandro, D. A., & Goldstein, D. J. (2010). Increased incidence of gastrointestinal bleeding following implantation of the HeartMate II LVAD. *J Card Surg, 25*(3), 352-356. doi: 10.1111/j.1540-8191.2010.01025.x

Stevens, K. R., Kreutziger, K. L., Dupras, S. K., Korte, F. S., Regnier, M., Muskheli, V., . . . Murry, C. E. (2009). Physiological function and transplantation of scaffold-free and vascularized human cardiac muscle tissue. *Proceedings of the National Academy of Sciences, 106*(39), 16568-16573.

Swedberg, K., Cleland, J., Dargie, H., Drexler, H., Follath, F., Komajda, M., . . . Haverich, A. (2005). Guidelines for the diagnosis and treatment of chronic heart failure: executive summary (update 2005) The Task Force for the Diagnosis and Treatment of Chronic Heart Failure of the European Society of Cardiology. *European heart journal, 26*(11), 1115-1140.

Taylor, D. A., Sampaio, L. C., & Gobin, A. (2014). Building New Hearts: A Review of Trends in Cardiac Tissue Engineering. *Am J Transplant*. doi: 10.1111/ajt.12939

Topkara, V. K., Kondareddy, S., Malik, F., Wang, I. W., Mann, D. L., Ewald, G. A., & Moazami, N. (2010). Infectious complications in patients with left ventricular assist device: etiology and outcomes in the continuous-flow era. *Ann Thorac Surg, 90*(4), 1270-1277. doi: 10.1016/j.athoracsur.2010.04.093

Vunjak-Novakovic, G., Tandon, N., Godier, A., Maidhof, R., Marsano, A., Martens, T. P., & Radisic, M. (2009). Challenges in cardiac tissue engineering. *Tissue Engineering Part B: Reviews, 16*(2), 169-187.

Weis, M., & von Scheidt, W. (1997). Cardiac allograft vasculopathy: a review. *Circulation, 96*(6), 2069-2077.

Wray, L. S., Tsioris, K., Gi, E. S., Omenetto, F. G., & Kaplan, D. L. (2013). Slowly degradable porous silk microfabricated scaffolds for vascularized tissue formation. *Adv Funct Mater, 23*(27), 3404-3412. doi: 10.1002/adfm.201202926

Zimmermann, W.-H., Didié, M., Döker, S., Melnychenko, I., Naito, H., Rogge, C., . . . Eschenhagen, T. (2006). Heart muscle engineering: an update on cardiac muscle replacement therapy. *Cardiovascular research, 71*(3), 419-429.

Zimmermann, W.-H., & Eschenhagen, T. (2003). Cardiac Tissue Engineering for Replacement Therapy. *Heart Failure Reviews, 8*(3), 259-269. doi: 10.1023/A:1024725818835

Zimmermann, W. H., Melnychenko, I., Wasmeier, G., Didie, M., Naito, H., Nixdorff, U., . . . Eschenhagen, T. (2006). Engineered heart tissue grafts improve systolic and diastolic function in infarcted rat hearts. *Nat Med, 12*(4), 452-458. doi: 10.1038/nm1394

CHAPTER 10: APPENDICES

APPENDIX A: MICROFABRICATION PROTOCOL

The following procedure was utilized to conduct the multiple steps necessary to fabricate the mold. The steps involved in this procedure include: wafer purification, photoresist spin coat, pre-bake, exposure to UV light, post-exposure bake, development, inspection, and post-processing. This procedure was designed by Professor Dirk Albrecht, Dept. of Biomedical Engineering, WPI. See Appendix A for the full Standard Operating Procedure (SOP) for Photolithography using SU8 Photoresist.

Prior to beginning the procedure, a series of values were determined in order to achieve the desired depth of channels. The photoresist available was SU-8 2035 and the desired depth of the channels was 100 µm. The following primary determinants were selected based on the photoresist specification sheet for SU-8 2000 series. See Appendix A for more information.

Spin-coating	1250 rpm	
Pre-bake (1)	5°C	5 min
Pre-bake (2)	5°C	15 min
Exposure time	14 sec	
Post-bake (1)	5°C	5 min
Post-bake (2)	5°C	9 min
Development time	8 min	

Dehydration Procedure:

The purpose of this step is to dehydrate the wafer, removing any excess moisture from the wafer.

1. Turn on blower and light on the clean hood.
2. Inside the clean hood, set the PMC Dataplate hot plate to 120°C. Press the following buttons: [SET], "Plate Temp" [1], [1], [2], [0], [ENT].
3. Place the wafer on the hot plate for 5 minutes, as shown below.

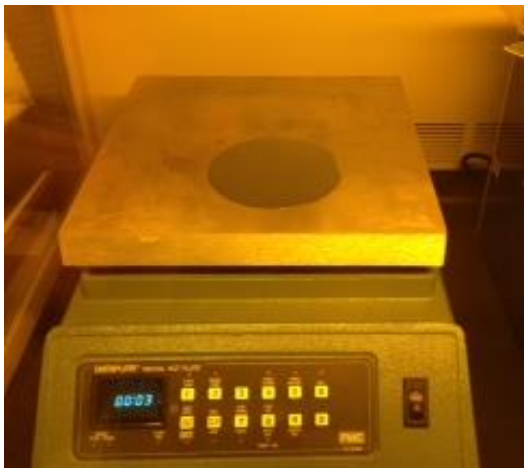

Figure A162: Wafer undergoing dehydration bake

4. To set the timer, press the following buttons: [SET], "Timer (h:m)" [4], [5], [ENT].
5. Remove the wafer from the hot plate and allow to cool to room temperature.

Spin-coating Procedure:

This procedure outlines the process of applying an even layer of photoresist to the wafer via spinning of the wafer at a determined speed.

1. Turn on the spin-coater using left power strip under the fume hood and ensure that the interior is completely coated with aluminum foil. Rotate the chuck to ensure that excess foil doesn't impede rotation.
2. Turn on the two 7'' Dataplate hotplates using the right power strip switch under the fume hood.
3. Set the left hot plate to 65°C and the right hot plate to 95°C.

4. On the spin-coater, press [Select Process] and edit the spin program to a spin speed of 1250 rpm. The other parameters should remain unchanged.
5. Select [Run Mode] and turn on the N_2 supply. After opening the main tank valve, ensure that the output pressure is 60-70 psi. Open the vacuum valve by aligning the black handle with the tubing, ensuring suction from the spin coating chuck.
6. Ensure that the wafer is clean and dry by blowing the wafer with the nitrogen gun.
7. Position the wafer on the chuck and use the alignment tool to ensure that the wafer is positioned on the center of the chuck. Only the edges of the wafer are touched with the alignment tool
8. After the wafer is aligned on the chuck, press [Vacuum]. The wafer should be secured to the chuck
9. In order to ensure that the wafer is aligned on the center of the chuck, press [START] to begin the spin program. If the wafer wobbles, press [STOP], then [Vacuum] in order to release the vacuum and alter the position of the wafer. It be necessary to reset the spin program by pressing [Edit Mode] then [Run Mode] and ensure that the display reads "Ready".
10. Slowly pour 8-10 ml of SU-8 2035 photoresist on to the wafer directly.
11. After about enough photoresist is applied to the wafer (to cover a diameter of about 5 cm) tilt the tube upwards and twist the tube to prevent excess dripping of photoresist.
12. Press [START] to begin the spin-coat. After the spin-coat is complete, ensure that the photoresist completely covered the wafer with no striations or streaks. Then, release the vacuum and close the vacuum valve.

Pre-bake Procedure:

The purpose of this procedure is to densify the photoresist following the spin-coating. In order to prevent thermal stresses and thus, cracking, the temperature is gradually increased and decreased by switching between the two hotplates of different temperatures.

1. Transfer the wafer from the spin-coater to the 65°C hot plate using tweezers. Bake the wafer for 5 minutes.
2. Transfer the wafer to the 95°C hot plate and bake for 15 minutes.
3. Return the wafer to the 65°C hot plate and allow cooling for 3 minutes. Then, remove the wafer and place on table surface within clean hood and allow cooling to room temperature.

UV Exposure Procedure:

The UV exposure process exposes the portion of the wafer that is uncovered by the photomask's black regions. The LED source releases a UV exposure of 365 nm. The photoresist that is exposed to the UV light is cross-linked, making is insoluble to developer. The portion of the wafer that is shielded from the UV exposure will be later dissolved by the development treatment.

1. Turn on the UV-KUB using the power switch, above the power cord. Press the silver power button on the front panel, lower right
2. Touch the screen and select [Settings] and [Drawer]. Wave your hand near the drawer to activate the sensor to open the drawer. Place the 4''x 5'' glass slide on the tray and wave your hand near the drawer to close it
3. Return to [Settings], touch the [X] on the upper right-hand corner of the screen. Select [Illumination]. The UV intensity should read 23.4 mW/cm^2.
4. Return to the main menu and select [Full Surface] then [New Cycle] then [Continuous]. Program the exposure duration to 8 seconds. The time is entered using the touchscreen numbers, then a unit ([h], [m], [s]). Press [v] to confirm the inputted time duration.
5. In order to test the exposure, press [Insolate]. After the drawer opens, wave your hand so that it closes. The screen should read, "Loading in Progress". Touch the screen to start the exposure. Ensure that the correct countdown time is initiated.
6. Transfer the wafer to the UV-KUB tray and center it on the circular pattern.
7. Position the photomask on the wafer. If there are any defects in the wafer, position the photomask so that black space covers any defects.
8. Place the 4''x 5'' glass slide over the photomask and wafer to ensure direct contact of the mask and wafer during UV exposure. Ensure that the slide, photomask, and wafer combination is positioned toward the back of the tray and ensure that the glass slide is completely covering the photomask.
9. Wave your hand near the door to close the tray and touch the screen. Press [Continue] to initiate the entered program.
10. When the exposure is finished, lift the glass side and remove the wafer from the tray with tweezers. Gently remove the photomask from the wafer with tweezers. Ensure that the pattern is not yet visible.

Post-Exposure Bake (PEB) Procedure:

This procedure completes the process of crosslinking the negative photoresist. The heating and cooling process prevents the wafer from undergoing thermal stresses.

1. Transfer the wafer to the 65°C hotplate in the clean hood. Cover with a foil tent and allow to bake for 5 minutes.
2. Transfer the wafer to the 95°C hotplate in the clean hood. Allow the wafer to bake for 9 minutes while keeping the wafer covered with the foil.
3. Return the wafer to the 65°C hotplate for 3 minutes while remaining covered. Then, place the wafer on a cleanroom wipe, in the clean hood, until the wafer reaches room temperature.

Development Procedure:

During the development process, unexposed negative photoresist is dissolved, leaving behind insoluble patterns.

1. Pour the developer solution into the developer dish at a depth of about 1 cm. Immerse the wafer in the developer and gently slosh/agitate, without splashing the developer. Keep wafer immersed in developer for about 8 minutes.
2. When the photoresist appears to be dissolved from the wafer, remove the wafer from the developer dish with tweezers and run the wafer under water in the clean hood sink.
3. After rinsing both sides of the wafer, dry the wafer with the nitrogen gun. Ensure that all water is removed from the features by positioning the gun close in proximity to the designs. The features should be visible and crisp, as shown below.

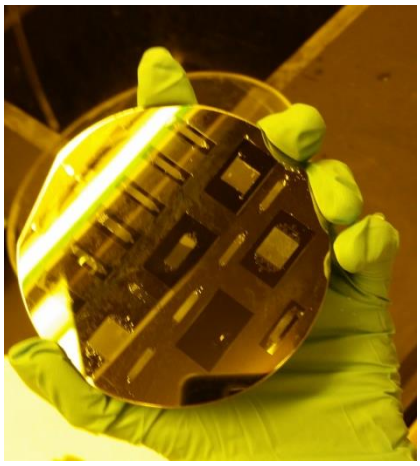

Figure A263: Wafer Post Development

4. Inspect the wafer for any residue. Perform a final cleaning of the wafer by gripping the wafer with tweezers while squirting developer onto the wafer. Again, rinse with water and dry with the nitrogen gun.

Inspection Procedure:

During this process, the quality of the development process is verified. By inspecting the wafer, any distortions or stains in the wafer will be identified.

1. Image the features of the wafer using the Zeiss Stemi-2000 stereo microscope to visualize the wafer in reflectance mode. If leftover residue is present within the features, repeat the development treatment.
2. Inspect the wafer again to ensure that the wafer was fabricated as desired.

Post-Bake Procedure:

This procedure is required to harden the developed photoresist.

1. Place the developed wafer on a hotplate that is no hotter than 65°C.
2. Set the ramp rate to 6°C/min by selecting [SET], "Ramp °C/hr" [6], [3], [6], [0], [ENT]. Set the temperature to 150°C and set the timer to 45 minutes. Set the timer to automatically turn off the hot plate after 45 minutes by selecting "Auto Off" [8]. Cover the wafer with foil.

The temperature of the wafer will slowly increase to 150°C during a 15 minute period. The temperature will reach 150°C and remain at this temperature for 30 minutes. The temperature will then gradually cool to room temperature, resulting in a total bake time of about 1 hour. After the bake, ensure that there are no cracks in the wafer.

APPENDIX B: PHOTOLITHOGRAPHY DATA SHEETS

The following charts and graphs were extracted from the specification sheet: SU-8 2000 Permanent Epoxy Negative Photoresist. Using these charts, the primary determinants required for wafer fabrication using SU-8 2035 with channel depth of 100µm were extracted.

Figure 1. SU-8 2000 Spin Speed versus Thickness

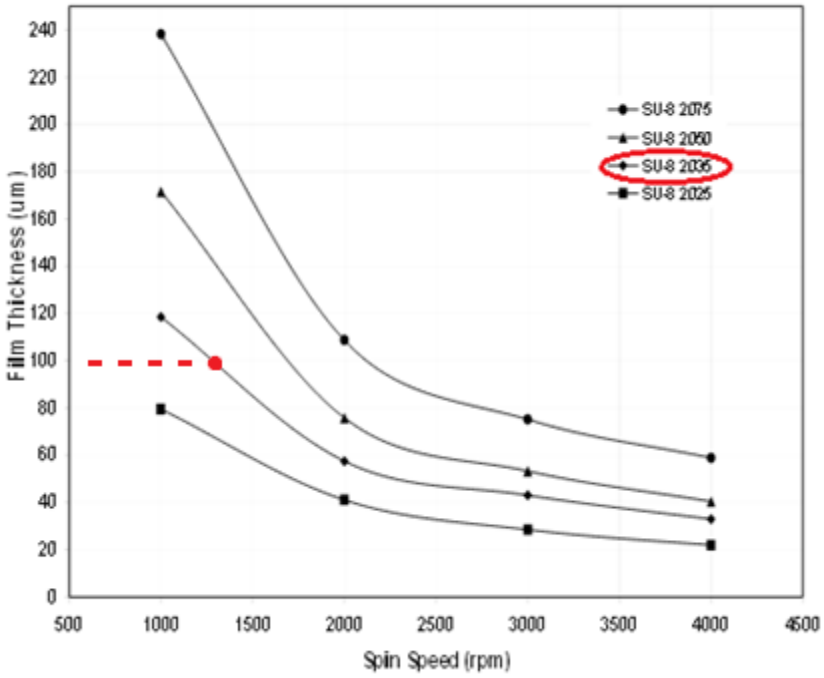

The graph above was used to determine the spin speed needed to achieve a film thickness of 100µm for the photoresist, SU-8 2035. As shown in the graph, the ideal spin speed is 1250 rpm

THICKNESS	SOFT BAKE TIMES	
	(65°C)	(95°C)
microns	minutes	minutes
25 -40	0 - 3	5 - 6
45 - 80	0 - 3	6 - 9
85 - 110	5	10 - 20
115 - 150	5	20 - 30
160 - 225	7	30 - 45

This chart was used to determine the ideal time for pre-bake conditions of the wafer. As indicated in this table, the ideal time for pre-bake is 5 minutes at 65°C and 10-20 minutes at 95°C.

THICKNESS	PEB TIME	PEB TIME
	(65°C)*	(95°C)
microns	minutes	minutes
25 -40	1	5 - 6
45 - 80	1 - 2	6 - 7
85 - 110	2 - 5	8 - 10
115 - 150	5	10 - 12
160 - 225	5	12 - 15

The chart, above, was utilized to determine the ideal times for post exposure baking (PEB) to ensure a thickness of 100µm. As shown above, the post bake conditions for this thickness is 2-5 minutes at 65°C and 8-10 minutes at 95°C.

THICKNESS	EXPOSURE ENERGY
microns	mJ/cm^2
25 - 40	150 - 160
45 - 80	150 - 215
85 - 110	215 - 240
115 - 150	240 - 260
160 - 225	260 - 350

Given the chart above, the exposure energy required to achieve the desired thickness is 215-240 mJ/cm2. The exposure energy can be converted to exposure time via the following equation:

$$Exposure\ time = \frac{exposure\ energy * multiplier * correction\ factor}{stability\ intensity}$$

THICKNESS microns	DEVELOPMENT TIME minutes
25 - 40	4 - 5
45 - 75	5 - 7
80 - 110	7 - 10
115 - 150	10 - 15
160 -225	15 - 17

This chart was utilized to determine the approximate time necessary for development. As indicated in the chart, 7-10 minutes of development exposure is necessary to create features with a thickness of 100µm.

APPENDIX C: SOFT LITHOGRAPHY PROTOCOL

After fabricating the mold, utilizing the procedure outlined above, the mold was prepared for soft lithography. The elastomeric polymer, PDMS, was casted over the mold using the procedure below. This procedure was designed by Professor Dirk Albrecht, Dept. of Biomedical Engineering, WPI, and outlines the multiple steps necessary for fluorination of the wafer, preparation of PDMS, casting and curing PDMS, cutting final PDMS device.

Fluorination Procedure:

The treatment of the Si surface with Tridecafluoro-1,1,2,2-tetrahydrooctyl)trichlorosilane (TFOCS) renders the surface hydrophobic and aids in maintaining the microfeatures during PDMS casting.

1. Set up the vacuum dissector in the fume hood. Line the bottom of the vacuum with aluminum foil. Line the sides of the vacuum with a layer of cardboard. Place the wafer in the vacuum so that it is leaning against the cardboard side, as indicated below.

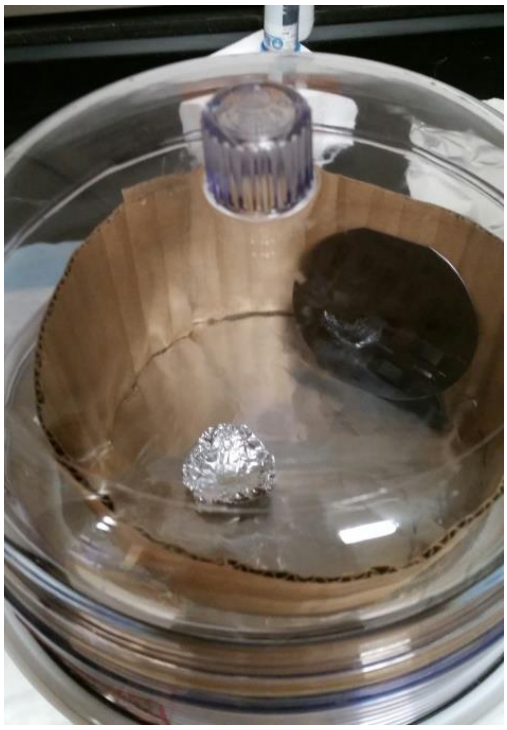

Figure C1: Fabricated wafer preparing for fluorination treatment

2. As displayed in the figure above, create an aluminum foil boat to contain the fluorination chemical.
3. Distribute 40 µL of (TFOCS) into the foil boat via a pipette tip. Place the pipette tip in the vacuum chamber (do not eject it).
4. Close the vacuum and allow to sit for 1 hour.
5. After 1 hour, remove the wafer and rinse with isopropyl. Then, rinse with distilled water. After thoroughly rinsing the wafer, dry the wafer with nitrogen gun, ensuring that all the features are dried.
6. After thorough evaporation of TFOCS in the clean hood, dispose of boat and pipette tip.

Procedure for PDMS Preparation:

This procedure consists of the mixing of Part A (monomer) with Part B (cross-linker). The ratio between Part A and Part B is 10:1, allowing for the ideal consistency of the cured PDMS polymer. In order to completely cover the wafer, 100 grams of PDMS was produced

1. A weight boat was positioned on the scaled. The scale was then set to 0.0 grams.

2. 100 grams of Part A was added to the weight boat, as read on the scale.
3. 10 grams of Part B were then added to the weight boat, as the scale read 110.0 grams.
4. Part A and Part B were thoroughly mixed via a folding technique.
5. After thorough mixing of the uncured PDMS, place the boat in the vacuum chamber. Gently apply suction to the chamber by releasing the vacuum valve. The vacuum will draw any bubbles in the PDMS to the surface, slowly removing all the air bubbles. The boat should remain in the vacuum for about an hour or until all the bubbles appear to be removed.

After an hour of degassing, gently release the suction so that air gradually fills the vacuum chamber. If the vacuum is released too quickly, the boat may flip over due to the sudden influx of air.

Procedure for Casting and Curing PDMS:

During this procedure, the PDMS is casted over the mold and cured.

1. Place the wafer mold in a round dish, ensuring that the bottom of the wafer is in complete contact with the bottom surface of the dish.
2. After the PDMS has been degassed for about an hour, pour the 110 grams of PDMS over the wafer so that the PDMS thoroughly covers the entire wafer and fills the dish. When distributing the PDMS, apply the PDMS from side to side, in a continuous motion, avoiding the creating of bubbles.
3. If any bubbles appear in the PDMS, surface bubbles can be removed via mouth blowing. Deeper bubbles will eventually travel to the surface of the PDMS and be released. And dust particles can be removed using a disposable pipette tip. Cover the PDMS with the dish lid.
4. When the PDMS appears clean and free of bubbles, as shown below, place the dish in the oven and allow to bake for approximately 4 hours at 65°C.

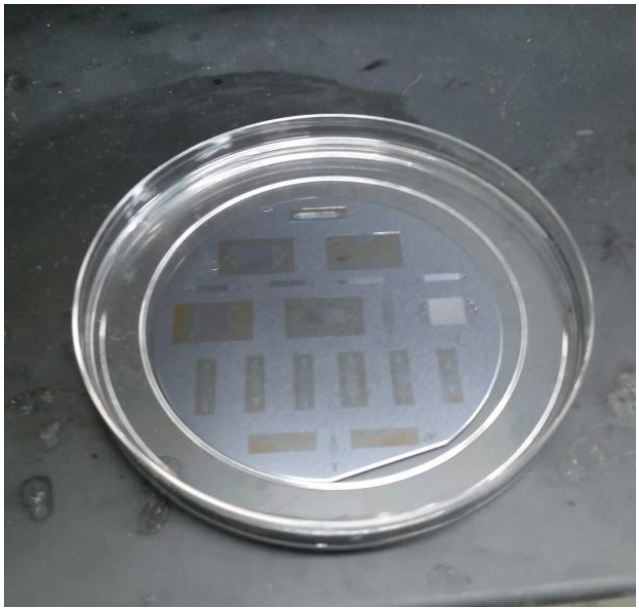

Figure C2: PDMS cast on fabricated wafer

Preparing the PDMS Device:

This procedure completes the production of the PDMS device.

1. Remove the wafer from the PDMS dish by cutting along the edge of the wafer with a razor blade.
2. Carefully remove the silicon wafer from the PDMS.
3. Identify the separation lines between designs and exert downward pressure on these lines with the razor blade, cutting out individual patterns.

This step concludes the process of creating PDMS molds of microfluidic patterns. Additional PDMS molds can be created using the same wafer and PDMS containing dish. Given the hydrophobicity of PDMS, these molds allow for the production of fibrin constructs with embedded microfluidic networks.

APPENDIX D: FIBRIN GEL MOLD FIDELITY DATA

Fibrin			Mold	
Branch	**Length**		**Branch**	**Length**
1	506.329		1	485.366
2	407.595		2	390.244
2	389.873		2	400.61
3	291.139		3	300
3	286.076		3	292.683
3	286.076		3	295.122
3	278.481		3	302.439
4	189.873		4	202.439
4	179.747		4	197.561
4	182.278		4	202.439
4	179.747		4	202.439
4	182.278		4	202.439
4	174.684		4	204.878
4	182.278		4	204.878
4	174.684		4	185.366